On Some Partial Differential Equation Models in Socio-Economic Contexts - Analysis and Numerical Simulations

Jan-Frederik Pietschmann
Trinity College
DAMTP, Center for Mathematical Sciences

A thesis submitted for the degree of
Doctor of Philosophy
May 3nd, 2011

to my grandparents

Franz und Hermine Barten

Johann und Hilde Pietschmann

Declaration

This dissertation is the result of my own work and includes nothing which is the outcome of work done in collaboration except where specifically indicated in the text.

Jan-Frederik Pietschmann

Acknowledgements

My first and greatest thanks goes to my Supervisor Peter A. Markowich. He provided me with a "kick-start" to the PhD by allowing me to take part in the Optimal Transport longterm program at IPAM in Los Angeles. After that, he helped me develop my mathematical capabilities by proposing demanding problems and by initiating contacts and collaborations with many mathematicians in the field of Partial Differential Equations. Moreover his sense of humour was especially helpful in situations where it seemed (and sometimes was) completely impossible to solve a problem. Second, I would like to thank Prof. Martin Burger from the University of Münster. During a number of collaborations, he answered countless questions and never gave me the feeling I was asking dull ones, which I think is a great achievement in itself. Furthermore, I would like to thank my colleagues at the Applied Partial Differential Equations group, especially Marie-Therese Wolfram, Alexander Lorz and Paolo Antonelli for many interesting discussions and, more importantly, the fun we had over the past 3 years. I especially acknowledge Marie's help on numerical (and many other) problems. I also owe a great deal to the other (present and former) members of the group, namely Daniel Brinkman, Marco Di Francesco, Guillaume Dujardin, Klemens Fellner, Clemens Heitzinger, Daniel Marahrens, Clément Mouhot, Norayr Matevosyan, Gael Raoul, Carola Schönlieb and Christof Sparber. In the research group in Münster, I would like to thank Bärbel Schlake for many discussions and tea breaks discussing mathematical and general problems related to our doctorates. I am also grateful to the complete institute in Münster, for providing me an office and including me in all their activities. I also acknowledge the hospitality of Marco Di Francesco in L'Aquila and Adrien Blanchet in Toulouse during extended research stays. I am grateful to Bertram Düring for being a great co-worker. My colleagues Carola Bibiane Schönlieb and Markus Wunsch I thank for being great flatmates during my time in Los Angeles. Finally, I'd like to thankmy parents, my sister Teresa and Maja for their support and their constant interest in the sometimes not very interesting details of my work.

All the work presented in this thesis has been supported by the Leverhulme Trust through the research grant entitled *Kinetic and mean field partial differential models for socio-economic processes* (PI Peter Markowich) and by Award No. KUK-I1-007-43, made by the King Abdullah University of Science and Technology (KAUST).

Abstract

This thesis deals with the analysis and numerical simulation of different partial differential equation models arising in socio-economic sciences. It is divided into two parts: The first part deals with a mean-field price formation model introduced by Lasry and Lions in 2007. This model describes the dynamic behaviour of the price of a good being traded between a group of buyers and a group of vendors. Existence (locally in time) of smooth solutions is established, and obstructions to proving a global existence result are examined. Also, properties of a regularised version of the model are explored and numerical examples are shown. Furthermore, the possibility of reconstructing the initial datum given a number of observations, regarding the price and the transaction rate, is considered. Using a variational approach, the problem can be expressed as a non-linear constrained minimization problem. We show that the initial datum is uniquely determined by the price (identifiability). Furthermore, a numerical scheme is implemented and a variety of examples are presented.

The second part of this thesis treats two different models describing the motion of (large) human crowds. For the first model, introduced by R.L. Hughes in 2002, several regularised versions are considered. Existence and uniqueness of entropy solutions are proven using the technique of vanishing viscosity. In one space dimension, the dynamic behaviour of solutions of the original model is explored for some special cases. These results are compared to numerical simulations. Moreover, we consider a discrete cellular automaton model introduced by A. Kirchner and A. Schadschneider in 2002. By (formally) passing to the continuum limit, we obtain a system of partial differential equations. Some analytical properties, such as linear stability of stationary states, are examined and extensive numerical simulations show capabilities and limitations of the model in both the discrete and continuous setting.

Contents

1 Introduction **5**

1.1 Mean Field Games 6

1.2 Crowd Motion 7

I A One Dimensional Price Formation Model **11**

2 Price Formation using a Mean Field Approach **13**

2.1 The Lasry-Lions Model for Price Formation 13

2.2 Stationary Solution - Bounded Interval 15

2.3 Local Existence 16

2.4 Towards a Global Existence Result 23

2.5 Numerical Results 39

2.5.1 Numerical Experiments on Large Domains 40

2.5.2 Numerical Experiments on Bounded Domains 42

3 Inverse Price Formation Problem **45**

3.1 Introduction 45

3.2 Identifiability 47

3.3 Reconstruction of the Initial Datum 48

3.3.1 Numerical Algorithms 49

3.3.2 Examples 50

II Crowd Motion **55**

4 The Hughes' model for pedestrian flow: The one-dimensional case **57**

4.1 Hughes' model . . . 58
4.2 An attempt to a mathematical theory: approximations . . . 59
4.3 The regularised model: existence and uniqueness theory . . . 62
4.3.1 A Priori Estimates on ϕ and ρ . . . 64
4.3.2 Stability estimates on ϕ . . . 71
4.3.3 The limit as $\varepsilon \to 0$ . . . 72
4.3.4 Uniqueness . . . 76
4.4 Numerics and Examples for the Hughes' model . . . 81
4.4.1 Characteristic Calculus . . . 81
4.4.2 Numerical simulations . . . 85
4.5 Alternative Regularization . . . 89

5 Continuous Limit of a Crowd Motion and Herding Model 93
5.1 Introduction . . . 93
5.2 The Microscopic Model . . . 95
5.2.1 Calculation of the Dynamic Floor Field . . . 96
5.2.2 Herding Effects . . . 97
5.3 Derivation of the Macroscopic Model . . . 97
5.4 Basic Properties of the Model . . . 100
5.4.1 Boundary Conditions . . . 100
5.4.2 Well-posedness . . . 101
5.4.3 Stationary Solutions . . . 101
5.5 Numerical Simulations . . . 109
5.5.1 Simulations in one space dimension . . . 110
5.5.2 Simulations in two space dimensions . . . 110
5.5.3 Monte-Carlo Simulation . . . 111
5.6 Examples . . . 112
5.6.1 Linear Stability . . . 112
5.6.2 Plateau Solutions . . . 112
5.7 Limitations of the Model: Non-convex Obstacles . . . 112

6 Conclusions and Future Work 119

Notation

As this thesis is mainly based on work that has already been published, the notation may differ in between the chapters. In these cases we mention all variants and mark in which chapter they are used.

Sets

$\mathbb{R}$	Set of real numbers
$\mathbb{N}$	Set of natural numbers
Ω	Domain in $\mathbb{R}^d$
$\partial\Omega$	Boundary of domain Ω
$\lvert\Omega\rvert$	Volume of Ω, i.e. $\int_\Omega \, dx$

Calculus Symbols

$\frac{df}{dx}$	Total derivative of a function f with respect to x
	Partial derivative of a function f with respect to t:
$\frac{\partial f}{\partial t}$	in Chapter 2
f_t	in Chapter 4
$\partial_t f$	in Chapter 5
∇f	Gradient of a function f
$\mathrm{div}(f)$	Divergence of a vector-valued function f
Δf	Laplacian of a function f
$\int_\Omega f \, dx$	Volume integral of a function f over Ω
$\int_{\partial\Omega} f \, ds$	Surface integral of a function f over $\partial\Omega$

Function Spaces

$C^k(\Omega)$	Space of k-continuously differentiable functions
$C_0^k(\Omega)$	Space of k-continuously differentiable functions having compact support
$L^p(\Omega)$	Space of p-integrable real-valued functions
$W^{k,p}(\Omega)$	Sobolev space of real-valued functions with p-integrable derivative up to order k
$W_0^{k,p}(\Omega)$	Subspace of functions in $W^{k,p}(\Omega)$ with trace zero
$H^k(\Omega)$	Sobolev space $W^{k,2}(\Omega)$
$H_0^k(\Omega)$	Sobolev space $W_0^{k,2}(\Omega)$
$H^{-k}(\Omega)$	Dual space of $H^k(\Omega)$
$BV(\Omega)$	Space of functions having bounded total variation
$L^p((0,T);X)$	Space of p-integrable functions with values in X
$H^m((0,T);X)$	Sobolev space of functions with values in X, quadratically integrable derivatives up to order m

Chapter 1

Introduction

In this thesis partial differential equation (PDE) models in the contexts of sociology and economics are analysed. The use of PDE models to explore socio and economic problems has become an active research area in the last decades. Many models are derived from microscopic systems consisting of a large number of individuals with a given interaction law. Then, a *coarse graining* procedure leads to the corresponding PDE model. We remark, however, that this strategy is not always possible, as will be explained using the example of human crowd motion later on. Nowadays, a large number of models treat many socio and economic effects. They range from classical economic problems such as the wealth distribution in a society, cf. [35, 34, 81], to less standard applications, such as criminal behaviour in urban areas, cf. [100, 94]. Another problem often discussed in this context is the formation of opinions in large groups. A possible approach is the use of kinetic models, see for example [33] and the references therein. We also mention that this field is closely related to socio- and econo-physics, cf. [20].
The thesis is divided into two major parts: First, we shall analyse a mean field game model describing the dynamics of the price of a good being traded between two groups. In the second part, two different models for the movement of human crowds are considered.

1.1 Mean Field Games

The first part of this thesis is concerned with a mean field game model in economics and finance which, among others, was introduced in a series of papers by J.-M. Lasry and P.-L. Lions [67, 65, 66, 69, 68, 70, 71]. The idea of mean field games is, roughly speaking, the following: One is interested in a situation involving a large number of *agents* or *players*. Each player has only limited information about the whole system. This information is global (or macroscopic) in the sense that it is given by the actions of all other agents or players, thus the name *mean field*. Each agent tries to follow an optimal strategy, based on the information available to him. Passing to the limit of infinitely many players, this approach results in one or a system of non-linear PDEs.
In this thesis, we shall study the particular example of a price formation model. It consists of a (large) group of buyers and a (large) group of vendors trading a good at a certain price $p = p(t)$. The model is given by a non-linear free boundary evolution equation that describes the dynamical behaviour of buyers and vendors which in turn define the price. It is set up on the whole real line, i.e. the price can, in principle, take arbitrarily large or small values. Already the original paper of Lasry & Lions, cf. [71], provided a sketch of a proof for global existence of a smooth solution. Furthermore, there exists a series of papers by Gualdani, Gonzalez and co-workers. In the first paper, they discussed the case of a symmetric initial data which leaves the price fixed for all times, cf. [44]. In the second paper they prove global existence on a bounded domain using a particle method, cf. [22] and finally examine the asymptotic behaviour, cf. [45].
In this thesis, we will prove local in time existence of a continuous solution. Then, we examine the difficulties that occur when trying to extend this local to a global solution. Finally, we will present some results for a regularised version of the model along with numerical examples.
We finally remark that recently global existence (both on bounded and unbounded domains) has been shown using an transformation between the original problem and the heat equation, cf. [18, 19].

The Inverse Problem

Solving the price formation model for a given initial state allows one to observe the dynamical behaviour of the densities of buyers and vendors and thus of the price (and the transaction rate). This is called the *direct* or *forward problem*. In practice, another

interesting problem is to determine the state of the system at a given time and use the model to be able to predict the price for future times. This, however, is by no means straight forward as the state of the system (i.e. the densities of buyers and vendors) cannot be observed directly. One approach to tackle this problem is to use so-called *data assimilation schemes*. Given a set of observations (in our case the price and transaction rate at several times), these schemes estimate the initial state of the system by minimising the error between the observations and the model predictions. We apply this procedure to the price formation model, prove identifiability of the initial datum and present several numerical examples.

1.2 Crowd Motion

The second part of this thesis deals with the motion of human crowds. In this context the term *crowd* denotes a large number of human beings residing in a certain (confined) venue. A typical example would be a soccer stadium or a pedestrian bridge. We emphasize that we exclude situations in which people are too far away from each other to directly interact. The term *motion* refers to the collective behaviour of the crowd, i.e. the movement of each person biased by the influence of its surroundings.

Video recordings of real crowds show that they exhibit a wide range of what is called *collective phenomena*. One common example among them is *lane formation*. This means, in a situation where two groups walk into opposite directions, the tendency to form lanes of people belonging to one group. This can be observed both in real word (e.g. on footpaths) as well as in artificial settings, cf. Figure 1.1.

A good understanding of crowd motion is of growing importance for several reasons. First of all, a growing fraction of humanity is living in urban regions, cf. Figure 1.2. These regions especially include facilities such as airports or shopping malls in which a large number of people is concentrated in a relatively small place. Appropriate mathematical models can help to optimize these buildings in order to avoid congestion and allow for faster operation. Even more important, they can be used to create and validate (using numerical simulation) evacuation plans which are of course of highest importance. This also applies to events such as rock concerts or sports games. A very illustrative example often used in the literature is the *Hajj*, the annual pilgrimage of Muslims to Mecca. In 2009 at least 2.5 million people participated in this event which takes place between the 8th and 12th day of Dhu al-Hijjah, the 12th and last month of the Islamic

Figure 1.1: Lane formation in an artificial experiment, [99].

calendar. Sadly, there have been disasters involving the death of pilgrims in the past. Using video recordings, it was possible to analyse the circumstances and to propose improved pedestrian routes, cf. [50, 3]. Therefore the ultimate goal in terms of mathematical modelling is to develop a model which is able to describe (at least qualitatively) the behaviour of human crowds over a large range of situations. Such a model does not yet exist and in the following we shall outline the difficulties in creating one. A major issue here is obviously the complexity of the humans involved. Their behaviour depends on the individual characteristics of each agent such as age, height, sex or even cultural heritage, cf. [21]. Furthermore the behaviour of each individual may change drastically depending on the situation (e.g. normal walking versus panic). However, even if it is assumed that all people behave exactly in the same way, the situation remains complicated. This becomes clearer by comparing a human crowd with a multi particle system from physics (e.g. an electron gas or a plasma). The usual strategy in physics to understand these complex systems is to start from a simple case, i.e. the interaction between only two particles. This process is governed by a simple physical law which then acts as a starting point for the understanding of the complete system using certain mathematical tools. In crowd motion, however, the interaction of a small number of people is already difficult to understand and therefore the principle "from simple to complex" does not work. As a result, most existing models are built upon simplified hypotheses and are mostly phenomenological. The only indication for the quality of a model is therefore its capability to reproduce observed behaviour such as the formation of lanes as described above but also characteristic patterns in the vicinity of exits can be used as a benchmark. A possible approach to overcome these problems would be to try to use data obtained from either real situations (e.g. video recordings) or artificial experiments, cf. [74, 91],

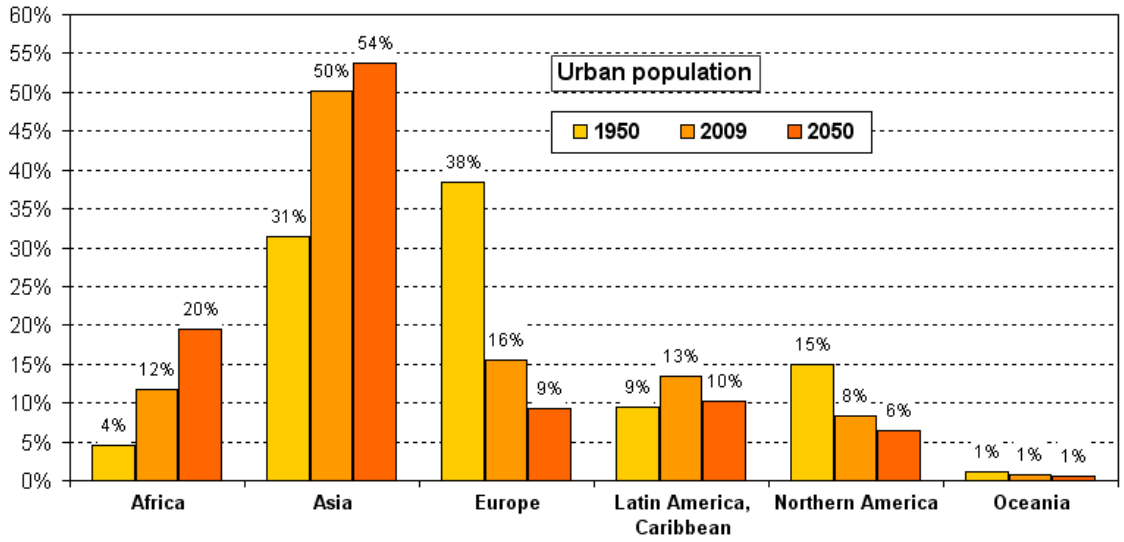

Figure 1.2: Distribution of the world urban population by major area, [84].

to inversely determine the mathematical structure of an appropriate model, cf. [12]. We shall now briefly discuss existing models. One can distinguish between two general approaches: microscopic and macroscopic models. In the microscopic framework, people are treated as individual entities (particles). The evolution of the particles in time is determined by physical and social laws which describe the interaction among the particles as well as their interactions with the physical surrounding. Examples for microscopic methods are social-force models (see [49] and the references therein), cellular automata, e.g [42, 83], queuing models e.g. [114] or continuum dynamic approaches like [109]. For an extensive review of different microscopic approaches we refer to [48]. Note that the microscopic approach in [109] uses the eikonal equation to compute the pedestrians' optimal path. This is a common feature with the model we will analyse in chapter 4. In contrast to microscopic models, macroscopic models treat the whole crowd as an entity without considering the movement of single individuals. The crowd is often represented by a density function depending on ('continuous') space and time. Classical approaches use well known concepts from fluid or gas dynamics, see [51]. More recent models are based on optimal transportation methods [82], mean field games, cf. [63] (see [71] for a general introduction) or non-linear conservation laws [25]. In [90], an approach based on time-evolving measures is presented. We finally note that crowd motion models share many features with traffic models, cf. [4]. In this thesis, two different models will be

analysed. First, we shall consider a model introduced by Hughes in 2002, cf. [54]. We present regularised versions (Subsection 4.2) and prove existence and uniqueness of entropy solutions. In Section 4.4 we will analyse some special cases for the non regularised problem and compare the results with our numerical simulations. In Chapter 5 we deal with the analysis and numerical simulation of a macroscopic model for the motion of a human crowd, derived by (formally) passing to a continuous limit from a microscopic cellular automata model developed by Kirchner and Schadschneider, cf. [59].

Part I

A One Dimensional Price Formation Model

Chapter 2

Price Formation using a Mean Field Approach

2.1 The Lasry-Lions Model for Price Formation

This chapter is organized as follows. After introducing the model, we discuss stationary solutions in Section 2.2. In Section 2.3 we show local existence of (2.3) for general initial data and discuss the maximal extension of the solution (Section 2.4). Finally we illustrate the behaviour of solutions with numerical experiments in Section 2.5. The groups of buyers and vendors are described by two non-negative density functions f_B and f_V, which satisfy the parabolic system

$$\begin{aligned} &\frac{\partial f_B}{\partial t} - \frac{\sigma^2}{2}\frac{\partial^2 f_B}{\partial x^2} = \lambda(t)\delta\left(x - p(t) + a\right), \quad \text{for } x < p(t) \\ &f_B \geq 0, \;\; f_B(x,t) = 0 \;\; \text{for } x \geq p(t) \end{aligned} \tag{2.1a}$$

and

$$\begin{aligned} &\frac{\partial f_V}{\partial t} - \frac{\sigma^2}{2}\frac{\partial^2 f_V}{\partial x^2} = \lambda(t)\delta\left(x - p(t) - a\right), \quad \text{for } x > p(t) \\ &f_V \geq 0, \;\; f_V(x,t) = 0 \;\; \text{for } x \leq p(t), \end{aligned} \tag{2.1b}$$

where

$$\lambda(t) = -\frac{\sigma^2}{2}\frac{\partial f_B}{\partial x}\left(p\left(t\right), t\right) = \frac{\sigma^2}{2}\frac{\partial f_V}{\partial x}\left(p\left(t\right), t\right) \tag{2.1c}$$

is the transaction rate and $x = p(t)$ denotes the price. The variable t denotes time and the space-like variable $x \in \mathbb{R}$ stands for the possible value of the price. The positive

parameter a measures the bid-ask spread (assumed to be equal to $2a$) and $\sigma > 0$ the randomness. A natural property of the model is that the total numbers of the buyers and vendors is preserved, i.e.

$$\frac{d}{dt}\int_{\mathbb{R}} f_B(x,t)\,dx = 0 \quad \text{and} \quad \frac{d}{dt}\int_{\mathbb{R}} f_V(x,t)\,dx = 0. \tag{2.2}$$

The preservation property (2.2) holds for the Dirac delta δ as well as for smoothed versions δ_ε with compact support in $(-a,a)$ and $\int \delta_\varepsilon = 1$.
By introducing the function (signed density of buyers-vendors)

$$f(x,t) = \begin{cases} f_B(x,t) & \text{if } x < p(t) \\ -f_V(x,t) & \text{if } x > p(t), \end{cases}$$

system (2.1) can be reduced to the following scalar free boundary value problem, with unknowns $f = f(x,t)$ and $p = p(t)$:

$$\frac{\partial f}{\partial t} - \frac{\sigma^2}{2}\frac{\partial^2 f}{\partial x^2} = \lambda(t)\left(\delta(x-p(t)+a) - \delta(x-p(t)-a)\right) \tag{2.3a}$$

$$f(x,t) > 0 \text{ if } x < p(t),\ \ f(x,t) < 0 \text{ if } x > p(t) \tag{2.3b}$$

with

$$f(x,0) = f_I(x),\ p(0) = p_0 \tag{2.3c}$$

(initial conditions). The compatibility conditions

$$f_I(p_0) = 0 \text{ and } f_I(x) > 0 \text{ for } x < p_0 \text{ and } f_I(x) < 0 \text{ for } x > p_0. \tag{2.4}$$

are assumed to hold. We reiterate $\lambda(t) = -\sigma^2 \frac{\partial f}{\partial x}(p(t),t)$. Note that this reduction requires that at $t = 0$, $f'(p_{0^+}) = f'(p_{0^-})$ or equivalently $(f_B)'(p_0,0) = -(f_V)'(p_0,0)$ (otherwise additional technicalities have to be taken care of). Also, we remark that by the shift $x = p(t) + y$ equation (2.3) is equivalent to

$$\begin{aligned} \frac{\partial g}{\partial t} &= \frac{\partial^2 g}{\partial y^2} - \frac{\partial g}{\partial y}(0,t)\left[\delta(y+a) - \delta(y-a)\right] + \dot{p}(t) g_y \\ \dot{p}(t) &= -\frac{g_{yy}(0,t)}{g_y(0,t)}, \end{aligned}$$

where we set $g(y,t) = f(y + p(t), t)$. Here the time derivative of the free boundary $\dot{p}(t)$ can be interpreted as the constraint that ensures $g(0,t) = 0$. Note that this formulation,

based on mapping the free boundary into the line $y = 0$, shows that the problem under consideration is highly nonlinear.

Existence and asymptotic behaviour in case of equally distributed buyers and vendors, i.e. $f_B(p_0 - x, t = 0) = f_V(p_0 + x, t = 0)$ for all $x \in \mathbb{R}$ has been addressed by Gonzalez and Gualdani in [44] recently. In this special case the price $p(t)$ is constant in time, i.e. $p(t) = p_0$ and the free boundary disappears from the problem, which becomes a linear parabolic IVP. For this special case they verified existence and proved exponential convergence of the solution towards its stationary state. An extension of their analysis to problems with initial condition close to equilibrium, on bounded domains, has been presented in [45], based on linearisation and semigroup techniques.

In [66] a strategy for carrying out an existence proof (by a time stepping argument, in the framework of nonlinear semigroups, introduced by Crandall and Liggett in [26]) is outlined, we shall however follow an entirely different 'direct' approach, based on classical solutions.

2.2 Stationary Solution - Bounded Interval

As a model we consider the stationary problem (2.3), posed on the bounded domain $(0, A)$, $(A > 0)$, subject to homogeneous Neumann boundary conditions:

$$\begin{aligned}
&\frac{\sigma^2}{2}\frac{\partial^2 f}{\partial x^2} = -\frac{\sigma^2}{2}\frac{\partial f}{\partial x}(p,t)\left(\delta(x-p+a) - \delta(x-p-a)\right)\\
&\frac{\partial f}{\partial x}(0) = \frac{\partial f}{\partial x}(A) = 0.
\end{aligned}$$

The solution, as given by J.-M. Lasry and P.-L. Lions in [71], satisfies:

$$\frac{\partial f}{\partial x} = 0 \text{ if } x < p - a \text{ or if } x > p + a \tag{2.5a}$$

$$\frac{\partial f}{\partial x} = \frac{\partial f}{\partial x}(p) \text{ if } p - a < a < p + a. \tag{2.5b}$$

For the equilibrium price p they obtained the algebraic equation

$$p = \frac{2M_- A - a(M_- - M_+)}{2(M_- + M_+)}, \tag{2.5c}$$

where $M_- = \int_0^p f dx$ (number of buyers) and $M_+ = \int_p^A (-f) dx$ (number of vendors), if the parameter are such that $p \in [a, A - a]$. Note that the price depends explicitly on the ratio of $\frac{M_-}{M_+}$. If the number of buyers increases or the number of vendors goes down the

price goes up, which is reasonable from an economical viewpoint.
We reiterate that the corresponding dynamic free boundary problem with close to equilibrium initial data and homogeneous Neumann boundary conditions has been analysed in [45]. We shall consider the case of a bounded price domain in our numerical experiments in Section 2.5.

2.3 Local Existence

Note that throughout this Section we use the letter C as well as C_1, C_2, ... for generic, not necessarily equal constants. When needed we shall specify on which parameters the constants depend. Without restriction of generality we set $\frac{\sigma^2}{2} = 1$ in the remaining parts of this paper.
At the beginning we would like to reiterate a classical estimate for the first derivative (with respect to x) of the solution of the heat equation

$$\begin{aligned} \frac{\partial u}{\partial t} &= \frac{\partial^2 u}{\partial x^2}, \qquad x \in \mathbb{R},\ t > 0 \\ u(x, t = 0) &= u_I(x), \qquad x \in \mathbb{R} \end{aligned}$$

with $u_I \in L^2(\mathbb{R})$. Multiplying by u and integrating, we obtain

$$\frac{1}{2}\frac{d}{dt}\int_{-\infty}^{\infty} u^2\, dx = -\int_{-\infty}^{\infty}\left(\frac{\partial u}{\partial x}\right)^2 dx.$$

Integrating this equation with respect to time and using the L^2-bound on the initial datum, this leads to

$$u \in L^\infty((0,\infty); L^2(\mathbb{R})),\ \frac{\partial u}{\partial x} \in L^2((0,\infty); L^2(\mathbb{R})).$$

Using again the equation we furthermore obtain

$$\frac{\partial u}{\partial t} \in L^2((0,\infty); H^{-1}(\mathbb{R})).$$

We now localize this estimate by choosing

$$\varphi \in \mathcal{C}_0^\infty(\mathbb{R}). \tag{2.6}$$

Then $v = u\varphi$ satisfies

$$\frac{\partial v}{\partial t} = \frac{\partial^2 v}{\partial x^2} + h \tag{2.7}$$

where

$$h = -2\frac{\partial u}{\partial x}\frac{\partial \varphi}{\partial x} - u\frac{\partial^2 \varphi}{\partial x^2} \in L^2((0,T);L^2(\mathbb{R})).$$

Thus multiplying (2.7) by $\frac{\partial^2 v}{\partial x^2}$ and integrating with respect to x we deduce

$$-\int_{\mathbb{R}} \frac{\partial^2 v}{\partial x \partial t}\frac{\partial v}{\partial x}\,dx = \int_{\mathbb{R}} \left(\frac{\partial^2 v}{\partial x^2}\right)^2 dx + \int_{\mathbb{R}} h\frac{\partial v}{\partial x}\,dx,$$

i.e.

$$\frac{1}{2}\frac{d}{dt}\int_{\mathbb{R}} \left(\frac{\partial v}{\partial x}\right)^2 dx = -\int_{\mathbb{R}} \left(\frac{\partial^2 v}{\partial x^2}\right)^2 dx - \int_{\mathbb{R}} h\frac{\partial^2 v}{\partial x^2}\,dx.$$

Therefore, by integrating with respect to t, we obtain

$$\frac{1}{2}\int_{\mathbb{R}} \left(\frac{\partial v}{\partial x}\right)^2 dx + \frac{1}{2}\int_0^T \int_{\mathbb{R}} \left(\frac{\partial^2 v}{\partial x^2}\right)^2 dx \le \frac{1}{2}\int_0^T \int_{\mathbb{R}} h^2\,dx + \frac{1}{2}\int_{\mathbb{R}} \left(\frac{\partial v_I}{\partial x}\right)^2 dx,$$

where v_I denotes the corresponding initial datum. We conclude

$$\frac{\partial v}{\partial x} \in L^\infty\left((0,T),L^2(\mathbb{R})\right),\ \frac{\partial^2 v}{\partial x^2} \in L^2((0,T);L^2(\mathbb{R})),$$

if $\frac{\partial v_I}{\partial x} \in L^2(\mathbb{R})$. Employing (2.7) then gives

$$\frac{\partial v}{\partial t} \in L^2((0,T);L^2(\mathbb{R})).$$

Iterating the above procedure with

$$z = v\psi, \quad \psi \in \mathcal{C}_0^\infty(\mathbb{R})$$

with $\operatorname{supp}\psi$ compactly contained in $\operatorname{supp}\phi$ and so on we obtain, after a simple exercise, for $\beta \in \mathbb{N}$:

$$\begin{aligned} \|u\|_{L^\infty((0,T);H^\beta(l_2))} &\le C\left(\|u\|_{L^2(((0,T));H^1(\mathbb{R}))} + \|u_I\|_{H^\beta(l_1)}\right) \\ &\le C\left(\|u_I\|_{L^2(\mathbb{R})} + \|u_I\|_{H^\beta(l_1)}\right) \end{aligned} \tag{2.8}$$

where l_1 and l_2 are real open intervals with l_2 compactly contained in l_1 and C depends only on l_1 and l_2. Now we pose the following assumption

(A1) The initial data f_I satisfies

$$f_I \in L^2(\mathbb{R}) \cap H^4(\Lambda) \cap L^1(\mathbb{R}) \cap \mathcal{C}(\mathbb{R}),$$

where $\Lambda = (p_0 - r_0, p_0 + r_0)$ for some $0 < r_0 < a$ and p_0 is such that $f_I(p_0) = 0$, $f_I > 0$ for $x < p_0$ and $f_I < 0$ for $p > p_0$.

Note that (A1) can certainly be weakened, as far as the local regularity close to p_0 is concerned, at the expense of additional technicalities. By a simple Min-Max-principle argument the solution f of (2.3) has a unique zero $x = p(t)$ for all t in its maximal interval of existence. In addition $\lambda(t) \geq 0$ (as long as the solution exists). The Maximum-Minimum principle implies:

$$f \geq u_1,\ x < p(t);\ f \leq u_2,\ x > p(t), \tag{2.9a}$$

where

$$\frac{\partial}{\partial t}u_1 = \frac{\partial^2}{\partial x^2}u_1,\ x < p(t);\ u_1(-\infty, t) = u_1(p(t), t) = 0,\ u_1(t = 0) = f_I \tag{2.9b}$$

$$\frac{\partial}{\partial t}u_2 = \frac{\partial^2}{\partial x^2}u_2,\ x > p(t);\ u_2(+\infty, t) = u_2(p(t), t) = 0,\ u_2(t = 0) = f_I. \tag{2.9c}$$

By classical arguments we shall now derive a fixed-point formulation of the system (2.3) that will be used to prove local existence. Let Γ denote the fundamental solution of the one-dimensional heat equation

$$\Gamma(x, t) = \frac{1}{\sqrt{4\pi t}} e^{-\frac{|x|^2}{4t}}. \tag{2.10}$$

Then the (mild) solution of (2.3) can be expressed using the Duhamel's principle

$$f(x, t) = \int_{\mathbb{R}} \Gamma(x - y, t) f_I(y)\, dy + \int_0^t \int_{\mathbb{R}} \Gamma(x - y, t - s)\lambda(s)q(y, s)dsdy, \tag{2.11}$$

where $q(x, t) = (\delta(x - p(t) + a) - \delta(x - p(t) - a))$. The explicit formulation of (2.11) is given by

$$\begin{aligned} f(x, t) = &\underbrace{\int_{\mathbb{R}} \frac{1}{\sqrt{4\pi t}} e^{-\frac{|x-y|^2}{4t}} f_I(y)dy}_{=:f_1(x,t)} \\ &+ \underbrace{\int_0^t \frac{\lambda(s)}{\sqrt{4\pi(t-s)}} \left(e^{-\frac{|x-p(s)+a|^2}{4(t-s)}} - e^{-\frac{|x-p(s)-a|^2}{4(t-s)}} \right) ds}_{=:f_2(x,t)} \\ &=: F[p, \lambda](x, t). \end{aligned} \tag{2.12}$$

By differentiation of (2.11) with respect to x and evaluation at $x = p(t)$ we obtain the Volterra integral equation of second kind for λ (given by (2.1c) with $\sigma^2/2 = 1$)

$$\lambda(t) = \lambda_0(t) + \int_0^t \lambda(s)K[p](s, t)ds, \tag{2.13}$$

where $K[p](s,t)$ is the difference of the x-derivatives of the heat kernel (2.10), evaluated at $x = p(t) - p(s) \mp a$, i.e.

$$K[p](s,t) = \frac{1}{2\sqrt{4\pi(t-s)}} \left(\frac{p(t)-p(s)+a}{(t-s)} e^{-\frac{|p(t)-p(s)+a|^2}{4(t-s)}} - \frac{p(t)-p(s)-a}{(t-s)} e^{-\frac{|p(t)-p(s)-a|^2}{4(t-s)}} \right). \tag{2.14}$$

The function λ_0 is given by

$$\lambda_0(t) = -\int_{\mathbb{R}} \frac{\partial \Gamma}{\partial x}(p(t)-y,t) f_I(y)\, dy =: \lambda_0[p](t).$$

Since $f(p(t),t) = 0$, we conclude that

$$-\dot{p}(t)\lambda(t) + \frac{\partial^2 f}{\partial x^2}(p(t),t) = 0. \tag{2.15}$$

Here we use the fact that near the free boundary f satisfies the heat equation and therefore replace $\frac{\partial f}{\partial t}$ by $\frac{\partial^2 f}{\partial x^2}$. Throughout our calculations we will frequently use

$$\lim_{z \to 0+} z^{-\gamma} e^{-\frac{\beta}{z}} = 0 \qquad \forall \gamma, \beta > 0. \tag{2.16}$$

Using the above considerations, we can write (2.3) as the following fixed-point problem:

1. Given $p = p(t)$ appropriately, we define

$$S[p](\lambda)(t) = \lambda_0[p](t) + \int_0^t \lambda(s) K[p](s,t) ds, \tag{2.17}$$

   where K is given by (2.14) and we prove that $S[p]$ has a unique fixed point λ in an appropriate set.

2. Given $\lambda = \lambda(t)$ from step 1, we define

$$L(p) = p_0 + \int_0^t \frac{\frac{\partial F[p,\lambda]}{\partial t}(x = p(\tau), \tau)}{\lambda(\tau)}\, d\tau, \tag{2.18}$$

   where F is given by (2.12) and prove the existence of a locally unique fixed point p.

Lemma 2.3.1 (Volterra equation)**.** *Let $p = p(t)$ and $\lambda_0 = \lambda_0(t)$ be in $\mathcal{C}([0,T])$ and let (A1) hold. Then there exists a unique solution $\lambda = \lambda(t)$ in $\mathcal{C}([0,T])$ of the second kind Volterra integral equation* (2.13)*. The $L^\infty((0,T))$ norm of the solution depends only on the modulus of continuity of p and on $\|\lambda_0\|_{L^\infty}$.*

Proof. The kernel $K[p](s,t)$ is continuous for $s \leq t$. An explicit upper bound is easily found due to (2.16) if $\max|p(t) - p(s)| < a$. Since by assumption λ_0 is continuous on $[0,T]$, the result follows from the standard theory of Volterra integral equations of the second kind (by Picard iteration, cf. [37]). □

Remark 2.3.2. *Clearly, $\lambda_0(t)$ is the x-derivative of the solution of the heat equation with initial datum $-f_I(x)$ evaluated at $(x,t) = (p(t),t)$. Thus, assumption (A1), giving local x-Lipschitz continuity of the solution of the heat equation with initial datum $-f_I$, implies that λ_0 is bounded in $\mathcal{C}([0,T])$, if $\|p - p_0\|_{\mathcal{C}([0,T])} \leq r_0$. In particular, note that by the localisation procedure leading to estimate (2.8) a bound on $\|\lambda_0\|_{\mathcal{C}([0,T])}$, which only depends on $\|f_I\|_{L^2(\mathbb{R})} + \|f_I\|_{H^2(\Lambda)}$ can be established if $\|p - p_0\|_{\mathcal{C}([0,T])} \leq r_0$.*

Lemma 2.3.3. *Let $p_1, p_2 \in \mathcal{C}([0,T])$ be such that*

$$\|p_i - p_0\|_{\mathcal{C}([0,T])} \leq r_0, \quad i = 1,2.$$

Then

$$\|\lambda_1 - \lambda_2\|_{\mathcal{C}([0,T])} \leq C_1 \left(\left\| \frac{\partial^2 f}{\partial x^2}_I \right\|_{L^\infty((p_0 - r_0, p_0 + r_0))} + \|f_I\|_{L^2(\mathbb{R})} + T\nu \right) e^{C_2 T} \|p_1 - p_2\|_{C([0,T])},$$

where $\lambda_1 = S[p_1]\lambda_1$, $\lambda_2 = S[p_2]\lambda_2$. The constants C_1, C_2 may depend on r_0 and ν is an upper bound for λ_1 in $L^\infty((0,T))$.

Proof. We have

$$\begin{aligned} \lambda_1 - \lambda_2 = \lambda_0[p_1](t) - \lambda_0[p_2](t) \\ + \int_0^t \left(K[p_1] - K[p_2] \right) \lambda_1(s) ds \\ + \int_0^t K[p_2] \left(\lambda_1(s) - \lambda_2(s) \right) ds. \end{aligned}$$

Using the Lipschitz continuity of the x-derivative of the solution of the heat equation with initial datum $-f_I$ we obtain

$$\begin{aligned} |(\lambda_1 - \lambda_2)(t)| \leq C_1 \left(\|f_I\|_{H^3(\Lambda)} + \|f_I\|_{L^2(\mathbb{R})} \right) \|p_1 - p_2\|_{C([0,T])} \\ + \nu C_2 T \|p_1 - p_2\|_{C([0,T])} + C_3 \int_0^t (\lambda_1(s) - \lambda_2(s)) ds. \end{aligned} \tag{2.19}$$

Here we used the localisation estimate (2.8), the boundedness of $K[p](t,s)$ as long as $s<t$ and $\|p-p_0\|\le r_0$ and the uniform Lipschitz continuity property

$$|K[p_1](s,t)-K[p_2](s,t)|\le C_3\|p_1-p_2\|_{C([0,T])},$$

if $s<t$, $\|p_i-p_0\|\le r_0$ for $i=1,2$. The Gronwall Lemma gives the result. □

Remark 2.3.4. *Using the same arguments we easily obtain the bound (as long as $\|p-p_0\|_{\mathcal{C}([0,T])}\le r_0$):*

$$\|\lambda\|_{\mathcal{C}([0,T])}\le C_3\left(\left\|\frac{\partial f}{\partial x}_I\right\|_{L^\infty((p_0-r_0,p_0+r_0))}+\|f_I\|_{L^2(\mathbb{R})}\right)e^{C_4T},\tag{2.20}$$

where C_3, C_4 may depend on r_0, too.

Lemma 2.3.5 (Positivity of λ for short time intervals)**.** *Let (A1) hold and assume $\|p-p_0\|_{\mathcal{C}([0,T])}\le r_0$. Then there exists a time $T=T(f_I)$, such that $\lambda=\lambda(t)$, the fixed-point of $S[p]$ on $\mathcal{C}([0,T])$, is positive for all $t\in[0,T]$.*

Proof. Note that $\lambda_0(0)=-\frac{\partial f_I}{\partial x}(p_0)$ is positive, we write

$$\lambda_0(t)=\lambda_0(0)+(w(p(t),t)-w(p_0,0)),\tag{2.21}$$

where w, as said before, solves the heat equation

$$\frac{\partial w}{\partial t}=\frac{\partial^2 w}{\partial x^2},\ x\in\mathbb{R},\ t>0,\tag{2.22a}$$

$$w(x,t=0)=-\frac{\partial f_I(x)}{\partial x}(x),\ x\in\mathbb{R}.\tag{2.22b}$$

Here w is locally Lipschitz in x and t, therefore we conclude that $\lambda_0(t)>\frac{\lambda_0(0)}{2}$ as long as $T=T(f_I)$ is sufficiently small. Note that T depends on f_I only through r_0, $1\Big/\frac{\partial f_I}{\partial x}(p_0)$, $\|f_I\|_{L^2(\mathbb{R})}$ and $\|f_I\|_{H^3(\Lambda)}$. Simple calculations show that $K[p](t,s)>0$ for $|p(s)-p(t)|<a$ and $0<s<t$. Therefore, choosing T small enough, we ensure that $\lambda(t)$ is strictly positive for all $t\le T$. □

Theorem 2.3.6 (Local Existence and Uniqueness)**.** *Under the assumption (A1), the system*

$$\lambda(t)=\lambda_0[p](t)+\int_0^t\lambda(s)K[p](s,t)ds\tag{2.23a}$$

$$0=-\dot p(t)\lambda(t)+\frac{\partial^2F[p,\lambda]}{\partial x^2}\left(x=p\left(t\right),t\right)\tag{2.23b}$$

supplemented by $p(0) = p_0$, has a unique solution $(\lambda, p) \in \mathscr{A} \times \mathcal{C}([0,T])$ on some time interval $[0,T]$, where $\mathscr{A}$ is given by

$$\mathscr{A} = \left\{ p \in \mathcal{C}([0,T]) \mid \quad \|p - p_0\|_{L^\infty((0,T))} \leq \frac{r_0}{2} \right\}.$$

Then the solution f of (2.3) is uniquely determined on the same time interval.

Proof. The local existence proof is based on Banach's Fixpoint theorem. Using Lemma 2.3.1 we conclude that the operator $S[p]$, given by (2.17), has a unique fixed-point. The function λ, being a fixed-point of the operator $S[p]$, is then used in the definition of the operator L given by (2.18).

First, we have to check that the operator L is a self-mapping of $\mathscr{A}$. Integration of (2.23b) gives

$$p(t) - p_0 = \int_0^t \frac{1}{\lambda(\tau)} \frac{\partial^2 F[p,\lambda]}{\partial x^2}(p(\tau),\tau) d\tau, \tag{2.24}$$

where $f = F[p,\lambda](x,t)$ is given by (2.12). Using estimate (2.16) we obtain for $t \in [0,T]$

$$\left| \frac{\partial^2 (f_1(p(t),t))}{\partial x^2} \right| \quad = \quad \left| \frac{\partial w}{\partial x}(p(t),t) \right| \leq C \left(\|f_I\|_{L^2(\mathbb{R})} + \|f_I\|_{H^3(\Lambda)} \right) =: M, \tag{2.25}$$

where w solves the IVP (2.22a). The second derivative of f_2 with respect to x is given by

$$\begin{aligned} \frac{\partial^2 f_2}{\partial x^2}(x,t) = \int_0^t \Bigg(& \frac{\lambda(\tau)}{4\sqrt{\pi(t-\tau)^3}} \left(\frac{|x - p(\tau) + a|^2}{2(t-\tau)} - 1 \right) e^{-\frac{|x-p(\tau)+a|^2}{4(t-\tau)}} \\ & - \frac{\lambda(\tau)}{4\sqrt{\pi(t-\tau)^3}} \left(\frac{|x - p(\tau) - a|^2}{2(t-\tau)} - 1 \right) e^{-\frac{|x-p(\tau)-a|^2}{4(t-\tau)^2}} \Bigg) \, d\tau. \end{aligned} \tag{2.26}$$

Inserting (2.25) and (2.26) into (2.24) and setting $x = p(\tau)$ we obtain the following estimate

$$\begin{aligned} |L(p)(t) - p_0| &\leq \int_0^t \frac{M}{\lambda(\tau)} d\tau \\ &+ \int_0^t \frac{1}{\lambda(\tau)} \int_0^\tau \left| \frac{\lambda(s)}{4\sqrt{\pi(\tau-s)^3}} \left(\frac{|p(\tau) - p(s) + a|^2}{4(\tau - s)} - 1 \right) e^{-\frac{|p(\tau)-p(s)+a|^2}{2(\tau-s)}} \right| ds d\tau \\ &+ \int_0^t \frac{1}{\lambda(\tau)} \int_0^\tau \left| \frac{\lambda(s)}{4\sqrt{\pi(\tau-s)^3}} \left(\frac{|p(\tau) - p(s) - a|^2}{4(\tau - s)} - 1 \right) e^{-\frac{|p(\tau)-p(s)-a|^2}{2(\tau-s)^2}} \right| ds d\tau \\ &\leq \left(M + Ct \max_{s \in [0,t]} \lambda(s) \right) \int_0^t \frac{d\tau}{\lambda(\tau)}, \end{aligned}$$

since λ is uniformly bounded away from 0 on $[0,T]$. By choosing T sufficiently small we ensure the self-mapping property of L. The contraction property of L follows from

$$\begin{aligned}\|L(p_2) - L(p_1)\|_{L^\infty((0,T))} &= \\ &= \max_{t\in[0,T]} \left| \int_0^t \left(\frac{1}{\lambda_1(\tau)} F[p_1,\lambda_1](p_1(\tau),\tau) - \frac{1}{\lambda_2(\tau)} F[p_2,\lambda_2](p_2(\tau),\tau) \right) d\tau \right| \quad (2.27) \\ &\leq CT\|p_2 - p_1\|_{L^\infty((0,T))},\end{aligned}$$

where λ_i is the fixed point of $S[p_i]$ for $i = 1, 2$. In (2.27) we used Lemma 2.3.3, simple estimates on the derivatives of the heat kernel and in particular (2.16). Once λ and p are known the linear parabolic equation (2.3a) can easily be integrated. □

Lemma 2.3.7. *Let $\lambda \in L^\infty((0,T))$, $p \in \mathcal{C}([0,T])$ and let (A1) hold. Then the solution f of (2.3) is in $\mathcal{C}((0,T];H^\beta(\mathbb{R}))$ for every $\beta < \frac{3}{2}$. Moreover the estimate*

$$\|f\|_{\mathcal{C}((0,T];H^\beta(\mathbb{R}))} \leq C_1\|f_I\|_{L^2(\mathbb{R})} + C_2\|\lambda\|_{L^2(0,T)}$$

holds with generic constants C_1 and C_2.

The proof follows from a simple computation based on the Fourier transformed equation (2.3).

Remark 2.3.8. *In Theorem 2.3.6, the time T, determining the length of the local existence interval, can easily be traced to depend only on the quantities $\|f_I\|_{H^4(\Lambda)}$, $\|f_I\|_{L^2(\mathbb{R})}$, r_0 and $1/|\frac{\partial}{\partial x} f_I(p_0)|$. In fact, T can be chosen universally, if $\|f_I\|_{L^2(\mathbb{R})}$, $\|f_I\|_{H^4(\Lambda)}$ and $1/|\frac{\partial}{\partial x} f_I(p_0)|$ vary in a bounded subset of the non-negative reals and if r_0 is bounded away from 0.*

2.4 Towards a Global Existence Result

To discuss global existence we make use of a blow-up alternative. For this we need to apply the local existence result on a sequence of time intervals

$$[0,T_0],[T_0,T_1],[T_1,T_2],\ldots,[T_{n-1},T_n],\ldots,$$

with $T_n > T_{n-1}$. Proceeding by induction, assume that the n-th time step has been carried out, giving a solution on $[T_{n-2},T_{n-1}]$ ($T_{n-2} \neq 0$). We have to verify that $f(T_{n-1})$ satisfies the assumptions (A1) with $r = r_{n-1} > 0$, such that the local existence-uniqueness

Theorem 2.3.6 can be reapplied to extend the solution on $[T_{n-2}, T_{n-1}]$. First of all we note that by construction

$$\sup_{t,s\in(T_{j-1},T_j)} |p(t) - p(s)| < a$$

for $j = 1, \dots, n-1$, so we can iterate the estimate (2.20) and obtain $\lambda \in L^\infty(0, T_{n-1})$. Thus by Lemma 2.3.7,

$$f \in \mathcal{C}((T_{n-2}, T_{n-1}]; H^\beta(\mathbb{R})) \text{ for all } \beta < \frac{3}{2},$$

so in particular

$$f(T_{n-1}) \in L^2(\mathbb{R}) \cap \mathcal{C}(\mathbb{R}).$$

Mass conservation (actually conservation of M_+ and M_-) then follows from the solution representation (2.12) by dominated convergence. Thus $f(T_{n-1}) \in L^1(\mathbb{R})$. To verify local regularity of $f(T_{n-1})$ around $x = p(T_{n-1})$, we recall the well known localisation estimate for solutions of the one-dimensional heat equation

$$\frac{\partial u}{\partial t} = \frac{\partial^2 u}{\partial x^2},\ x \in \mathbb{R},\ t > 0,$$

which states that there are constants $D_{l,k} > 0$ such that

$$\sup_{(x,t)\in C_{\frac{r}{2}}(x_0,t_0)} \left| \frac{\partial^{l+k} u}{\partial t^l \partial x^k}(x,t) \right| \le D_{l,k} \frac{1}{r^{k+2l+3}} \|u\|_{L^1(C_r(x_0,t_0))}$$

for all $k, l \in \mathbb{N} \cup \{0\}$. Here the parabolic downward cylinder $C_r(x_0, t_0)$ centered at (x_0, t_0) is given by

$$C_r(x_0, t_0) = \{(x,t) \mid |x - x_0| \le r,\ t_0 - r^2 \le t \le t_0\},$$

see [40, Section 2.3, p. 61]. Now, having constructed $f = f(x,t),\ t \le T_{n-1}$, we choose $0 < r_{n-1} < a$ such that

$$C_{r_{n-1}}(p(T_{n-1}), T_{n-1}) \subseteq \{(x,t) \mid p(t) - a < x < p(t) + a, 0 \le t \le T_{n-1}\}.$$

In particular, let $w = w_t(\delta), \delta > 0$, be the modulus of continuity of $p = p(t)$ at time t. Therefore it suffices to set $r_n = \frac{q_n}{2}$, where

$$w_{T_{n-1}}(q_n^2) = a - q_n$$

(chose the minimal solution). Then f satisfies the heat equation in an open cylinder, which contains $C_{r_{n-1}}\left(p\left(T_{n-1}\right), T_{n-1}\right)$, and

$$\sup_{x\in\left(p(T_{n-1})-\frac{r_{n-1}}{2},p(T_{n-1})+\frac{r_{n-1}}{2}\right)}\left|\frac{\partial f(x,T_{n-1})}{\partial x^k}\right| \leq D_{l,k}\frac{M_+ + M_-}{r_{n-1}^{k+1}},\ k\in\mathbb{N}\cup\{0\} \qquad (2.28)$$

holds due to mass conservation. We conclude that (A1) is satisfied at $t = T_{n-1}$, so the local existence and uniqueness Theorem 2.3.6 can be applied and f can be extended to $[0, T_n]$ for some $\Delta T_{n-1} := T_n - T_{n-1} > 0$ sufficiently small. Now there are two possibilities: Either $T_n \to +\infty$, which implies global in time existence of a unique solution of (2.3) or $T_n \to T_{\max} < \infty$. In the latter case either, possibly after extraction of a subsequence:

$$\text{(C1)}\quad \gamma_n := \|f(T_n)\|_{L^2(\mathbb{R})} + \|f(T_n)\|_{H^4((p(T_n)-r_n,p(T_n)+r_n))} \to \infty \text{ as } n\to\infty$$

or, again after possible extraction of a subsequence,

$$\text{(C2)}\quad \left|\frac{\partial}{\partial x}f(p(T_n),T_n)\right| = \lambda(T_n)\to 0 \text{ as } n\to\infty$$

or after maybe extracting another subsequence

$$\text{(C3)}\quad r_n \to 0 \text{ as } n\to\infty,$$

as otherwise the local solution argument could be restarted in $T - \epsilon_1$, with $\epsilon_1 > 0$ sufficiently small and - due to Remark 2.3.8 - a solution could be obtained on $[T_{\max} - \epsilon_1, T_{max} + \epsilon_2]$ for some $\epsilon_2 > 0$.

Before we proceed with discussing global versus local existence we prove that $\frac{\partial f}{\partial x}(p(t), t) < 0$ on $[0, T]$, assuming that $p = p(t)$ is in $\mathcal{C}([0, T])$. Note that every solution f of the heat equation in a cylinder $D := (a, b)\times[T_1, T]$ is analytic in the spatial variable, for each time $t \in (T_1, T]$ (where the non-empty interval (a, b) is contained in, say, $(p(T) - \frac{a}{4}, p(T) + \frac{a}{4})$ and $T_1 < T$ but sufficiently close to T, see [40, p. 62]. From this we conclude, that if all spatial derivatives of f at $z_0 := (p(T), T)$ are zero we obtain that $f(x, T) = 0$ for all $x \in (a, b)$. This implies that f vanishes identically in D, according to the min-max principle, applied in the small downward cylinders $D_1,\ D_2$ to the left and resp., to the right of $p(T)$, such that the free boundary does not intersect the cylinders D_1 and D_2. Without loss of generality we may drop this last case. Thus there exists $K \in \mathbb{N}$ such

that the K-th order spatial derivative of f is not zero at $(p(T), T)$:

$$\begin{aligned}&\frac{\partial^K f}{\partial x^K}(p(T), T)) \neq 0,\\ &\frac{\partial^l f}{\partial x^l}(p(T), T)) = 0, \text{ for } l = 1, 2, ..., K-1.\end{aligned}$$

Now let us consider $f \in \mathcal{C}^{2K+1}$ (using again the localisation estimate) in both x and t coordinates and

$$\frac{\partial^2 f}{\partial x^2} = f_t \qquad \text{in } D := (a, b) \times [T_1, T], \tag{2.29a}$$

$$\frac{\partial f}{\partial x} < 0 \qquad \text{on } B := \{(x, t) \in D : \ f(x, t) = 0\}. \tag{2.29b}$$

We know that B is a graph of a function $p(t)$ in D and:

$$\begin{cases} f(x,t) > 0 & \text{when } x < p(t),\\ f(x,t) = 0 & \text{when } x = p(t),\\ f(x,t) < 0 & \text{when } x > p(t). \end{cases} \tag{2.30}$$

Lemma 2.4.1. *We have $\frac{\partial f}{\partial x}(p(T), T) < 0$, if p is continuous up to $t = T$.*

Remark 2.4.2. *For the proof of Lemma 2.4.1 it is sufficient to show that p is differentiable at $t = T^-$. Then the parabolic version of the Hopf Lemma can be applied and gives precisely $\frac{\partial f}{\partial x}(p(T), T) < 0$ (since f is negative for $x < p(t)$ and positive for $x > p(t)$).*

Proof. We state the proof in four steps:

I. We know that at time $\{t = T\}$

$$f > 0 \text{ for } x < p(T) \text{ and } f < 0 \text{ for } x > p(t).$$

Therefore we conclude that

$$\begin{gathered}K = 2N + 1 \ \text{ for some } N \in \mathbb{N}\\ \tfrac{\partial^{2N+1}}{\partial x^{2N+1}} f(p(T), T) < 0.\end{gathered}$$

II. Differentiation of equation (2.29a) with respect to time yields

$$\frac{\partial^2 f}{\partial t^2} = \frac{\partial}{\partial t}\left(\frac{\partial^2 f}{\partial x^2}\right) = \frac{\partial^4 f}{\partial x^4}.$$

Reiterating the above equation for the mixed derivatives we obtain:

$$\begin{aligned}\frac{\partial^l f}{\partial t^l} &= \frac{\partial^{2l} f}{\partial x^{2l}},\\ \frac{\partial^{l+k} f}{\partial t^l \partial x^k} &= \frac{\partial^{2l+k} f}{\partial x^{2l+k}},\end{aligned}$$

for $l, k \in 0 \cup \mathbb{N}$ such that $2l + k = 0, 1, ..., K$.

III. Let us write the Taylor expansion of f at z_0 with the mean-value Lagrange remainder of $(N+1)$-order.

$$\begin{aligned}f(x,t) = &\sum_{\substack{0\le l,k:\\ l+k\le N}} \frac{1}{l!k!}\frac{\partial^{l+k}}{\partial t^l \partial x^k} f\left(p(T),T\right)\left(x-p(T)\right)^k (t-T)^l\\ &+ \sum_{\substack{0\le l,k\\ l+k=N+1}} \frac{1}{l!k!} a_{l,k}(x,t)(x-p(T))^k (t-T)^l\end{aligned} \tag{2.31}$$

where

$$a_{l,k}(x,t) = \frac{\partial^{l+k}}{\partial t^l \partial x^k} f\left(\xi_l(x,t), \mu_k(x,t)\right) = \frac{\partial^{2l+k}}{\partial x^{2l+k}} f\left(\xi_l(x,t), \mu_k(x,t)\right).$$

Here $\xi_l(x,t),\ \mu_k(x,t)$ are some intermediate points in (a,b) and $(0,T)$ respectively. Let us note, that $l+k \le N$ implies $2l+k \le 2N$ since $l \le N$. Therefore we conclude that

$$\frac{\partial^{l+k}}{\partial t^l \partial x^k} f\left(p(T),T\right) = 0$$

since all spatial derivatives of order less than $K = 2N+1$ vanish at that point. Thus the first sum in (2.31) vanishes and we are left to deal with the remainder, where $2l + k = N + 1 + l$ and $l \le N + 1$.

IV. We calculate the remainder:

$$\begin{aligned}f(x,t) =&\frac{a_{N+1,0}(x,t)}{(N+1)!}(t-T)^{N+1} + \frac{a_{N,1}(x,t)}{N!}(x-p(T))(t-T)^N\\ &+ \sum_{\substack{0\le l<N\\ 1<k\le N+1\\ l+k=N+1}} \frac{1}{l!k!} a_{l,k}(x,t)(x-p(T))^k (t-T)^l\end{aligned} \tag{2.32}$$

Dividing both sides of (2.32) by $(t-T)^{N+1}$, evaluating at $x = p(t)$ and keeping in mind that $f(p(t), t) = 0$ we obtain:

$$0 = \frac{f(p(t),t)}{(t-T)^{N+1}} = \frac{1}{(N+1)!}a_{N+1,0}\left(p(t),t\right) + \frac{1}{N!}a_{N,1}\left(p\left(t\right),t\right)\frac{p(t)-p(T)}{t-T} + \sum_{1<k\leq N+1}\frac{1}{k!(N+1-k)!}a_{N+1-k,k}(p(t),t)\left(\frac{p(t)-p(T)}{t-T}\right)^{k} \tag{2.33}$$

Next we take a close look at terms in the sum:

(i) When $l = N+1$ and $k = 0$, then $2l + k = 2N + 2$:

$$a_{N+1,0}(x,t) = \frac{\partial^{N+1}}{\partial t^{N+1}}f(x,t) = \frac{\partial^{2N+2}}{\partial x^{2N+2}}f(x,t) = O(1). \tag{2.34}$$

(ii) When $l = N$ and $k = 1$, then $2l + k = 2N + 1$:

$$a_{N,1}(x,t) = \frac{\partial^{2N+1}}{\partial x^{2N+1}}f(\xi_N(x,t),\mu_1(x,t)).$$

thus there exist positive constants ε, δ such that:

$$a_{N,1}(x,t) \leq -\epsilon < 0 \ \text{ in } \mathbb{K}_\delta := \{(x,t)\ |(x,t) - (p(T),T)| < \delta\}. \tag{2.35}$$

(iii) When $l < N$, then $2l + k = N + 1 + l < 2N + 1$ and we have:

$$a_{l,k}(x,t) = o(1).$$

Let

$$z(t) := \frac{p(t)-p(T)}{t-T},$$

then (2.33) can be written as

$$0 = \frac{1}{(N+1)!}a_{N+1,0}(p(t),t) + \frac{1}{N!}a_{N,1}(p(t),t)z(t) + \sum_{1<k\leq N+1}\frac{1}{k!(N+1-k)!}a_{N+1-k,k}(p(t),t)z^{k}(t) \tag{2.36}$$

Since all coefficients $a_{N+1-k,k}(p(t),t)$ in the last part of the above sum vanish as t goes to T, we conclude (using the implicit function theorem) that

$$\begin{aligned}\frac{p(t)-p(T)}{t-T} = z(t) &= -\frac{1}{N+1}\frac{a_{N+1,0}(p(t),t)}{a_{N,1}(p(t),t)} + o(1)\\ &= -\frac{1}{N+1}\frac{\frac{\partial^{2N+2}}{\partial x^{2N+2}}f(p(T),T)}{\frac{\partial^{2N+1}}{\partial x^{2N+1}}f(p(T),T)} + o(1),\end{aligned}$$

as $t \to T$ and $x \to p(T)$. Thus $p(t)$ left-differentiable at $t = T$, and thus, by the parabolic version of the Hopf Lemma, $f(p(T),T) < 0$ and $N = 1$ follows.

□

Theorem 2.4.3. *Let $T_{\max} < \infty$. Then either*

$$(a)\ \limsup_{t \to T_{max}^-} p(t) = \infty$$

or

$$(b)\ \liminf_{t \to T_{max}^-} p(t) = -\infty$$

or

$$(c)\ -\infty < \liminf_{t \to T_{max}^-} p(t) < \limsup_{t \to T_{max}^-} p(t) < \infty.$$

Proof. Assume that $T_{\max} < \infty$ and $p \in \mathcal{C}([0, T_{\max}])$. Returning to the blow up alternative we can exclude (C2) because of Lemma 2.4.1. Also, since p is uniformly continuous on $[0, T_{\max}]$ we conclude from the above construction of the sequence r_n that $r_n \geq R$, where R satisfies $R = \frac{Q}{2}$ and Q is the minimal solution of

$$w(Q^2) = a - Q.$$

Here $w(\delta) := \sup_{t \in (0,T)} w_t(\delta)$ is the global modulus of continuity of $p = p(t)$ on $[0, T]$. Therefore (C3) is also excluded. To exclude (C1) it is sufficient to iterate the estimates (2.20) and (2.28) on the intervals $[T_{n-2}, T_{n-1}],\ n = 1, 2, 3, \ldots$. $T_{\max} = \infty$ follows, which is a contradiction. Thus $p = p(t)$ is discontinuous at $T_{\max}$ if $T_{\max} < \infty$, which implies (a),(b) or (c). □

Next we state an interesting result on the large time behaviour of the function $\lambda = \lambda(t)$.

Lemma 2.4.4 (Unboundedness of λ in the L^1 norm)**.** *Let assumption (A1) be satisfied and let $T_{max} = +\infty$. Then*

$$\int_0^\infty \lambda(s)\, ds = \infty$$

holds.

Proof. First we derive the following formulas for the (negative and positive) mass.

$$\begin{aligned} M_- &= \int_{-\infty}^{p(t)} f(x,t)\,dx = \int_{-\infty}^{p(t)} \int_{-\infty}^{\infty} \Gamma(x-y,s) f_I(y) dy ds \\ &+ \frac{1}{\sqrt{\pi}} \int_0^t \lambda(s) \int_{-\infty}^{\frac{p(t)-p(s)+a}{2\sqrt{t-s}}} e^{-u^2}\,du ds - \frac{1}{\sqrt{\pi}} \int_0^t \lambda(s) \int_{-\infty}^{\frac{p(t)-p(s)-a}{2\sqrt{t-s}}} e^{-u^2}\,du ds \\ &= \int_{-\infty}^{p(t)} \int_{-\infty}^{\infty} \Gamma(x-y,s) f_I(y) dy ds + \frac{1}{\sqrt{\pi}} \int_0^t \lambda(s) \int_{\frac{p(t)-p(s)-a}{2\sqrt{t-s}}}^{\frac{p(t)-p(s)+a}{2\sqrt{t-s}}} e^{-u^2}\,du ds \\ &= \frac{1}{\sqrt{\pi}} \int_{-\infty}^{\infty} \int_{-\infty}^{\frac{p(t)-y}{\sqrt{4t}}} e^{-u^2} du f_I(y) dy + \frac{1}{\sqrt{\pi}} \int_0^t \lambda(s) \int_{\frac{p(t)-p(s)-a}{2\sqrt{t-s}}}^{\frac{p(t)-p(s)+a}{2\sqrt{t-s}}} e^{-u^2}\,du ds. \end{aligned} \tag{2.37}$$

and

$$M_+ = \frac{1}{\sqrt{\pi}} \int_{-\infty}^{\infty} \int_{\frac{p(t)-y}{\sqrt{4t}}}^{\infty} e^{-u^2} du f_I(y) dy - \frac{1}{\sqrt{\pi}} \int_0^t \lambda(s) \int_{\frac{p(t)-(s)-a}{2\sqrt{t-s}}}^{\frac{p(t)-p(s)+a}{2\sqrt{t-s}}} e^{-u^2}\,du ds, \tag{2.38}$$

(obtained by analogous calculations). We write

$$\begin{aligned} M_- &= \frac{1}{\sqrt{\pi}} \int_{-\infty}^{p_0} \int_{-\infty}^{\frac{p(t_n)-y}{\sqrt{4t_n}}} e^{-u^2}\,du\, f_I(y)\,dy \\ &- \frac{1}{\sqrt{\pi}} \int_{p_0}^{\infty} \int_{-\infty}^{\frac{p(t_n)-y}{\sqrt{4t_n}}} e^{-u^2}\,du\,|f_I(y)|\,dy + A(t_n) \end{aligned}$$

and

$$\begin{aligned} -M_+ &= \frac{1}{\sqrt{\pi}} \int_{-\infty}^{p_0} \int_{\frac{p(t_n)-y}{\sqrt{4t_n}}}^{\infty} e^{-u^2}\,du\, f_I(y)\,dy \\ &- \frac{1}{\sqrt{\pi}} \int_{p_0}^{\infty} \int_{\frac{p(t_n)-y}{\sqrt{4t_n}}}^{\infty} e^{-u^2}\,du\,|f_I(y)|\,dy - A(t_n). \end{aligned}$$

where $A(t)$ is given by

$$A(t) = \frac{1}{\sqrt{\pi}} \int_0^{\infty} \lambda(s) 1_{s<t} \int_{\frac{p(t)-p(s)-a}{2\sqrt{t-s}}}^{\frac{p(t)-p(s)+a}{2\sqrt{t-s}}} e^{-u^2}\,du ds.$$

Next we assume that $\int_0^{\infty} \lambda(s)\,ds < \infty$ and choose a sequence t_n such that $t_n \to \infty$ as $n \to \infty$. Thus

$$\begin{aligned} A(t_n) &= \frac{1}{\sqrt{\pi}} \int_0^{\infty} \lambda(s) 1_{s<t_n} \int_{\frac{p(t_n)-p(s)-a}{2\sqrt{t_n-s}}}^{\frac{p(t_n)-p(s)+a}{2\sqrt{t_n-s}}} e^{-u^2}\,du ds \\ &\le \frac{1}{\sqrt{\pi}} \int_0^{\infty} \lambda(s) 1_{s<t_n} \int_{-\infty}^{\infty} e^{-u^2}\,du ds. \end{aligned}$$

Now if $s < t_n$ we obtain

$$\frac{p(t_n) - p(s) - a}{\sqrt{t_n - s}} = \underbrace{\frac{p(t_n)}{\sqrt{t_n - s}}}_{=:\alpha_n(s)} - \underbrace{\frac{p(s) + a}{\sqrt{t_n - s}}}_{=:\beta_n}$$

$$\frac{p(t_n) - p(s) + a}{\sqrt{t_n - s}} = \frac{p(t_n)}{\sqrt{t_n - s}} - \underbrace{\frac{p(s) - a}{\sqrt{t_n - s}}}_{=:\gamma_n}.$$

Since $\lim_{n\to\infty} \beta_n(s) = \lim_{n\to\infty} \gamma_n(s) = 0$ for all $s > 0$ we have:

$$\begin{aligned}\int_{\frac{p(t_n)-p(s)-a}{2\sqrt{t_n-s}}}^{\frac{p(t_n)-p(s)+a}{2\sqrt{t_n-s}}} e^{-u^2}\, duds &= \int_{\alpha_n(s)+\gamma_n(s)}^{\alpha_n(s)+\beta_n(s)} e^{-u^2}\, duds \\ &= e^{-\xi_n^2}(\beta_n - \gamma_n) \to 0 \text{ as } n \to \infty,\end{aligned}$$

for some $\xi_n \in (\alpha_n(s) + \gamma_n(s), \alpha_n(s) + \beta_n(s))$. From dominated convergence we conclude

$$A(t_n) \to 0 \ \text{ as } \ n \to \infty.$$

Furthermore we note that

$$\frac{1}{\sqrt{\pi}} \int_{-\infty}^{\frac{p(t_n)-y}{\sqrt{4t_n}}} e^{-u^2}\, du = \underbrace{\frac{1}{\sqrt{\pi}} \int_{-\infty}^{\frac{p(t_n)}{\sqrt{4t_n}}} e^{-u^2}\, du}_{=:\sigma_n} + \frac{1}{\sqrt{\pi}} \int_{\frac{p(t_n)}{\sqrt{4t_n}}}^{\frac{p(t_n)-y}{\sqrt{4t_n}}} e^{-u^2}\, du.$$

The second integral is bounded from above by

$$\int_{-\infty}^{\infty} e^{-u^2}\, du$$

and thus, by dominated convergence, pointwise tends to zero as $n \to \infty$. Now, using again (2.37) and (2.38), we can write

$$M_- = \sigma_n M_- - \sigma_n M_+ + B_n,$$

where B_n tends to 0 as n tends to infinity. We obtain in the limit $n \to \infty$ (after maybe passing to a subsequence), with $\sigma = \lim_{n\to\infty} \sigma_n$,

$$(1 - \sigma)M_- + \sigma M_+ = 0$$

which is contradiction as $0 \le \sigma \le 1$, $M_- > 0$, $M_+ > 0$. □

To conclude this section, we present a result about the regularity of the free boundary for equation (2.3) when the delta-distributions in the parabolic equation are replaced by smoothed approximations D. We assume the following:

(A2) D in $\mathcal{C}_0^\infty(-a,a)$, $D \geq 0$ and $\int_{-a}^{a} D\, dx = 1$.

and consider the (smoothed) FBP:

$$\begin{aligned} &\frac{\partial f}{\partial t} - \frac{\partial^2 f}{\partial^2 x} = \lambda(t)\left(D(x-p(t)+a) - D(x-p(t)-a)\right) \\ &f(x,t) > 0 \text{ if } x < p(t),\ f(x,t) < 0 \text{ if } x > p(t) \end{aligned} \tag{2.39}$$

with

$$f(x,0) = f_I(x),\ p(0) = p_0. \tag{2.40}$$

Note that we do not go through the local existence arguments previously discussed for the smoothed model, the arguments are very similar to the case with the delta distributions.

Lemma 2.4.5 (Local boundedness of the free boundary)**.** *Let $p = p(t)$ be the free boundary, assume that $\frac{d}{dx} f_I$ is in $L^2(\mathbb{R})$ and that (A1) holds. Then there is $C > 0$ such that*

$$|p(t)| \leq C,\ t \in [0, T_{max}).$$

Proof. We start by deriving a bound on $\lambda(t) = -\frac{\partial f}{\partial x}(p(t),t)$, where f satisfies (2.39). Differentiating the equation w.r.t. x, multiplying by $\frac{\partial f}{\partial x}$ and integrating over $\mathbb{R}$ leads to

$$\begin{aligned} \frac{1}{2}\frac{d}{dt}\int_{\mathbb{R}} \left(\frac{\partial f}{\partial x}\right)^2 dx &= -\int_{\mathbb{R}} \left(\frac{\partial^2 f}{\partial x^2}\right)^2 dx \\ &\quad + \int_{\mathbb{R}} \lambda(t) \frac{\partial f}{\partial x}(x,t)\left(D'(x-p(t)+a) - D'(x-p(t)-a)\right) dx \\ &\leq -\int_{\mathbb{R}} \left(\frac{\partial^2 f}{\partial x^2}\right)^2 dx + K\lambda(t) \left\| \frac{\partial f}{\partial x} \right\|_{L^2(\mathbb{R})} \\ &\leq -\int_{\mathbb{R}} \left(\frac{\partial^2 f}{\partial x^2}\right)^2 dx + K \left\| \frac{\partial f}{\partial x} \right\|_{L^\infty(\mathbb{R})} \left\| \frac{\partial f}{\partial x} \right\|_{L^2(\mathbb{R})}, \end{aligned}$$

where $K = 2\|D'\|_{L^2(\mathbb{R})} < \infty$, as $D(x)$ and its derivatives are bounded. Next, we reiterate the estimate

$$\left\| \frac{\partial f}{\partial x} \right\|_{L^\infty} \leq C\left(\left\| \frac{\partial f}{\partial x} \right\|_{L^2} + \left\| \frac{\partial^2 f}{\partial x^2} \right\|_{L^2} \right) \tag{2.41}$$

and conclude

$$\begin{aligned}\frac{1}{2}\frac{d}{dt}\int_{\mathbb{R}}\left(\frac{\partial f}{\partial x}\right)^2 dx &\leq -\int_{\mathbb{R}}\left(\frac{\partial^2 f}{\partial x^2}\right)^2 dx + CK\left\|\frac{\partial f}{\partial x}\right\|^2_{L^2(\mathbb{R})} + CK\left\|\frac{\partial f}{\partial x}\right\|_{L^2(\mathbb{R})}\left\|\frac{\partial^2 f}{\partial x^2}\right\|_{L^2(\mathbb{R})} \\ &\leq -\int_{\mathbb{R}}\left(\frac{\partial^2 f}{\partial x^2}\right)^2 dx + CK\left\|\frac{\partial f}{\partial x}\right\|^2_{L^2(\mathbb{R})} + \frac{1}{2}\left\|\frac{\partial^2 f}{\partial x^2}\right\|^2_{L^2(\mathbb{R})} + \frac{(CK)^2}{2}\left\|\frac{\partial f}{\partial x}\right\|_{L^2(\mathbb{R})}.\end{aligned}$$

Therefore we obtain

$$\frac{1}{2}\frac{d}{dt}\int_{\mathbb{R}}\left(\frac{\partial f}{\partial x}\right)^2 dx + \frac{1}{2}\int_{\mathbb{R}}\left(\frac{\partial^2 f}{\partial x^2}\right)^2 dx \leq C_2\int_{\mathbb{R}}\left(\frac{\partial f}{\partial x}\right)^2 dx \tag{2.42}$$

with some constant $C_2 \geq \max\left\{CK, \frac{(CK)^2}{2}\right\}$. Integration with respect to t results in

$$\begin{aligned}\int_{\mathbb{R}}\left(\frac{\partial f}{\partial x}(t)\right)^2 dx + \frac{1}{2}\int_0^T\int_{\mathbb{R}}\left(\frac{\partial^2 f}{\partial x^2}(s)\right)^2 dxds \leq C(T)\int_{\mathbb{R}}\left(\frac{\partial f}{\partial x}(t=0)\right)^2 dx. \\ \forall t\in[0,T],\, T\leq T_{max}.\end{aligned} \tag{2.43}$$

From this we conclude

$$\frac{\partial f}{\partial x} \in L^\infty((0,T);L^2(\mathbb{R})),\ \frac{\partial^2 f}{\partial x^2} \in L^2((0,T);L^2(\mathbb{R})).$$

The estimate (2.41) gives

$$\frac{\partial f}{\partial x} \in L^2((0,T);H^1(\mathbb{R})).$$

As $\lambda(t) = -\frac{\partial f}{\partial x}(p(t),t)$ this also means $\lambda \in L^2((0,T))$.

We continue by stating an explicit formula for f, using again Duhamel's principle.

$$\begin{aligned}f(x,t) = &\int_{\mathbb{R}}\frac{1}{\sqrt{4\pi t}}e^{-\frac{|x-y|^2}{4t}}f_I(y)dy \\ &+\int_0^t\frac{\lambda(s)}{\sqrt{4\pi(t-s)}}\left(\int_{\mathbb{R}}D(x-p(s)+a)e^{-\frac{|x-y|^2}{4(t-s)}}\,dy\right. \\ &\qquad\left.-\int_{\mathbb{R}}D(x-p(s)-a)e^{-\frac{|x-y|^2}{4(t-s)}}\,dy\right)ds\end{aligned}$$

Now we use this representation of f to calculate the masses M_+ and M_-. In analogy to (2.37) and (2.38) we obtain:

$$\begin{aligned}M_- = &\frac{1}{\sqrt{\pi}}\int_{-\infty}^{\infty}\int_{-\infty}^{\frac{p(t)-y}{\sqrt{4t}}}e^{-u^2}du f_I(y)dy \\ &+\frac{1}{\sqrt{\pi}}\int_0^t\lambda(s)\int_{\mathbb{R}}D(y')\int_{\frac{p(t)-p(s)-a-y'}{\sqrt{4(t-s)}}}^{\frac{p(t)-p(s)+a-y'}{\sqrt{4(t-s)}}}e^{-\frac{u^2}{2}}\,dudy'ds\end{aligned} \tag{2.44}$$

and

$$M_+ = \int_{p(t)}^{\infty} f(x,t)\,dx = \frac{1}{\sqrt{\pi}} \int_{-\infty}^{\infty} \int_{\frac{p(t)-y}{\sqrt{4t}}}^{\infty} e^{-u^2} du f_I(y) dy \\ + \frac{1}{\sqrt{\pi}} \int_0^t \lambda(s) \int_{\mathbb{R}} D(y') \int_{\frac{p(t)-p(s)-a-y'}{\sqrt{4(t-s)}}}^{\frac{p(t)-p(s)+a-y'}{\sqrt{4(t-s)}}} e^{-\frac{u^2}{2}}\, du dy' ds. \tag{2.45}$$

Assume now that $D \in L^1(\mathbb{R})$ and that there exists a sequence $t_n \nearrow T_{max}$ as $n \to \infty$ such that $p(t_n) \to \infty$ as $n \to \infty$. Since $f_I \in L^1(\mathbb{R})$ and since $\lambda \in L^2((0,T_{max}))$ we conclude, by using dominated convergence in both integrals of (2.45) that $M_+ \to 0$ as $n \to \infty$. This contradicts mass conservation on $[p(t_n), \infty)$. If $p(t_n) \to -\infty$ as $t_n \nearrow T_{max}$ we proceed analogously with the formula (2.44) for M_-. □

Theorem 2.4.6. *Let (A1), (A2) hold, $\frac{d}{dx} f_I$ in $L^2(\mathbb{R})$. Then either*

1.) $T_{max} = \infty$,

2.) $-\infty < p^- := \liminf_{t \nearrow T_{max}} p(t) < \limsup_{t \nearrow T_{max}} p(t) =: p^+ < +\infty$.

Furthermore if 2.) holds, then $f \equiv 0$ in the interval (p^-, p^+).

Proof. We first note that all previous results for equation (2.3) also hold for (2.39). Thus combining Theorem 2.4.3 with Lemma 2.4.5 we conclude

$$-\infty < \liminf_{t \nearrow T_{max}} p(t) < \limsup_{t \nearrow T_{max}} p(t) < +\infty \tag{2.46}$$

if T_{max} is finite. We continue by showing that $f \in \mathcal{C}([0,T_{max}]; \mathcal{C}(\mathbb{R}))$. First we reiterate that $\frac{\partial f}{\partial x} \in L^2((0,T_{max}); H^1(\mathbb{R}))$. Next we notice $\frac{\partial^2 f}{\partial x^2} \in L^2((0,T_{max}); L^2(\mathbb{R}))$ from which we conclude $\frac{\partial^3 f}{\partial x^3} \in L^2((0,T_{max}); H^{-1}(\mathbb{R}))$ and thus

$$\frac{\partial^2 f}{\partial x \partial t} = \frac{\partial^3 f}{\partial x^3} + \lambda(t)(D'(x - p(t) + a) - D'(x - p(t) - a)) \in L^2((0,T_{max}); H^{-1}(\mathbb{R})).$$

We now use Theorem 3 from [40, Section 5.9, p. 287] to conclude

$$\frac{\partial f}{\partial x} \in \mathcal{C}([0,T_{max}]; L^2(\mathbb{R})).$$

Since it is easy to show that $f \in \mathcal{C}([0,T_{max}]; L^2(\mathbb{R}))$ we obtain

$$f \in \mathcal{C}([0,T_{max}]; H^1(\mathbb{R})).$$

As in one dimension the space H^1 can be embedded (via Morrey's inequality) into a space of (Hölder) continuous functions, we finally conclude

$$f \in \mathcal{C}([0, T_{max}]; \mathcal{C}(\mathbb{R})). \tag{2.47}$$

To prove that $f(x, T_{max}) = 0$ in (p^-, p^+), we first fix $x \in (p^-, p^+)$ and choose a sequence t_n such that $t_n \nearrow T_{max}$ as $n \to \infty$ and $f(x, t_n) < 0$ for all n (note that there is a sequence $\tau_n \nearrow T_{max}$ as $n \to \infty$, such that $p(\tau_n) = x$ and $f(x, t) > 0$ for $t \in (\tau_{2k+1}, \tau_{2k+2})$, $f(x, t) < 0$ for $t \in (\tau_{2l}, \tau_{2l+1})$). Then we conclude, by the continuity of f, that

$$f(x, T_{max}) \leq 0.$$

Analogously, we obtain $f(x, T_{max}) \geq 0$ and thus

$$f(x, T_{max}) = 0 \quad \forall x \in (p^-, p^+).$$

□

Corollary 2.4.7. *Let (A1), (A2) hold and additionally $f_I \in H^2(\mathbb{R})$. Then, $\lambda(t) \to 0$ as $t \nearrow T_{max}$.*

Proof. It is simple to show that

$$f \in \mathcal{C}([0, T_{max}]; H^2(\mathbb{R})).$$

Thus $f \in \mathcal{C}([0, T_{max}]; \mathcal{C}^1(\mathbb{R}))$. Since $f(x, T_{max}) = 0$ for $x \in (\liminf_{t \nearrow T_{max}}, \limsup_{t \nearrow T_{max}})$ the statement follows. □

The existence-uniqueness theory presented in this paper does not exclude the occurence of a 'fat' free boundary in finite time. Although $f(t)$ approaches $f(T_{max})$ in a very smooth way, the local existence theorem cannot be restarted at $t = T_{max}$ since no uniquely defined initial value for the free boundary p can be found to solve the integral-differential system (2.23a), (2.23b). In fact, this can be dealt with by looking for weaker solutions in the framework of nonlinear semigroups, i.e. by employing an implicit Euler-type time discretization of the form

$$\frac{f^{n+1} - f^n}{\Delta t} = \left(\frac{\partial^2 f}{\partial x^2}\right)^{n+1} + \lambda^{n+1} \left(D(x - p^{n+1} + a) - D(x - p^{n+1} - a)\right), \tag{2.48}$$

where $f^n \approx f(t_n)$, $\lambda^n \approx \lambda(t_n)$ and $p^n \approx p(t_n)$ with $t_n := n\Delta t$ for some $\Delta t > 0$. It has to be shown that - given g^n appropriately - the elliptic equation (2.48) can be solved for

f^{n+1}, p^{n+1} with $\lambda^{n+1} := -\left(\frac{\partial f}{\partial x}\right)^{n+1}$. Thus we consider (following [71]) the stationary problem, for $\kappa > 0$:

$$\kappa^2 f - \frac{d^2 f}{dx^2} = g + \lambda(D(x-p+a) - D(x-p-a)) \tag{2.49a}$$

$$f(x) > 0 \text{ if } x < p,\ f(x) < 0 \text{ if } x > p. \tag{2.49b}$$

Here, $\kappa^2 = \frac{1}{\Delta t}$, where D denotes either the Dirac delta or an approximation (as above). Furthermore g is a given smooth function (which can be thought of as the result of the previous iteration). We proceed as in [71] and write down the solution of equation (2.49a) via convolution with the Green's function of $-\frac{d^2}{dx^2} + \kappa^2$, i.e.

$$\frac{1}{2\kappa} e^{-\kappa|x|}. \tag{2.50}$$

In the case where $D = \delta$, we obtain

$$f = G + \frac{\lambda}{2\kappa}\left(e^{-\kappa|x-p+a|} - e^{-\kappa|x-p-a|}\right), \tag{2.51}$$

with $G = \frac{1}{2\kappa} e^{-\kappa|x|} * g$. We notice $f(p) = G(p)$ and therefore p can be determined uniquely as long as G has exactly one zero. To determine $\lambda = -\frac{\partial f}{\partial x}(p)$ we differentiate (2.51) and set $x = p$. Thus

$$\frac{\partial f}{\partial x}(p) = \frac{dG}{dx}(p) + e^{-\kappa a}\frac{df}{dx}(p). \tag{2.52}$$

This equation can be solved to obtain $\frac{df}{dx}(p)$, as $e^{-\kappa a} < 1$.

Remark 2.4.8. *In the case where D is an approximation of the Dirac delta, equation* (2.52) *has to be replaced by*

$$\frac{\partial f}{\partial x}(p) = \frac{dG}{dx}(p) \underbrace{-\frac{1}{2\kappa}\int_{-a}^{a} \frac{\partial D}{\partial x}(z)\left(e^{\kappa(z-a)} - e^{-\kappa(z+a)}\right) dx}_{=:A(\kappa)} \frac{\partial f}{\partial x}(p). \tag{2.53}$$

$A(\kappa)$ is, for $\kappa > 0$ strictly less than 1 as $A(0) = 1$, $\lim_{\kappa \nearrow +\infty} A(\kappa) = 0$ (since $\int_{\mathbb{R}} D(x)\, dx = 1$) and A is decreasing. Thus, this equation can be solved to obtain $\frac{\partial f}{\partial x}(p)$.

What is left is to show that G really has only one zero, even if g has a 'fat' zero(-interval). The case when g has a unique zero in $\mathbb{R}$ was dealt with in [71]. We proceed

similarly but assume that there are $-\infty \leq \underline{p} < \overline{p} < +\infty$ and $g(x) > 0$ for $x < \underline{p}$, $g(x) = 0$ for $\underline{p} \leq x \leq \overline{p}$ and $g(x) < 0$ for $x > \overline{p}$. We calculate:

$$2\kappa G(x) = \int_{-\infty}^{\underline{p}} e^{-\kappa|x-y|} g_+(y)dy - \int_{\overline{p}}^{\infty} e^{-\kappa|x-y|}|g_-(y)|dy$$

For $x > \overline{p}$ we obtain

$$\begin{aligned}
&\int_{-\infty}^{\underline{p}} e^{-\lambda|x-y|} g_+(y)dy - \int_{\overline{p}}^{\infty} e^{-\lambda|x-y|}|g_-(y)|dy \\
&= e^{-\lambda x} \underbrace{\left(\int_{-\infty}^{\underline{p}} e^{\lambda y} g_+(y)dy - \int_{\overline{p}}^{x} e^{\lambda y}|g_-(y)|dy - e^{2\lambda x} \int_{x}^{\infty} e^{-\lambda y}|g_-(y)|dy \right)}_{=:S_+(x)}
\end{aligned}$$

For $x < \underline{p}$ analogous calculations lead to

$$\begin{aligned}
&\int_{-\infty}^{\underline{p}} e^{-\lambda|x-y|} g_+(y)dy - \int_{\overline{p}}^{\infty} e^{-\lambda|x-y|}|g_-(y)|dy \\
&= e^{\lambda x} \underbrace{\left(e^{-2\lambda x} \int_{-\infty}^{x} e^{\lambda y} g_+(y)dy + \int_{x}^{\underline{p}} e^{-\lambda y} g_+(y)dy - \int_{\overline{p}}^{\infty} e^{-\lambda y}|g_-(y)|dy \right)}_{=:S_-(x)}.
\end{aligned}$$

We have

$$\begin{aligned}
S'_-(x) &= -2\lambda e^{-2\lambda x} \int_{-\infty}^{x} e^{\lambda y} g_+(y)dy \\
S'_+(x) &= -2\lambda e^{2\lambda x} \int_{x}^{\infty} e^{-\lambda y}|g_-(x)|dy
\end{aligned}$$

and thus $S_-(x)$ is decreasing for $x < \underline{p}$, $S_+(x)$ for $x > \overline{p}$. Furthermore, we have

$$S_-(\underline{p}) = e^{-2\lambda \underline{p}} \int_{-\infty}^{\underline{p}} e^{\lambda y} g_+(y)dy - \int_{\overline{p}}^{\infty} e^{-\lambda y}|g_-(y)|dy \tag{2.54}$$

$$S_+(\overline{p}) = \int_{-\infty}^{\underline{p}} e^{\lambda y} g_+(y)dy - e^{2\lambda \overline{p}} \int_{\overline{p}}^{\infty} e^{-\lambda y}|g_-(y)|dy \tag{2.55}$$

Now, we can state

Lemma 2.4.9. *Let $D(x) = \delta(x)$ or let (A2) hold and*

$$g(x) \begin{cases} > 0, & x < \underline{p}, \\ = 0, & x \in [\underline{p}, \overline{p}], \\ < 0, & x > \overline{p}. \end{cases}$$

Then, under the additional assumption

$$\int_{-\infty}^{\underline{p}} e^{-\lambda y} g_+(y)\, dy - \int_{\overline{p}}^{\infty} e^{-\lambda y}|g_-(y)|\, dy > 0 > \int_{-\infty}^{\underline{p}} e^{\lambda y} g_+(y)\, dy - \int_{\underline{p}}^{\infty} e^{\lambda y}|g_-(y)|\, dy \tag{2.56}$$

there exactly exists one $\tilde{p} \in (-\infty, \infty)$ *such that*

$$G(\tilde{p}) = 0.$$

Proof. First we notice that (2.56) means precisely $S_-(-\infty) > 0 > S_+(\infty)$. Also, note that for $x \in (\underline{p}, \overline{p})$ we have

$$\begin{aligned} 2\kappa G(x) &= \int_{-\infty}^{\underline{p}} e^{-\lambda|x-y|} g_+(y) dy - \int_{\overline{p}}^{\infty} e^{-\lambda|x-y|}|g_-(y)| dy && (2.57)\\ &= e^{-\lambda x}\int_{-\infty}^{\underline{p}} e^{\lambda y} g_+(y)\, dy - e^{\lambda x}\int_{\overline{p}}^{\infty} e^{-\lambda y}|g_-(y)|\, dy && (2.58)\\ &=: H(x). && (2.59) \end{aligned}$$

By differentiation we conclude $H' < 0$. Using (2.54) and (2.55) we find

$$\begin{aligned} S_-(\underline{p}) &= e^{-\lambda \underline{p}} H(\underline{p}), && (2.60)\\ S_+(\overline{p}) &= e^{\lambda \overline{p}} H(\overline{p}), && (2.61) \end{aligned}$$

and thus

$$\begin{aligned} \operatorname{sgn} H(\underline{p}) &= \operatorname{sgn} S_-(\underline{p}), && (2.62)\\ \operatorname{sgn} H(\overline{p}) &= \operatorname{sgn} S_+(\overline{p}). && (2.63) \end{aligned}$$

Now we consider the following cases

case 1: $S_-(\underline{p}) \le 0$.

We imediately conclude (as S_- is decreasing) that there exists a $\tilde{p} \in (-\infty, \underline{p}]$ sucht that

$$S_-(\tilde{p}) = 0 \quad \text{and} \quad H(\underline{p}) \le 0. \tag{2.64}$$

Since $H' < 0$ we conclude $H(\overline{p}) < 0$ and thus $S_+(\overline{p}) < 0$. Since $S_+' < 0$ on $(\overline{p}, \infty)$ we finally obtain that there exists exactly one $\tilde{p}$ such that $G(\tilde{p}) = 0$.

case 2: $S_-(\underline{p}) > 0$.

First we notice that in this case $S_- > 0$ on $(-\infty, \underline{p})$ and that $H(\underline{p}) > 0$. We also reiterate $H' < 0$ on $(\underline{p}, \overline{p})$. Now there are two possibilities:

case 2a: $H(\overline{p}) > 0$ and thus $S_+(\overline{p}) > 0$.

Since S_+ decays on $(\overline{p}, \infty)$ and since $S_+(\infty) < 0$ we conclude again that there exists a $\tilde{p} \in [\overline{p}, \infty)$ such that

$$S_+(\tilde{p}) = G(\tilde{p}) = 0. \tag{2.65}$$

case 2b: $H(\overline{p}) \leq 0$. Then we conclude in the same way as in 2a) that there is a $\tilde{p} \in [\underline{p}, \overline{p}]$ such that $G(\tilde{p}) = 0$.

Putting all these cases together we finally obtain that there exist a $\tilde{p} \in (-\infty, \infty)$ such that

$$G(\tilde{p}) = 0.$$

□

Thus, at least in the implicit Euler discretized framework, a fat free boundary is smoothed out after a single time step. This is the basis for proving that the solution of the free boundary problem (2.29), (2.30) can be extended beyond, albeit as a mild solution according to nonlinear semigroup theory. To be precise, it has to be shown that the constraint (2.56) is maintaned by the discrete evolution and that the discretisation converges to a mild solution of the FBP. This programme has already been outlined in [71].

2.5 Numerical Results

In this section we present numerical results which were created in collaboration with M.-T. Wolfram. For actual numerical computations there is no need to use the fully implicit scheme presented in the previous section. Instead, we use an implicit-explicit scheme to solve (2.3) on a bounded domain. Let f_I and p_0 denote the initial data satisfying the compatibility condition (2.4). Then

1. Solve (2.3) for $f(x, t_j)$, given $p(t_{j-1})$,

2. Update the free boundary $p(t_j)$ such that $f(p(t_j), t_j) = 0$

3. Set $j = j + 1$, go to 1.

Equation (2.3) is discretized in space using a finite difference method, where the convection term $\frac{\partial f}{\partial x}(p(t), t)$ is approximated by its upwind difference quotient. The resulting ODE system is solved using an implicit Euler method, resulting in the following numerical discretization at $x = x_n$ and $t = t_{j+1}$

$$\begin{aligned}\frac{f_n^{j+1} - f_n^j}{\tau} = \frac{\sigma^2}{2}\frac{f_{n+1}^{j+1} - 2f_n^{j+1} + f_{n-1}^{j+1}}{h^2} - \\ - \frac{\sigma^2}{2}\frac{1}{h}\left[-q(x_n)^+ f_{k-1}^{j+1} + |q(x_n)| f_k^{j+1} + q(x_n)^- f_{k+1}^{j+1}\right]\end{aligned} \tag{2.66}$$

where $q(x_n) = (\delta(x_n - p(t_{k-1}) - a) - \delta(x_n - p(t_{k-1}) + a))$, $q^+ = \max(q, 0)$, $q^- = \min(q, 0)$ and k denotes the index such that $f(p(t_{k-1}), t_j) = 0$. Here h denotes the mesh size, τ the time steps of the implicit Euler method. The Dirac δ is approximated by a Gaussian

$$\delta_\varepsilon(x) = \frac{1}{\varepsilon\sqrt{\pi}} e^{-\frac{x^2}{\varepsilon^2}}$$

where ε is chosen such that $\delta(a) = \delta(-a) = 10^{-6}$.

Proposition 2.5.1. *Let $p(t_{j-1})$ be given and $f(p(t_{j-1}), t_j) = 0$. If $\tau < 2k \max(q)$, then the matrix defined by (2.66) is strictly diagonally dominant, hence regular.*

Proof. The function $q(x)$ is positive on $[p(t) - 2a, 0)$, negative on $(0, p(t) + 2a]$ and has a compact support on $[p(t) - 2a, p(t) + 2a]$. Therefore we consider the following different cases. If $x_n < p(t) - 2a$ then $q(x_n)$ equals zero and (2.66) is the standard discretization of the heat equation. If $x_n \in [p(t) - 2a, 0)$ then $q(x_n) > 0$ and if $\tau < 2h \max(q)$ then

$$|a_{ii}| > \sum_{i \neq j} |a_{ij}|.$$

The same argument holds for $x_n \in [0, p(t) + 2a)$, therefore the system matrix is strictly diagonally dominant. □

2.5.1 Numerical Experiments on Large Domains

In this Section we present long-time numerical experiments on large domains to illustrate the behaviour of solutions on the unbounded domains. We observe that depending on

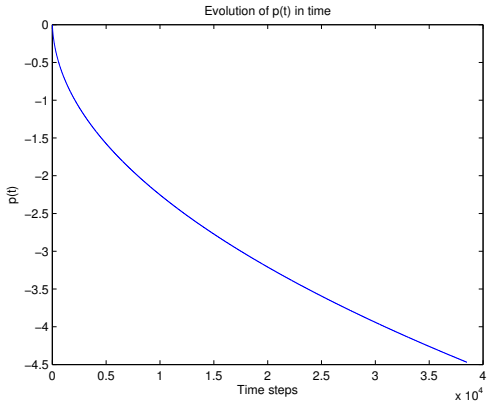

Figure 2.1: Evolution of the price $p(t)$ in time for $M_1 < M_2$

the initial masses M_1 or M_2, the price $p(t)$ either decreases or increases with a rate proportional to $\sqrt{t}$.

We choose $\Omega = [-400, 400]$, discretized with a non-equidistant mesh of meshsize $h_1 = 10^{-3}$ in $x \in [p(t)-4a, p(t)+4a]$ and $h_2 = 1$ for $x \in [-400, p(t)-4a)$ or $x \in (p(t)+4a, 400]$ and $a = 1$. We solve the discrete scheme (2.66) on the time interval $[0, 400]$, with time steps $\tau = 5 \times 10^{-3}$. The initial datum we chose is

$$f_I(x) = \begin{cases} 10^{-6} & \text{for } x \in [-400, -1) \\ 2.2222x^3 - 0.2222x^2 - 2.4444x & \text{for } x \in [-1, 1.1] \\ -10^{-6} & \text{for } x \in (1.1, 400] \end{cases}$$

with initial masses $M_1 = 0.5927$ and $M_2 = 0.7642$. The evolution of the price $p(t)$ is depicted in Figure 2.1. In fact the price $p(t)$ is proportional to $\sqrt{t}$.

In the second example we choose an initial guess with $M_2 < M_1$, given by $f_I(x) = 0.5882x^3 + 0.0588x^2 - 0.5294x$ on the interval $(-1, 0.9)$ and $f_I(x) = \pm 10^{-6}$ outside this interval. All other parameters take the same values as in the previous example. Since $M_1 = 0.1373$ and $M_2 = 0.1037$, the price increases again proportionally to $\sqrt{t}$, which can be seen in Figure 2.2.

Note that the second derivative of f at $x = p_0$ determines the initial direction of $p(t)$, since

$$\dot{p}(t) = -\frac{\frac{\partial^2 f}{\partial x^2}(p(t), t)}{\frac{\partial f}{\partial x}(p(t), t)}, \quad \frac{\partial^2 f_I}{\partial x^2}(p_0) = 0.$$

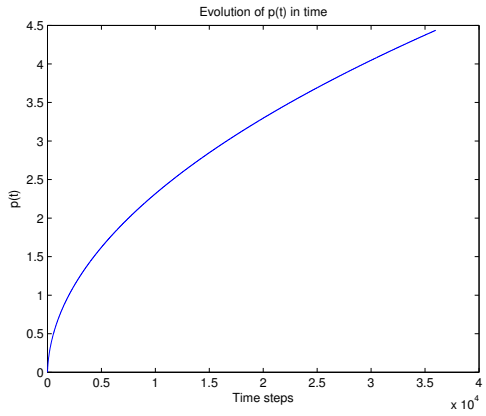

Figure 2.2: Evolution of the price $p(t)$ in time for $M_1 > M_2$

Therefore we can construct examples, where the price is not monotonously increasing or decreasing in time. We choose the following initial guess

$$f_I(x) = \begin{cases} 10^{-5} & \text{for } x \in [-100, -3.1547) \\ -1.5x^2 - 6x - 4 & \text{for } x \in [-3.1547, -1) \\ -2.5x^3 - 3x^2 - x & \text{for } x \in [-1, 0.1) \\ 1.071x^2 - 2.142x + 0.071 & \text{for } x \in [0.1, 1.96) \\ -10^{-5} & \text{for } x \in [1.96, 100], \end{cases}$$

depicted in Figure 2.3(a). The function f_I is concave at $x = 0$, but $M_1 > M_2$. Due to the negative curvature of f_I at $x = 0$, the price $p(t)$ initially decreases, but since $M_1 > M_2$ it starts to increase after some iterations. In this example we are only interested in the initial behaviour, therefore we choose $\Omega = [-100, 100]$ and calculate the first 400 time steps with $\tau = 5 \times 10^{-3}$. The evolution of the price $p(t)$ is depicted in Figure 2.3(b).

2.5.2 Numerical Experiments on Bounded Domains

Finally we would like to illustrate the behaviour of solutions on bounded domains. Here the solutions converge quickly to their stationary state, which can be calculated explicitly using (2.5).

We choose $\Omega = [0, 1]$ with an equidistant mesh of meshsize $h = 10^{-3}$ and a temporal

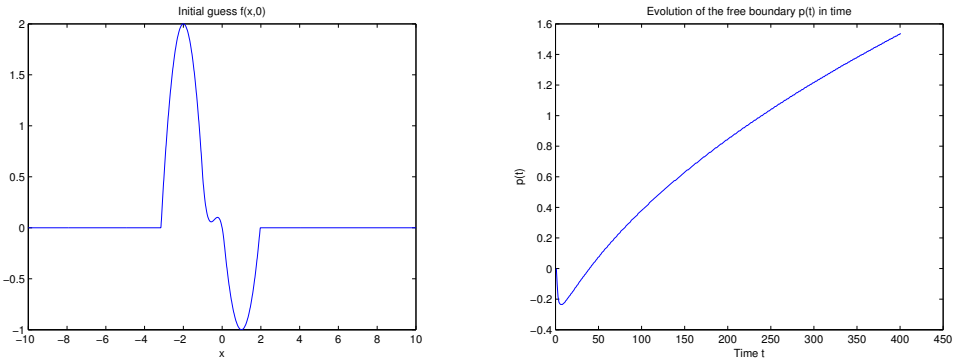

(a) Zoom of initial guess $f_I(x)$

(b) Evolution of $p(t)$

Figure 2.3: Non-monotonous behaviour of $p(t)$

meshsize $\tau = 10^{-3}$. The initial data is given by the cubic polynomial

$$f_I(x) = 145.833x^3 - 233.333x^2 + 87.5x,$$

which has the root at $x = 0.6$. Therefore $p_0 = 0.6$ and the initial masses are $M_1 = 3.675$ and $M_2 = 1.2443$. The parameter a is set to 0.1 and $\frac{\sigma^2}{2} = 1$. To ensure the mass preservation property, system (2.3) is supplemented with homogeneous Neumann boundary conditions at $x = 0$ and $x = 1$. Figure 2.4(a) illustrates the evolution of the density $f(x,t)$ in time. The solution converges quickly to the stationary profile given by (2.5). The numerically calculated price "converges" towards $p(t) = 0.709$ (see Figure 2.4(b)), the stationary price calculated from (2.5) is given by $p_{stat} = 0.71$.
In case of symmetric initial data the moving boundary is constant in time, i.e. $p(t) = p_0$ (cf. [44]). In order to test the numerical method we choose $f_I(x) = \sin(2\pi x)$ and the same discretization in space and time as in the previous example. The evolution of $f(x,t)$ is illustrated in Figure 2.5(a). As expected the numerically calculated price $p(t)$ is constant in time, see Figure 2.5(b).

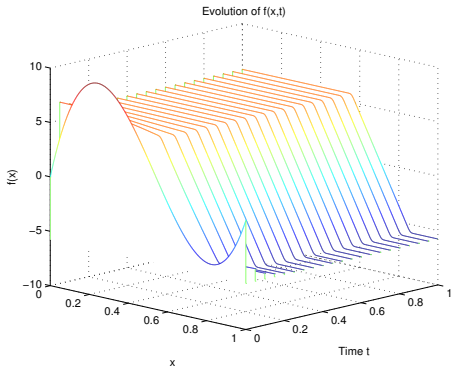

(a) Evolution of $f(x,t)$

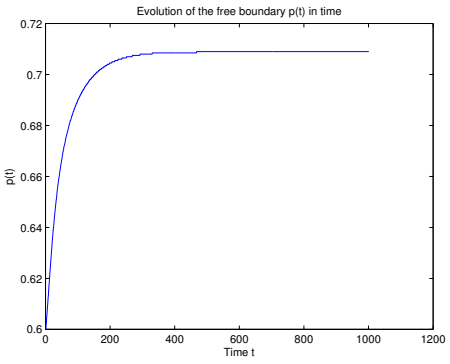

(b) Evolution of $p(t)$

Figure 2.4: Solution of mean-field equation (2.3)

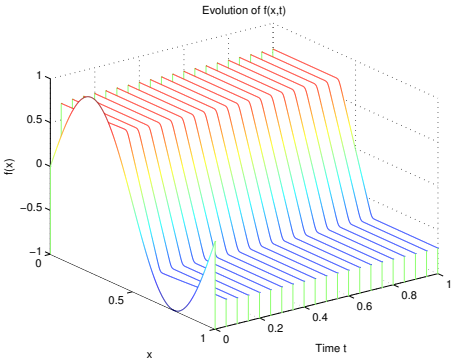

(a) Evolution of $f(x,t)$

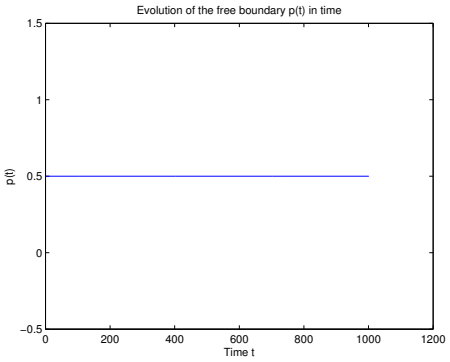

(b) Evolution of $p(t)$

Figure 2.5: Solution of mean-field equation (2.3) with symmetric initial data

Chapter 3

Inverse Price Formation Problem

The work in this Chapter has been caried out in collaboration with M. Burger, F. Lenz and P.A. Markowich.

3.1 Introduction

We again consider the price formation model from the previous chapter:

$$\frac{\partial f}{\partial t} - \frac{\partial^2 f}{\partial x^2} = \lambda(t)(\delta(x - p(t) + a) - \delta(x - p(t) - a)),\ x \in \mathbb{R}, t \in \mathbb{R}_+ \tag{3.1a}$$

$$\lambda(t) = -\frac{\partial f}{\partial x}(p(t), t), \tag{3.1b}$$

$$f(x, 0) = f_I,\ p(0) = p_0, \tag{3.1c}$$

with compatibility conditions

$$f_I(p_0) = 0 \text{ and } f_I(x) > 0 \text{ for } x < p_0 \text{ and } f_I(x) < 0 \text{ for } x > p_0.$$

However, this time we are not interested in the direct problem, i.e. the problem of determining a solution f to (3.1a)-(3.1c) with given initial datum f_I. Instead, we ask the question whether it is possible, given measurements of $p(t)$ (and possibly $\lambda(t)$) over a certain time interval I, to use the model to predict the price for future times (i.e. times exceeding I). This problem is of the class of inverse problem (cf. [38] and the references therein). More precisely, it is a so-called data assimilation problem: In data assimilation, the goal is to determine the state of a system at a certain time t^*, denoted by x_{t^*}, from a number of measurements. If data has only been measured at one point in time (or

in a very short interval), the problem is called *static*. The goal is then to identify the state of the system at the time the measurements were taken. In our case, data can be measured over a relatively large interval. This is called the *dynamic* data assimilation problem. We assume that measurements are given in an interval $[t^*, t^* + \Delta t]$ which is called the *assimilation window*. We also distinguish between stochastic or deterministic problems depending on whether the model incorporate noise via a stochastic term or not. For a broader overview on data assimilation, see [73] and the references therein. In many applications, the dimension (or number, in the discrete setting) of observations available is small compared to the state space of the system. A prime example is weather forecasting, where currently used models typically consist of about $O(10^7)$ state variables while only measurements of order $O(10^6)$ are available, cf. [85]. In general, the strategy to solve a data assimilation problem is to minimize the squared difference between the observations and the predictions by the model over all admissible states x_{t^*}. In some application it is reasonable to assume a given background information x_0^b (e.g. a previous forecast) which is also incorporated in the minimization problem. In its most general form, the discrete approach can be written as

$$\mathcal{J}(x_{t^*}) = \frac{1}{2}(x_{t^*} - x_0^b)^T B^{-1}(x_{t^*} - x_0^b) + \frac{1}{2}\sum_1^N (y_i - \mathcal{H}(x_i))^T R_i^{-1}(y_i - \mathcal{H}(x_i)) \to \arg\min_{x_{t^*}}$$

where by y_i we denote the observed data at time t_i and $\mathcal{H}$ is the observation operator, B^{-1} and R_i^{-1} are given weights. The states x_i, $i = 1, \ldots, N$ are subject to the system equations

$$x_{i+1} = \mathcal{M}_{i+1,i}(x_i),\ i = 0, \ldots, N-1.$$

Here, $\mathcal{M}_{i+1,i}$ is an operator that propagates the state of the system from time i to $i+1$. For the price formation model this means that we want to estimate the initial datum f_I at time $t = 0$ from measurements of the price $p(t)$ in the interval $[0, t_1]$. Once the initial state is determined, we can use (3.1a) to predict the price for times larger than t_1. There are two possible sources of error: measurement error in the observations and general modelling error. The definition of a measurement error for a price is a bit delicate as a price can, at least in principle, be obtained exactly. However, an error can still be introduced if the exact information of the price is not available, e.g. due to rounding errors. The modelling error, which is likely to play an important role, is not yet included in our current approach.

3.2 Identifiability

In this Section, we shall show that two different initial data cannot result in the same price, i.e. the identification of the initial datum is unique. As described in Section 2.1, the transformation $y = x - p(t)$ eliminates the free boundary but results in the following highly non-linear problem

$$\frac{\partial g}{\partial t} = \frac{\partial^2 g}{\partial y^2} - \frac{\partial g}{\partial y}(0,t)\left[\delta(y+a) - \delta(y-a)\right] + \dot{p}(t) g_y$$
$$\dot{p}(t) = -\frac{g_{yy}(0,t)}{g_y(0,t)}.$$

For given p the problem reduces to

$$\frac{\partial g}{\partial t} = \frac{\partial^2 g}{\partial y^2} - \frac{\partial g}{\partial y}(0,t) d(y) + m(t)\frac{\partial g}{\partial y} \tag{3.2}$$
$$\frac{\partial g}{\partial y}(0,t) = \lambda(t) \tag{3.3}$$

with $d(y) := [\delta(y+a) - \delta(y-a)]$, and $m(t) := \dot{p}(t)$.

Lemma 3.2.1. *Let g_1, g_2 be two solutions to (3.2), (3.3) for the same, given $p(t)$. Under the additional regularity assumptions*

$$g_1,\ g_2 \in \mathcal{C}^1([0;T]; \mathcal{C}^2(\mathbb{R}) \cap L^1(\mathbb{R})),$$
$$\frac{\partial g_i}{\partial y},\ \frac{\partial^2 g_i}{\partial y^2} \in \mathcal{C}([0;T]; L^1(\mathbb{R})),\ i = 1,2$$

we have $g_1 = g_2$.

Proof. The strategy of the proof is to show that all moments $\bar{g} := g_1 - g_2$ are zero. As the space of (Hermite) polynomials is dense in L^2 this will suffice to conclude $\bar{g} = 0$. The function $\bar{g}$ is a solution to

$$\frac{\partial \bar{g}}{\partial t} = \frac{\partial^2 \bar{g}}{\partial y^2} + \dot{p}(t)\frac{\partial \bar{g}}{\partial y}.$$

Applying the Fourier transform to $\bar{g}$ results in

$$\hat{g}_t(s,t) = (-s^2 + is\dot{p}(t))\hat{g}(s,t),$$

and thus

$$\hat{g}(s,t) = e^{-s^2 + is\dot{p}(t)}\hat{g}(s,0).$$

Now applying the inverse Fourier transform and evaluating g and its first derivative at $x = 0$ yields

$$0 = \bar{g}(0,t) = \frac{1}{2\pi}\int_{-\infty}^{\infty} e^{-s^2+is\dot{p}(t)}\hat{g}(s,0)\,ds,$$
$$0 = \frac{\partial \bar{g}}{\partial y}(0,t) = \frac{1}{2\pi}\int_{-\infty}^{\infty} se^{-s^2+is\dot{p}(t)}\hat{g}(s,0)\,ds.$$

For $t = 0$ we see that already the zeroth and first moment of $\hat{g}(s,0)\,dx$ are zero (since the exponential function is strictly positive). Differentiating the above equations with respect to t and evaluating at $t = 0$ gives the same result for all higher moments.

□

3.3 Reconstruction of the Initial Datum

In this Section we consider the reconstruction of the initial datum using measurements of the price. We will work in the original formulation of the problem (3.2), (3.3). Furthermore, we will restrict ourselves to the bounded domain $\Omega = [0,1]$, to make the numerical treatment of the problem possible. By

$$p_m(t), \quad 0 \le t \le t_1,$$

we denote the measured price. We supplement (3.1a) with the following boundary conditions

$$\frac{\partial f}{\partial x}(0,t) = \frac{\partial f}{\partial x}(1,t) = 0. \tag{3.4}$$

These boundary conditions preserve the conservation of total mass featured by the original problem on the whole real line. To shorten the notation, we introduce

$$g(x,t) := \lambda(t)(\delta(x - p(t) + a) - \delta(x - p(t) - a)),$$

i.e.

$$\frac{\partial f}{\partial t} - \frac{\partial^2 f}{\partial x^2} = g(x,t).$$

If we would solve this equation with the correct datum f_I, the condition $f(p(t),t) = 0$ would be exactly fulfilled. This motivates to use the deviation of $f(p_m(t),t)$ a data

term. Introducing an additional regularization, the corresponding Lagrange functional with Lagrange parameter μ, μ_0 is given by

$$\mathcal{L} = \frac{\alpha}{2}\int_0^{t_1}\int_\Omega (f(x,t))^2\delta(x-p_m(t))\,dxdt + \beta\int_0^{t_1}\int_\Omega \mu(x,t)\left[\partial_t f - \partial_{xx} f - g(x,t)\right]\,dxdt \\ + \int_0^1 \mu_0(x)[f(x,0)-f_I]\,dx + \frac{\gamma}{2}\int_0^1 (\partial_x f_I)^2\,dx$$

with α, β, γ being constants weighting the different terms. The derivatives of $\mathcal{L}$ with respect to their arguments are

$$\frac{\partial\mathcal{L}}{\partial f}w = \int_0^{t_1}\int_\Omega \left[-\partial_t\mu - \partial_{xx}\mu + \alpha f\delta(x-p_m(t))\right] w\,dxdt + \int_0^1 \mu w|_{t=T}^{t=0}\,dx + \int_0^1 \mu(x,0)w\,dx$$
$$\frac{\partial\mathcal{L}}{\partial\mu}v = \int_0^{t_1}\int_\Omega v\left[\partial_t f - \partial_{xx} f - g(x,t)\right]\,dxdt + \int_0^1 v(x,0)[f(x,0)-f_I]\,dx$$
$$\frac{\partial\mathcal{L}}{\partial f_I}k = \gamma\int_0^1 \partial_x f_I\partial_x k\,dx + \int_0^1 \mu(x,0)k\,dx = -\gamma\int_0^1 \partial_{xx} f_I k\,dx + \int_0^1 \mu(x,0)k\,dx.$$

Choosing $\mu_0(x) = \mu(x,0)$, the first order optimality conditions read

$$\partial_t f - \partial_{xx} f = g(x,t), \qquad f(x,0) = f_I,\ \partial_x f|_{x=0,1} = 0 \tag{3.5a}$$
$$-\partial_t\mu - \partial_{xx}\mu + \alpha f\delta(x-p(t)) = 0, \qquad \mu(x,T) = 0,\ \ \partial_x\mu|_{x=0,1} = 0 \tag{3.5b}$$
$$\gamma\partial_{xx} f_I = \mu(x,0), \qquad \partial_x f_I|_{x=0,1} = 0. \tag{3.5c}$$

3.3.1 Numerical Algorithms

To numerically solve the optimality conditions (3.5a), (3.5b), we discretise space and time using steps Δx and Δt, respectively and write

$$f_k^j = f(k\Delta x, j\Delta t),\ \ \mu_k^j f(k\Delta x, j\Delta t),\ \ \text{etc.} \tag{3.6}$$

For both equations, we use the implicit-explicit scheme presented in Section 2.5. To determine the f_I, we employ a standard gradient descent scheme, cf. [86]. Starting with an initial guess f_I^0, each step in this method consists of

1. Solve (3.5a) with $f_I = f_I^j$ and obtain f^{j+1}
2. Solve (3.5b) with $f = f^{j+1}$ and obtain μ^{j+1}
3. Perform the update by solving for f_I^{j+1}

$$f_I^{j+1} = f_I^j - \tau\left[\gamma\partial_{xx}(f_I)^{j+1} - \mu_k^{j+1}\right],$$

where τ is a given damping parameter. If $\gamma > 0$, we employ an implicit Euler scheme to perform the update. This procedure is repeated until the desired accuracy or the maximum number of iterations is reached.

3.3.2 Examples

In this Subsection, we present several numerical examples. We use artificial data created by the algorithm described in Section 2.5, with $\Delta t = 10^{-3}$ and $\Delta x = 10^{-3}$. In the first example, we use the same space and time discretisation in the reconstruction algorithm to test if, under optimal conditions, it converges to the correct solution. To avoid *inverse crimes*, i.e. to avoid exceptionally good results obtained when the same code is used to create artificial data as to perform the reconstruction, cf. [111], we shall in the next example use a different time and space discretisation in the reconstruction. We chose $\Delta t = 8.3 \cdot 10^{-4}$, $\Delta x = 8.3 \cdot 10^{-4}$ for this and all subsequent examples. The damping parameter is chosen as $\tau = 0.01$. We use the following 'true' initial datum

$$f_I^{\text{true}} = 711.1x^3 - 995.5x^2 + 284.4x.$$

As initial guess for the gradient descent scheme we take

$$f_I^{\text{guess}} = 0.8(711.1(x + 0.02)^3 - 995.5(x + 0.02)^2 + 284.4(x + 0.02)).$$

For both functions the corresponding prices are shown in Fig. 3.1. The assimilation interval will always be $[0, 0.1]$ and we use the reconstructed initial datum to forecast the price in $[0.1, 0.2]$.

Example 1: Perfect Observations

The aim of this experiment is to test the implementation of the reconstruction scheme and its convergence to the 'true' solution. As this convergence may become arbitrarily slow, we choose a large number of iteration steps, i.e. 4000. In Fig. 3.2, the results are shown. The algorithms obviously converges, however the convergence becomes very slow after approximately 1200 iterations. This reflects the linear convergence behaviour of gradient-type methods.

Example 2: Inverse Crime

Next we repeat the experiment from example 1, however this time with a different time and space discretisation for the reconstruction algorithm to avoid the so-called inverse

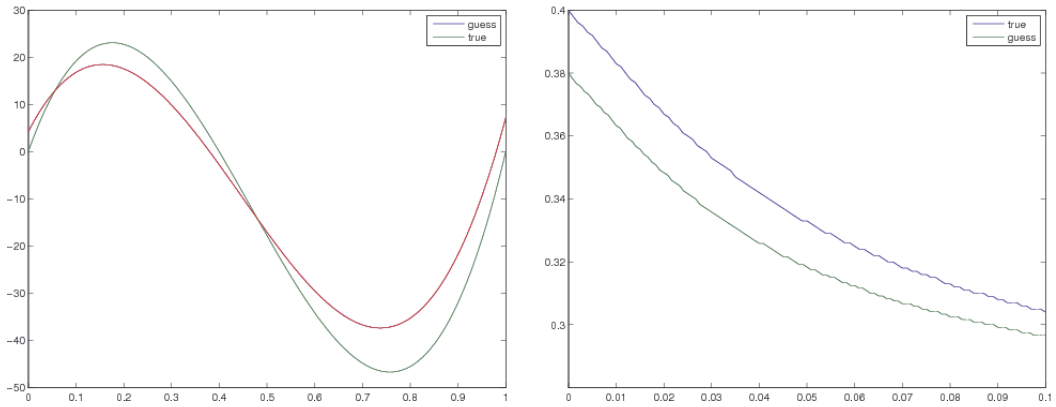

Figure 3.1: The 'true' $(711.1x^3 - 995.5x^2 + 284.4x)$ and perturbed initial datum $(0.8(711.1(x+0.02)^3 - 995.5(x+0.02)^2 + 284.4(x+0.02)))$ and the corresponding prices

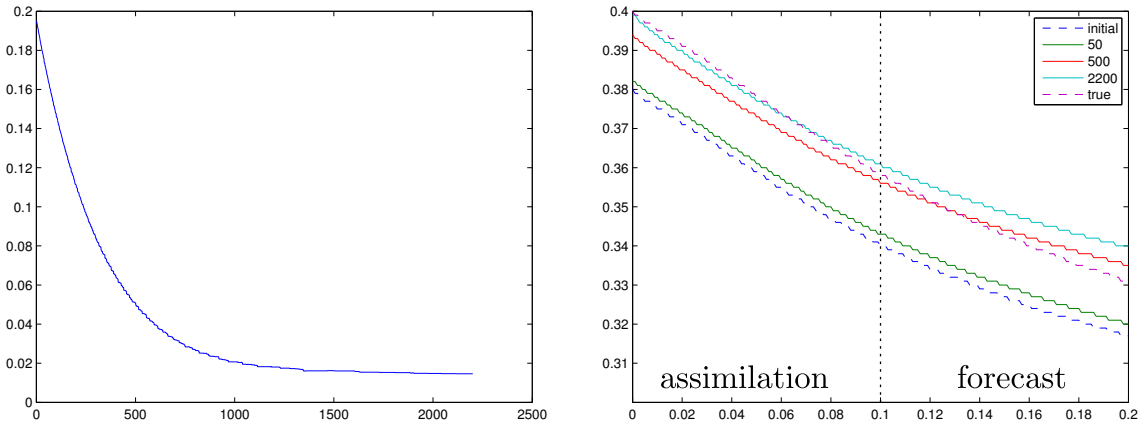

Figure 3.2: Example 1: L^2-Error between 'true' and reconstructed price (left) and reconstructed and forecasted price for different number of iterations (right).

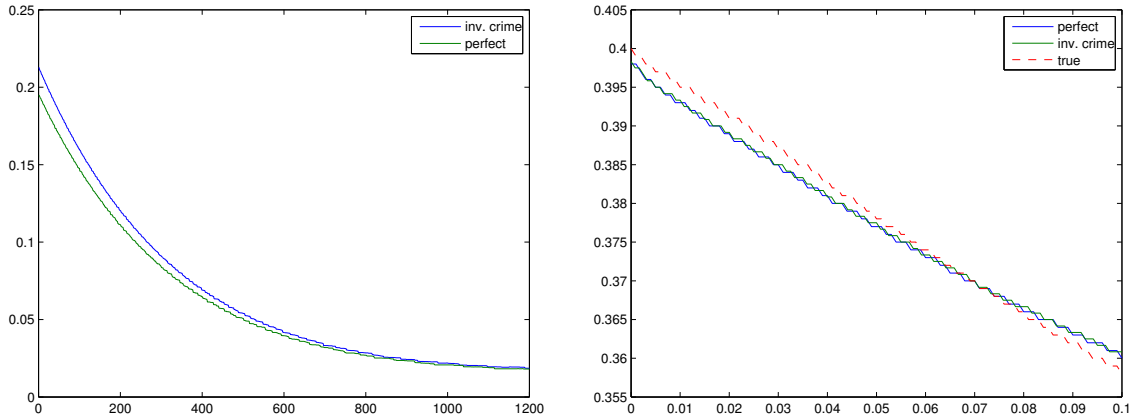

Figure 3.3: Example 2: L^2-Error between 'true' and reconstructed price, with and without different space- and time discretisations (left), the corresponding reconstructed prices (right).

crime explained above. We perform 1200 iterations. The results are shown in Fig. 3.3. As expected, the results are not as good as in Example 1, however, we still obtain very good convergence towards the 'true' solution.

Example 3: Noisy Observations

In this example, we examine the influence of noise in the measurements. We perturb the data by 0, 5, 10 and 20 percent noise, measured in the L^2-norm. The results are depicted in Fig. 3.4. For small noise levels, the convergence is basically equal to the case without noise. This is due to the strong smoothing effects of the optimality conditions. However, as the noise level increases, its effect, and thus the error in the reconstructed price, becomes stronger.

Example 4: Imperfect Observations

In this final example we examine the case in which the price measurements are not given at every discrete time step point in the assimilation window. As expected, the rate of convergence degrades the more data point are removed.

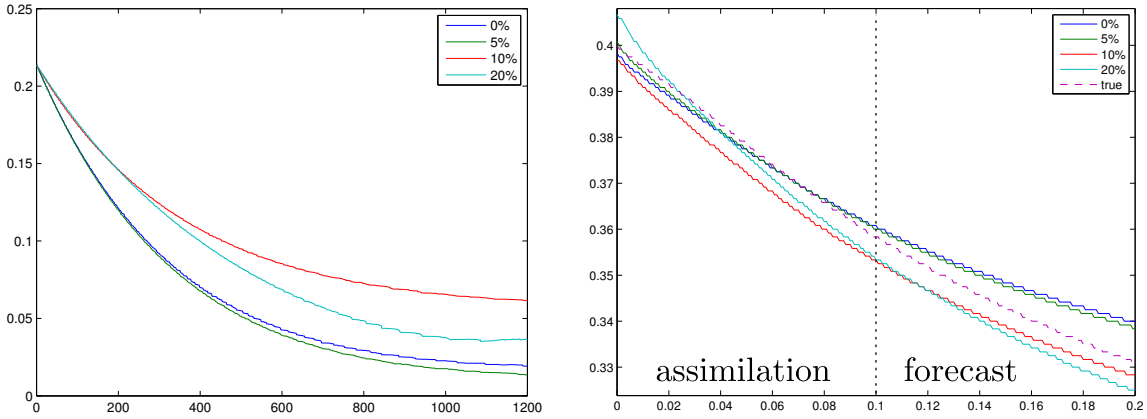

Figure 3.4: L^2-Error between 'true' and reconstructed price for 0, 5 and 10 and 20 percent noise (left), corresponding reconstructed prices (right).

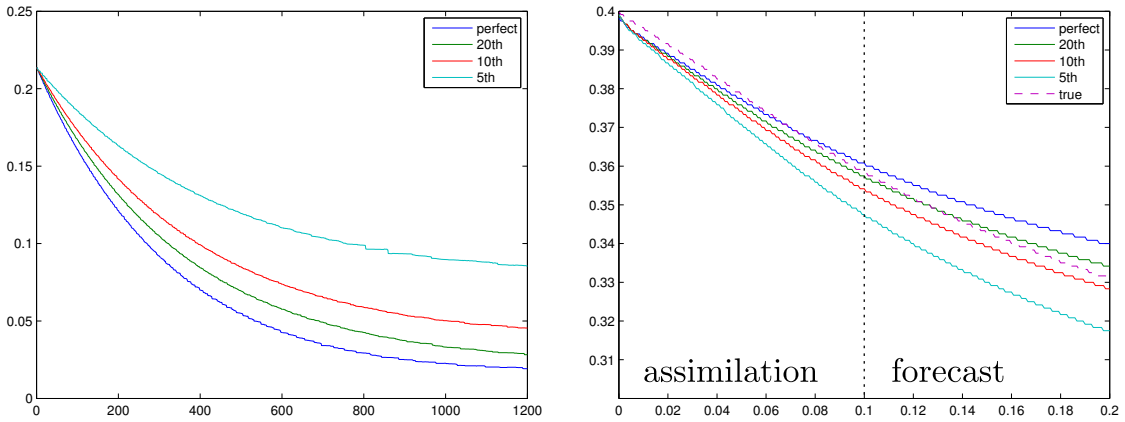

Figure 3.5: L^2-Error between 'true' and reconstructed price for perfect data and every 20th, 10th and 5th data point removed (left), corresponding reconstructed prices (right).

Part II

Crowd Motion

Chapter 4

The Hughes' model for pedestrian flow: The one-dimensional case

In this Chapter we shall analyse a model introduced by R. L. Hughes in 2002 [54]. Hughes' model treats human crowds as "thinking" fluids and has been applied to diverse scenarios like the Battle of Agincourt and the annual Muslim Hajj [55]. It is given by

$$\rho_t - \operatorname{div}(\rho f^2(\rho)\nabla\phi) = 0, \tag{4.1a}$$

$$|\nabla\phi| = \frac{1}{f(\rho)}. \tag{4.1b}$$

Here x denotes the position variable with $x \in \Omega$, a bounded domain in $\mathbb{R}^d$ with smooth boundary $\partial\Omega$, $t \geq 0$ is time and $\rho = \rho(x,t)$ is the crowd density. The function $f = f(\rho)$ is given by $f(\rho) = 1 - \rho$, modelling the existence of a maximal density of individuals which can be normalized to 1 by a simple scaling. System (4.1) is supplemented with the following boundary conditions for ϕ

$$\phi(x,t) = 0, \qquad x \in \partial\Omega,\ t \geq 0 \tag{4.2}$$

and the initial condition

$$\rho(x,0) = \rho_I(x) \geq 0. \tag{4.3}$$

We shall be more precise about the boundary conditions for ρ and give a more detailed interpretation of the model in the next section.

Note that if the term $\frac{1}{f(\rho)}$ in (4.1b) is replaced by 1, the system decouples and (4.1a) reduces to a non-linear conservation law with discontinuous flux. This type of equation

has already been analysed and simulated, cf. [56, 60]. Even though Hughes' system (4.1) shares some features with this class of equations it is methodologically much more challenging. This is due to the non-linearity of the eikonal equation (4.1b) as well as the implicit time dependence of the potential $\nabla\phi$ in (4.1a). In fact, for the unique viscosity solution ϕ of the eikonal equation, no more regularity than Lipschitz continuity can be expected. In this Chapter we present an existence and uniqueness theory for a regularised version of (4.1) in one space dimension. Additionally, we discuss the behaviour of simple solutions for the original system (4.1) and validate these results numerically.

Numerical simulations are already available in literature, see Ling et al. [76]. Their approach does not cover the case of discontinuous flux inside the computational domain. Nevertheless we follow the iterative procedure presented in [76], i.e. first solve the Eikonal equation (4.1b) then the conservation law (4.1a). Numerical methods for non-linear conservation laws with discontinuous flux can be found in literature, e.g. [108]. We will use the approach presented by J. Towers for our numerical simulations. Note that equation (4.1a) is similar to the Lighthill-Witham-Richards traffic flow model [75, 93], and similar numerical schemes can be used. Various approaches can be found in the literature, e.g. [15, 14, 115, 116]. These schemes are usually based on numerical methods for non-linear conservation laws, for a general introduction we refer to [72, 107] and the references therein.

The chapter is organized as follows: In the remaining part of the introduction, we shall explain the model in more detail (Subsection 4.1) and present regularised versions (Subsection 4.2). In Section 4.3, we prove existence and uniqueness of entropy solutions for a regularised model and in Section 4.4 we will analyse some special cases for the non regularised problem and compare these results with our numerical simulations.

4.1 Hughes' model

We start with a brief motivation of Hughes' model (4.1) (for further details see [54]). The density of individuals $\rho = \rho(x,t)$ satisfies the continuity equation

$$\rho_t + \operatorname{div}(\rho V) = 0, \tag{4.4}$$

and we use the following 'polar decomposition' notation for the velocity field $V(x,t)$

$$V(x,t) = |V(x,t)|Z(x,t), \quad |Z(x,t)| = 1. \tag{4.5}$$

In order to prescribe a logistic dependency of $|V|$ with respect to ρ we choose the classical linear expression

$$|V(x,t)| = 1 - \rho.$$

As for the directional unit vector $Z(x,t)$, we assume it to be parallel to the gradient of the potential $\phi(x,t)$. Such potential is determined by solving the eikonal equation in (4.1). The potential ϕ rules the common sense of the task (the task is represented by the boundary $\partial\Omega$). More precisely, the pedestrians tend to minimize their estimated travel time to the target. In a naive way, this could be modelled by prescribing the eikonal equation

$$|\nabla\phi| = 1, \qquad \phi|_{\partial\Omega} = 0,$$

which has the unique semi-concave solution $\phi(x) = \mathrm{dist}(x, \partial\Omega)$ at least in the case of a convex domain Ω. However, it is reasonable to assume that individuals temper their estimated travel time by avoiding extremely high densities, i. e.

$$|\nabla\phi| = \frac{1}{1-\rho}, \qquad \phi|_{\partial\Omega} = 0, \tag{4.6}$$

which implies a 'density driven' rearrangement of the level sets of ϕ. This leads to $Z(x,t) = \frac{\nabla\phi(x,t)}{|\nabla\phi(x,t)|} = (1-\rho)\nabla\phi$ and therefore the continuity equation in (4.1) is justified.

4.2 An attempt to a mathematical theory: approximations

A successful attempt to develop a mathematical theory for the model (4.1) has never been carried out so far. The non-linearity with respect to ρ in the continuity equation forces using the notion of entropy solutions for scalar conservation laws, as it is well known that weak L^∞ solutions to such kind of equations are in general not unique. On the other hand, the vector field $\nabla\phi$ may clearly develop discontinuities in subsets of Ω which may vary in time.

In general, the subsets of discontinuity of $\nabla\phi$ depend on ρ non-linearly and non–locally. This may be seen by simple examples in one space dimension. Moreover, the presence of the term $1-\rho$ in the right-hand-side of the eikonal equation renders the problems even more difficult, because of the possible blow–up of $|\nabla\phi|$ as ρ approaches the density $\rho = 1$.

A full understanding of the model is highly non-trivial, even in one space dimension, where the model can be decoupled by solving the eikonal equation by integration.

In order to overcome such difficulties, we propose reasonable approximations to the Hughes' model (4.1), basically consisting of a regularization of the potential to avoid the discontinuity of $|\nabla\phi|$. At a first glance, a very natural way to approximate the equation for the potential would be simply adding a small 'viscosity', i. e.

$$-\delta\Delta\phi + |\nabla\phi|^2 = \frac{1}{f(\rho)^2}, \qquad \delta > 0.$$

Such an approximation still has the drawback of (possibly) producing a blow up of the right hand side when the density approaches the overcrowding value $\rho = 1$. This problem can be bypassed considering instead

$$-\delta\Delta\phi + f(\rho)^2|\nabla\phi|^2 = 1, \qquad \delta > 0. \tag{4.7}$$

On the other hand, the development of a satisfactory existence and uniqueness theory by using the coupling (4.7) is seriously complicated by the presence of the density dependent coefficient multiplying the Hamilton-Jacobi term $|\nabla\phi|^2$.

The model for which we shall develop a full existence and uniqueness theory uses the following elliptic regularization of the eikonal equation in (4.1), namely

$$-\delta_1\Delta\phi + |\nabla\phi|^2 = \frac{1}{(f(\rho)+\delta_2)^2}, \quad \delta_1, \delta_2 > 0. \tag{4.8}$$

The sign in front of δ_1 (δ in the alternative equation (4.7)) is chosen such that we would recover the unique viscosity solution in a possible limit $\delta_1 \to 0$. The second order term in (4.8) is meant to smooth the potential ϕ in order to avoid discontinuities for $|\nabla\phi|$. The elliptic operator in (4.8) is a classical elliptic Hamilton-Jacobi operator, and it is therefore easier to deal with compared to the one in (4.7). On the other hand equation (4.8) contains one further approximation on the right-hand-side which can be motivated as follows.

Without the elliptic regularization, the potential ϕ in (4.8) would satisfy

$$|\nabla\phi| = \frac{1}{(1-\rho+\delta_2)} \tag{4.9}$$

Then, the polar decomposition of the velocity field introduced in (4.4) reads in this case

$$\begin{aligned} &V = |V|Z, \quad |Z| = 1 \\ &|V| = f(\rho)^2|\nabla\phi| = \frac{f(\rho)^2}{\delta_2 + f(\rho)} = \frac{(1-\rho)^2}{\delta_2 + (1-\rho)}, \quad Z = \frac{\nabla\phi}{|\nabla\phi|}. \end{aligned} \tag{4.10}$$

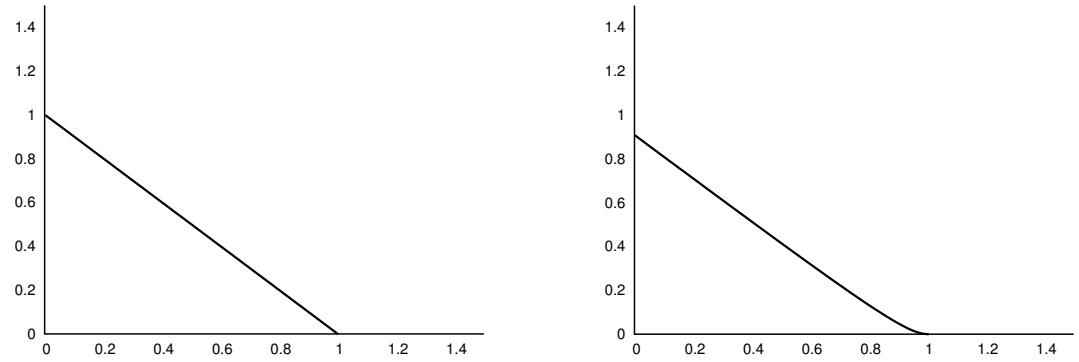

Figure 4.1: Comparison between the scalar 'logistic' speed $|V|$ of the pedestrian in Hughes' model (4.1) (left) and the model with elliptic coupling (4.8)

The profile of $|V|$ as a function of ρ in (4.10) has essentially the same properties of the logistic function $|V|(\rho) = 1 - \rho$ of the original Hughes's model, except that the vacuum at $\rho = 1$ is achieved with a zero derivative and the maximal velocity is slightly penalized, i. e. $|V|_{max} = 1/1 + \delta_2$ instead of $|V|_{max} = 1$ of the original model (cf. Figure 4.1).

As for the unit vector Z, which is parallel to $\nabla\phi$, the only difference with the original model is that individuals 'sense' the target as the density reaches the maximum value $\rho = 1$. In this case $|\nabla\phi| = 1/\delta_2$, i. e. the slope of $\nabla\phi$ is very high in absolute value (δ_2 is thought as a small parameter), but not infinite as in the original model. On the other hand, when $\rho = 1$, $|V|$ vanishes, and therefore the above mentioned difference is not effective (individuals do not move at all when $\rho = 1$!).

We shall first cover the one dimensional existence and uniqueness theory for the regularised model with elliptic coupling (4.8) introduced in the previous subsection, more precisely we shall study the model system

$$\begin{cases} \rho_t - (\rho f^2(\rho)\phi_x)_x = 0 \\ -\delta_1\phi_{xx} + |\phi_x|^2 = \dfrac{1}{(f(\rho) + \delta_2)^2}. \end{cases} \tag{4.11}$$

As the continuity equation in (4.11) features non-linear convection, we shall address the existence and uniqueness theory in the framework of weak entropy solutions, cf. for instance [62]. The results are contained in Section 4.3. More precisely, the notion of solution is stated in Definition 4.3.1, the existence result is provided in Theorem 4.3.10, and the uniqueness result is proven in Theorem 4.3.12.

The problem (4.11) is posed on the bounded interval $x \in [-1, 1]$ with homogeneous

Dirichlet boundary conditions. We shall follow the approach by Bardos et al. [17] (see also [32, 7, 79]) to recover suitable boundary conditions for a scalar conservation law. This aspect is explained at the beginning of the next section.

4.3 The regularised model: existence and uniqueness theory

In this section we establish our existence and uniqueness results for the regularised Hughes' model system (4.11) with $f(\rho) = (1 - \rho)$. For future use we denote

$$g(\rho) := \rho f(\rho)^2.$$

System (4.11) is coupled with the initial condition

$$\rho(x, 0) = \rho_I(x) \geq 0, \tag{4.12}$$

and with the Dirichlet boundary conditions

$$\min_{k \in [0, \operatorname{Tr}\rho]} \{g(\operatorname{Tr}(\rho)) - g(k)\} = 0, \tag{4.13}$$

$$\phi(\pm 1, t) = 0. \tag{4.14}$$

Here $\operatorname{Tr}\rho$ denotes the trace of ρ on the boundary. More precisely,

$$\operatorname{Tr}\rho(-1, t) = \lim_{x \to -1^+} \rho(x, t), \qquad \operatorname{Tr}\rho(1, t) = \lim_{x \to 1^-} \rho(x, t).$$

It was originally proven in [17] that (4.13) is the correct way to pose Dirichlet boundary conditions for a scalar conservation law, mainly for two reasons: first, (4.13) comes as a natural condition from the vanishing viscosity limit of solutions with zero Dirichlet boundary data; second, (4.13) encloses the natural interplay between the boundary datum and the value of the solution which is transported via characteristics in the linear case (the boundary datum needs to be posed only if characteristics at the boundary are directed towards the interior of the domain). The boundary condition provided in [17] assumes the simplified form (4.13) since we shall deal with non-negative solutions and due to a trivial monotonicity property of the potential ϕ (cf. Lemma 4.3.11 below). We remark here that the boundary condition (4.13) reduces to

$$g(\operatorname{Tr}\rho) \geq g(k) \qquad \text{on} \quad x = \pm 1, \quad \text{for all } k \in [0, \operatorname{Tr}\rho],$$

which expresses the fact that the allowed densities on the boundary are those for which the function g is *non-decreasing*. A deeper understanding of the boundary conditions for nonlinear conservation laws in one space dimension can be also found in [32].

We shall prove that the system (4.11) has a unique solution (ρ, ϕ) in a sense made precise by the following definition. For the density component ρ we will use the classical notion of entropy solutions originally introduced by Kružkov in [62] and adapted to boundary value problems by Bardos et al. in [17].

Definition 4.3.1 (Entropy Solution)**.** *Let $\rho_I \in BV([-1,1])$. A couple (ρ, ϕ) is a weak* entropy *solution to the system* (4.11) *if*

- $\rho \in BV([-1,1]\times[0,T)) \cap L^\infty([-1,1]\times[0,T))$
- $\phi \in W^{2,\infty}([-1,1])$
- ρ *and* ϕ *satisfy the inequality*

$$\iint\limits_{\Omega_T} |\rho - k|\psi_t \, dxdt + \int_{-\infty}^{\infty} \rho_I \psi_0 dx - \iint\limits_{\Omega_T} \operatorname{sgn}(\rho - k)[g(\rho) - g(k)]\psi_x \phi_x \, dxdt$$
$$+ \iint\limits_{\Omega_T} \operatorname{sgn}(\rho - k) g(k) \psi \phi_{xx} dxdt - \operatorname{sgn}(k) \int_0^T [g(\operatorname{Tr}\rho) - g(k)]\phi_x \psi|_{x=\pm 1} dt \geq 0, \tag{4.15}$$

  for every Lipschitz continuous test function ψ on $[-1,1]\times[0,T)$ having compact support.

- ϕ *and* ρ *satisfy the second equation in* (4.11) *almost everywhere in x and t.*

As usual in the context of conservation laws, we shall approximate the targeted model (4.11) via a vanishing viscosity approach, namely we shall work on the system

$$\rho_t - (\rho f^2(\rho)\phi_x)_x = \varepsilon \rho_{xx} \tag{4.16a}$$
$$-\delta_1 \phi_{xx} + |\phi_x|^2 = \frac{1}{(f(\rho) + \delta_2)^2}, \tag{4.16b}$$

for a small $\varepsilon > 0$. System (4.16) is coupled with homogeneous boundary condition

$$\rho(x,t)|_{x=\pm 1} = 0 \qquad \phi(x,t)|_{x=\pm 1} = 0,$$

and the initial condition

$$\rho(x,0) = \rho_I(x).$$

Existence of unique (smooth) solutions to the above regularised problem follow from standard results. For the elliptic coupling see e.g. [64, Chapter 3, Lemma 1.1] and [64, Chapter 3, Thm. 1.2]. For the parabolic approximation we refer to [113, Section 5, Thm. 5.3 and Thm. 5.4]. The proof of this theorem is based on semi group techniques. The strategy is to first linearise the equation to an evolution equation with a linear but time depending operator. Under the given assumptions, it is known that there exists a solution to such an equation (see e.g. [105]). Then, the solution to the non-linear equation in obtained using a fixed-point argument.

In the next subsections we shall first derive suitable a-priori estimates on ϕ and ρ, then we shall recall our notion of entropy solution, and finally prove existence and uniqueness of the limit as $\varepsilon \to 0$.

4.3.1 A Priori Estimates on ϕ and ρ

We shall now derive some a-priori estimates for the elliptic coupling, i.e.

$$\begin{aligned} -\delta_1 \phi_{xx} + \phi_x^2 &= F_{\delta_2}(\rho) := \frac{1}{(\delta_2 + f(\rho))^2} \\ \phi(\pm 1) &= 0. \end{aligned} \tag{4.17}$$

Our strategy is the following: we shall first replace the term $f(\rho)$ by

$$\widetilde{f}(\rho) := \begin{cases} f(\rho) & \text{if} \quad \rho \in [0,1] \\ 0 & \text{otherwise} \end{cases}$$

in order to have the right-hand side $F_{\delta_2}(\rho)$ uniformly bounded and non-degenerate. The result is stated in the Lemmas 4.3.2 and 4.3.3. Then, we use the estimates on the elliptic coupling in order to prove that the density ρ satisfies $\rho \in [0,1]$, see Lemma 4.3.4. Since the solution to the $\widetilde{f}$-modified system coincides with the one to (4.11), by uniqueness of smooth solutions to the regularised problem (4.11) we conclude that the estimates for ρ and ϕ hold without replacing f by $\widetilde{f}$. In order to simplify the notation, we shall drop the tilde symbol above f.

Let us introduce the *Hopf–Cole* transformation

$$\psi(x,t) := e^{-\frac{\phi(x,t)}{\delta_1}}, \tag{4.18}$$

which implies

$$\psi_x = -\frac{\psi\phi_x}{\delta_1}, \quad \psi_t = -\frac{\psi\phi_t}{\delta_1}, \quad \phi_x = -\delta_1\frac{\psi_x}{\psi}, \quad \phi_t = -\delta_1\frac{\psi_t}{\psi} \tag{4.19}$$

$$\psi_{xx} = -\frac{\phi_{xx}\psi}{\delta_1} - \frac{\phi_x\psi_x}{\delta_1} = \frac{\psi}{\delta_1^2}\left(-\delta_1\phi_{xx} + \phi_x^2\right) = \frac{\psi}{\delta_1^2}F_{\delta_2}(\rho). \tag{4.20}$$

Therefore, ψ satisfies

$$\begin{cases} \delta_1^2\psi_{xx} = \psi F_{\delta_2}(\rho) \\ \psi(\pm 1) = 1. \end{cases} \tag{4.21}$$

As a first estimate, we prove that ψ is uniformly bounded in $H^1(\Omega)$ and in $L^\infty(\Omega)$.

Lemma 4.3.2. *There exists a constant $C > 0$ depending only on δ_1 and δ_2 such that*

$$\|\psi\|_{H^1([-1,1])} \leq C, \qquad \|\psi\|_{L^\infty([-1,1])} \leq C, \qquad \|\psi_{xx}\|_{L^\infty([-1,1])} \leq C. \tag{4.22}$$

Proof. Let us introduce the variable

$$\widetilde{\psi} := \psi - 1,$$

which satisfies

$$\begin{cases} \delta_1^2\widetilde{\psi}_{xx} = \widetilde{\psi}F_{\delta_2}(\rho) + F_{\delta_2}(\rho) \\ \widetilde{\psi}(\pm 1) = 0. \end{cases} \tag{4.23}$$

Multiplication of (4.23) by $\widetilde{\psi}$ and integration over $[-1, 1]$ leads to (after integration by parts)

$$-\delta_1^2\int \widetilde{\psi}_x^2 dx = \int \widetilde{\psi}^2 F_{\delta_2}(\rho)dx + \int \widetilde{\psi}F_{\delta_2}(\rho)dx.$$

Since

$$\frac{1}{(1+\delta_2)^2} \leq F_{\delta_2}(\rho) \leq \frac{1}{\delta_2^2}, \tag{4.24}$$

by a trivial use of Young's inequality we get

$$\int \widetilde{\psi}_x^2 dx + \int \widetilde{\psi}^2 dx \leq C,$$

for a constant C depending on δ_1 and δ_2. Sobolev's inequality then implies

$$\|\psi\|_{L^\infty} \leq C.$$

The last assertion in (4.22) follows by the equation (4.21). □

Next we prove that ψ is non-negative on $[-1,1]$ and uniformly bounded from below by a positive constant, which implies the desired estimates on the ϕ variable.

Lemma 4.3.3. *There exists a constant $C > 0$ such that*

$$\psi(x,t) \geq C \tag{4.25}$$

for all $(x,t) \in [-1,1] \times [0,+\infty)$. Moreover,

$$\|\phi\|_{H^1([-1,1])} \leq C, \qquad \|\phi\|_{L^\infty([-1,1])} \leq C, \qquad \|\phi_{xx}\|_{L^\infty([-1,1])} \leq C. \tag{4.26}$$

Proof. Let us consider the original equation (4.17) satisfied by ϕ. We have

$$\delta_1 \phi_{xx} + \frac{1}{\delta_2^2} \geq \delta_1 \phi_{xx} + F_{\delta_2}(\rho) = \phi_x^2 \geq 0,$$

which can be written as

$$\left(\delta_1 \phi + \frac{|x|^2}{2\delta_2}\right)_{xx} \geq 0.$$

Therefore the function $\delta_1\phi + \frac{|x|^2}{2\delta_2}$ attains its maximum at the boundary, ϕ is bounded from above and $\psi = e^{-\phi/\delta_1}$ is bounded away from zero. The statements (4.26) follow as a consequence of (4.25) and of (4.19)-(4.20). □

We conclude by proving that ρ is always bounded above by the maximal density $\rho = 1$.

Lemma 4.3.4 (Boundedness of ρ)**.** *Assume that $\rho_I \leq 1$. Then the solution to* (4.16a) *with $f(\rho) = (1-\rho)$ satisfies $\rho(x,t) \leq 1$ for all $(x,t) \in [-1,1] \times [0,+\infty)$.*

Proof. We first define the function

$$\eta(\rho) = \begin{cases} 0 & \rho \leq 0, \\ \frac{\rho^2}{4\gamma} & 0 < \rho \leq 2\gamma, \\ \rho - \gamma & \rho > 2\gamma. \end{cases} \tag{4.27}$$

and use it to approximate $(\rho-1)_+$ (the positive part of $(\rho-1)$). Here $\gamma > 0$ is a small parameter. Our goal is to show that this positive part, being zero at $t = 0$, does not

increase. We consider

$$\begin{aligned}
\frac{d}{dt}\int \eta(\rho-1)\,dx &= \int \eta'(\rho-1)(\varepsilon\rho_x + (\rho(1-\rho)^2\phi_x)_x\,dx \\
&= -\varepsilon\int \eta''(\rho-1)\rho_x^2\,dx + \varepsilon\eta'(\rho-1)\rho_x|_{x=\pm1} \\
&\quad - \int_{0\le(\rho-1)\le\gamma} \eta''(\rho-1)\rho(1-\rho)^2\rho_x\phi_x\,dx + \eta'(\rho-1)\rho(1-\rho)\phi_x|_{x=\pm1} \\
&\le -2\varepsilon\int \eta''(\rho-1)\rho_x^2\,dx - C_\varepsilon\int_{0\le(\rho-1)\le\gamma} \eta''(\rho-1)\rho^2(1-\rho)^4|\phi_x|^2\,dx \\
&\le -2\varepsilon\int \eta''(\rho-1)\rho_x^2\,dx - C_{\varepsilon,\delta}\gamma^3(1+\gamma)^2,
\end{aligned}$$

where $C_{\varepsilon,\delta}$ depends on ε, δ_1 and δ_2. Here, we employed Young's inequality and the Dirichlet boundary conditions. Furthermore we used the ε-independent L^∞ bound on ϕ_x we obtained in Lemma 4.3.3. Letting $\gamma\to 0$, we infer

$$\frac{d}{dt}\int(\rho-1)_+\,dx = \lim_{\gamma\to0} -\varepsilon\int \eta_\gamma''(\rho-1)|\rho_x|^2\,dx \le 0,$$

and thus the integral is decreasing in time. As $(\rho-1)_+$ is a positive function and zero at $t=0$, we conclude that is stays zero for all times and thus that ρ is always bounded by 1. □

Note that using the same technique, but approximating the negative part of ρ we also obtain that the solution is almost everywhere non-negative (since $\rho_I \ge 0$).

BV estimate on ρ

We are now ready to prove the crucial BV estimate on ρ which serves as a tool to get compactness in the limit as $\varepsilon\to0$. Furthermore, it will guarantee the existence of $\operatorname{Tr}\rho$, see [17, Lemma 1]. Let us start with estimating the L^1 norm of ρ_x.

Lemma 4.3.5. *Suppose $\rho_I \in W^{1,1}([-1,1])$. Then, there exists a constant $C>0$ independent on ε such that*

$$\|\rho_x(t)\|_{L^1(\Omega)} \le (\|(\rho_I)_x\|_{L^1(\Omega)} + C)e^{Ct}$$

for all $t\ge0$.

Before we start the proof let us define an approximation $\eta_\gamma(z)$ of the function $|z|$ as $\gamma \to 0$ such that

$$\begin{aligned} &\eta_\gamma(z) \to |z|, \quad \eta'_\gamma(z) \to \operatorname{sign}(z), \quad \eta'_\gamma(z)z \to |z| \qquad \text{as } \ \gamma \to 0 \\ &\eta'_\gamma(z)z \geq 0, \quad \eta''_\gamma(z) \geq 0 \\ &\eta''_\gamma(z) \leq \mathbf{1}_{[-\gamma,\gamma]}(z)\frac{C}{\gamma} \end{aligned} \tag{4.28}$$

for some constant $C > 0$.

Remark 4.3.6 (Properties of η)**.** *We remark that the definition of η implies the following properties, which shall be often used in the sequel:*

- *All integrals of the form*

$$\int_\Omega \eta''_\gamma(f(x))f(x)^2\,dx \leq \frac{C}{\gamma}\int_{|f(x)|\leq\gamma} f(x)^2\,dx \leq C\gamma|\Omega|$$

  tend to zero as $\gamma \to 0$.

- *Furthermore, with $g \in \mathcal{C}^1(\mathbb{R}_+)$, $f, h \in L^1(\Omega)$, $k \in \mathbb{R} > 0$ we have*

$$\begin{aligned} &\int_\Omega \eta''_\gamma(f(x)-k)(g(f(x))-g(k))h(x)\,dx \\ &\leq \frac{C}{\gamma}\int_{0<|f(x)-k|\leq\gamma} \|g'\|_{L^\infty(\mathbb{R}_+)}|f(x)-k||h(x)|\,dx \\ &\leq \frac{C}{\gamma}\gamma\|g'\|_{L^\infty(\mathbb{R}_+)}\int_{0<|f(x)-k|\leq\gamma} |h(x)|\,dx \to 0, \end{aligned}$$

  as $\gamma \to 0$.

Proof of Lemma 4.3.5. We deduce that

$$\begin{aligned} &\frac{d}{dt}\int \eta_\gamma(\rho_x)dx = \int \eta'_\gamma(\rho_x)\rho_{xt}dx = \int \eta'_\gamma(\rho_x)(g(\rho)\phi_x)_{xx}dx + \varepsilon\int \eta'_\gamma(\rho_x)\rho_{xxx}dx \\ &= \int \eta'_\gamma(\rho_x)(g'(\rho)\rho_x\phi_x)_x + \int \eta'_\gamma(\rho_x)(g(\rho)\phi_{xx})_x - \varepsilon\int \eta''_\gamma(\rho_x)\rho_{xx}^2dx \\ &= -\int \eta''_\gamma(\rho_x)\rho_{xx}g'(\rho)\rho_x\phi_x dx + \int \eta'_\gamma(\rho_x)g'(\rho)\rho_x\phi_{xx}dx \\ &\quad + \int \eta'_\gamma(\rho_x)g(\rho)\phi_{xxx}dx - \varepsilon\int \eta''_\gamma(\rho_x)\rho_{xx}^2dx \\ &\leq -\frac{\varepsilon}{2}\int \eta''_\gamma(\rho_x)\rho_{xx}^2dx + C(\varepsilon)\int \eta''_\gamma(\rho_x)\phi_x^2\rho_x^2dx + C\int|\rho_x|dx + C. \end{aligned} \tag{4.29}$$

Here the last step is justified by the identities (4.19) and (4.20), by (4.25), and by

$$\|\psi_{xxx}(t)\|_{L^1(\Omega)} \leq C\|\rho_x(t)\|_{L^1(\Omega)} + C, \text{ since } \psi_{xxx} = F_{\delta_2}(\rho)\psi_x + \psi F'_{\delta_2}(\rho)\rho_x.$$

The sum of the boundary terms

$$\int \eta'_\gamma(\rho_x)(\varepsilon\rho_{xx} + g'(\rho)\rho_x\phi_x + g(\rho)\phi_{xx})\, d\sigma_x = \int \eta'_\gamma(\rho_x)\rho_t\, d\sigma_x$$

vanishes, as ρ_t is constant along the boundary. Due to Rem. 4.3.6, the second term on the right hand side of (4.29) vanishes as $\gamma \to 0$, therefore we obtain the desired assertion in the limit (after integration with respect to time). □

Before estimating the L^1 norm of ρ_t we have the following technical lemma.

Lemma 4.3.7. *There exists a constant $C > 0$ independent of ε and of t such that*

$$\|\psi_t(t)\|_{L^\infty(\Omega)} \leq C\|\rho_t(t)\|_{L^1(\Omega)} \tag{4.30}$$

$$\|\psi_{xxt}(t)\|_{L^1(\Omega)} \leq C\|\rho_t(t)\|_{L^1(\Omega)} \tag{4.31}$$

$$\|\psi_{xt}(t)\|_{L^\infty(\Omega)} \leq C\|\rho_t(t)\|_{L^1(\Omega)}. \tag{4.32}$$

Proof. We start with the proof of estimate (4.30). Differentiation of (4.21) with respect to time yields

$$\psi_{xxt} = \frac{1}{\delta_1^2}\left(\psi_t F_{\delta_2}(\rho) + \psi F'_{\delta_2}(\rho)\rho_t\right). \tag{4.33}$$

Next we multiply (4.33) by ψ_t and integrate over $[-1, 1]$. Using the fact that $\psi_t = 0$ at the boundary, we integrate by parts to obtain

$$-\delta_1^2 \int \psi_{xt}^2 dx = \int F_{\delta_2}(\rho)\psi_t^2 dx + \int F'_{\delta_2}(\rho)\rho_t\psi\psi_t dx.$$

In view of (4.24) and Lemma 4.3.3 we can find a constant $C = C(\delta_1, \delta_2) > 0$ such that

$$\|\psi_t(t)\|^2_{H^1(\Omega)} \leq C\|\psi_t(t)\|_{L^\infty(\Omega)}\|\rho_t(t)\|_{L^1(\Omega)},$$

and the Sobolev inequality $\|\psi_t(t)\|_{L^\infty(\Omega)} \leq \|\psi_t(t)\|_{H^1(\Omega)}$ implies the assertion.

The inequality (4.31) follows by a direct use of the equation (4.21) and by (4.30). Finally, the last statement (4.32) follows from the inequality

$$\|\psi_{xt}(t)\|_{L^\infty(\Omega)} \leq \|\psi_{xxt}(t)\|_{L^1(\Omega)},$$

which is a consequence of the fact that $\int \psi_{xt} dx = \psi_t(1, t) - \psi_t(-1, t) = 0$ and that every $W^{1,1}$ function in one space dimension admits an absolutely continuous representant. □

We are now ready to estimate the L^1 norm of the time derivative.

Lemma 4.3.8. *Assuming $\rho_I \in W^{2,1}([-1,1])$ and $\varepsilon > 0$, there exists a constant $C > 0$ independent on ε such that*

$$\|\rho_t(t)\|_{L^1(\Omega)} \leq Ce^{Ct},$$

for all $t \geq 0$.

Proof. Again we consider the approximation η_γ of the absolute value, given by (4.28). We deduce that

$$\begin{aligned}
&\frac{d}{dt}\int \eta_\gamma(\rho_t)dx = \int \eta'_\gamma(\rho_t)\rho_{tt}dx = \int \eta'_\gamma(\rho_t)(g(\rho)\phi_x)_{tx}dx + \varepsilon\int \eta'_\gamma(\rho_t)\rho_{xxt}dx \\
&= \int \eta'_\gamma(\rho_t)(g'(\rho)\rho_t\phi_x)_x + \int \eta'_\gamma(\rho_t)(g(\rho)\phi_{xt})_x - \varepsilon\int \eta''_\gamma(\rho_t)\rho_{xt}^2dx \\
&= -\int \eta''_\gamma(\rho_t)\rho_{xt}g'(\rho)\rho_t\phi_x dx + \int \eta'_\gamma(\rho_t)g'(\rho)\rho_x\phi_{xt}dx \\
&\quad + \int \eta'_\gamma(\rho_t)g(\rho)\phi_{xxt}dx - \varepsilon\int \eta''_\gamma(\rho_t)\rho_{xt}^2dx \\
&\leq -\frac{\varepsilon}{2}\int \eta''_\gamma(\rho_t)\rho_{xt}^2dx + C(\varepsilon)\int \eta''_\gamma(\rho_t)\phi_x^2\rho_t^2dx \\
&\quad + C\|\phi_{xt}(t)\|_{L^\infty(\Omega)}\int |\rho_x|dx + C\int |\phi_{xxt}|dx.
\end{aligned}$$

All boundary terms in the above calculation are zero as ρ_t and thus $\eta'_\gamma(\rho_t)$ is zero on the boundary. The second term on the r.h.s. above vanishes as $\gamma \to 0$. As for the other terms, we can differentiate (4.18) to easily obtain

$$\|\phi_{xt}(t)\|_{L^\infty(\Omega)} \leq C\|\psi_{xt}(t)\|_{L^\infty(\Omega)} + C\|\psi_t(t)\|_{L^\infty(\Omega)} \leq C\|\rho_t(t)\|_{L^1(\Omega)}$$

and

$$\|\phi_{xxt}(t)\|_{L^1(\Omega)} \leq C\|\psi_{xxt}(t)\|_{L^1(\Omega)} + C\|\psi_{xt}(t)\|_{L^1(\Omega)} + C\|\psi_t(t)\|_{L^1(\Omega)} \leq C\|\rho_t(t)\|_{L^1(\Omega)}.$$

Therefore, integration with respect to time and Lemma 4.3.5 results in

$$\|\rho_t(t)\|_{L^1(\Omega)} \leq (\|(\rho(0)_t\|_{L^1(\Omega)} + C)e^{Ct},$$

for all $t \geq 0$. Using the fact that ρ_I is in $W^{2,1}(\Omega)$ and that ε is bounded, we can use equation (4.16a) to estimate

$$\|\rho_t(0)\|_{L^1(\Omega)} \leq \|g'(\rho_I)\phi_x(t)\|_{L^\infty(\Omega)}\|(\rho_I)_x\|_{L^1(\Omega)} + \varepsilon\|(\rho_I)_{xx}\|_{L^1(\Omega)}.$$

We thus conclude that $\|\rho_t(0)\|_{L^1(\Omega)}$ is bounded as well completing the proof. □

4.3.2 Stability estimates on ϕ

Next, we prove some stability estimates for the elliptic equation (4.17) with respect to the variable ρ. These estimates will be useful later on to prove uniqueness of an entropy solution ρ in the limit.

Given two densities ρ and $\bar{\rho}$, let ϕ and $\bar{\phi}$ solve

$$\begin{aligned} -\delta_1\phi_{xx} + \phi_x^2 &= F_{\delta_2}(\rho), \\ -\delta_1\bar{\phi}_{xx} + \bar{\phi}_x^2 &= F_{\delta_2}(\bar{\rho}), \end{aligned}$$

with boundary conditions $\phi(\pm 1) = \bar{\phi}(\pm 1) = 0$. For both solutions we consider the corresponding Hopf–Cole transformation

$$\psi(x,t) := e^{-\frac{\phi(x,t)}{\delta_1}} \qquad \bar{\psi}(x,t) := e^{-\frac{\bar{\phi}(x,t)}{\delta_1}}.$$

Then we can deduce the following lemma:

Lemma 4.3.9. *There exists a constant $C > 0$ independent on ε and on t such that*

$$\|\phi(t) - \bar{\phi}(t)\|_{L^1(\Omega)} \le C\|\rho(t) - \bar{\rho}(t)\|_{L^1(\Omega)} \tag{4.34}$$

$$\|\phi_{xx}(t) - \bar{\phi}_{xx}(t)\|_{L^1(\Omega)} \le C\|\rho(t) - \bar{\rho}(t)\|_{L^1(\Omega)} \tag{4.35}$$

$$\|\phi_x(t) - \bar{\phi}_x(t)\|_{L^\infty(\Omega)} \le C\|\rho(t) - \bar{\rho}(t)\|_{L^1(\Omega)}. \tag{4.36}$$

Proof. Let us multiply equation

$$\delta_1^2(\psi_{xx} - \bar{\psi}_{xx}) = (\psi - \bar{\psi})F_{\delta_2}(\rho) + \bar{\psi}(F_{\delta_2}(\rho) - F_{\delta_2}(\bar{\rho})) \tag{4.37}$$

by $\eta_\gamma'(\psi - \bar{\psi})$, with η_γ given by (4.28) and integrate over $[-1,1]$. Integration by parts implies

$$\begin{aligned} -\delta_1^2 &\int (\psi_x - \bar{\psi}_x)^2 \eta_\gamma''(\psi - \bar{\psi})dx \\ &= \int (\psi - \bar{\psi})\eta_\gamma'(\psi - \bar{\psi})F_{\delta_2}(\rho)dx + \int \bar{\psi}\eta_\gamma'(\psi - \bar{\psi})[F_{\delta_2}(\rho) - F_{\delta_2}(\bar{\rho})]dx. \end{aligned}$$

We use the properties of η_γ and (4.24) to obtain, as $\gamma \to 0$

$$C(\delta)\int |\psi - \bar{\psi}|dx \le \int F_\delta(\rho)|\psi - \bar{\psi}|dx \le \int \bar{\psi}|F_\delta(\rho) - F_\delta(\bar{\rho})|dx \le C\int |\rho - \bar{\rho}|dx.$$

Next we can deduce (4.34) by using the Hopf–Cole transformation as usual. To prove (4.35), multiply (4.37) by $\operatorname{sign}(\psi_{xx} - \bar{\psi}_{xx})$ and integrate over $[-1,1]$ to obtain

$$\delta_1^2 \int |\psi_{xx} - \bar{\psi}_{xx}|dx \le C\int |\psi - \bar{\psi}|dx + C\int |\rho - \bar{\rho}|dx.$$

Next we obtain (4.35) by using (4.34) and passing to the variable ϕ. Inequality (4.36) follows by the Sobolev inequality as at the end of the proof of Lemma 4.3.7. □

4.3.3 The limit as $\varepsilon \to 0$

Our next goal is to study the behaviour of the solution $(\rho^\varepsilon, \phi^\varepsilon)$ to the system (4.16) as the parameter ε tends to zero. Using Lemma 4.3.5 and Lemma 4.3.8 we know that ρ^ε is in the space of functions having bounded variation $BV(\Omega)$. Therefore, we can employ the classical Helly's theorem on strong L^1–compactness of functions with bounded BV–norm, cf. [41] for instance. Thus, ρ^ε has a strong limit in L^1 up to subsequences. As for the ϕ variable, since ρ_x is uniformly estimated in L^1, differentiating the elliptic equation with respect to x implies that ϕ^ε_{xxx} is uniformly bounded in L^1 and therefore ϕ^ε_{xx} is strongly compact in L^1. Denoting by (ρ, ϕ) the limit $\varepsilon \to 0$ of $(\rho^\varepsilon, \phi^\varepsilon)$, as the convergence is strong in L^1 and due to the estimates on ϕ proven in subsection 4.3.1, it is immediately clear that ϕ solves the second equation in (4.11) and ρ is a weak solution of

$$\rho_t - (\rho f^2(\rho)\phi_x)_x = 0. \tag{4.38}$$

In the remainder of this section, we will show that (ρ, ϕ) is in fact the unique entropy solution to the system (4.11) in the sense of Definition 4.3.1. First we shall state the existence theorem.

Theorem 4.3.10 (Existence of entropy solutions)**.** *There exists an entropy solution* (ρ, ϕ) *to system* (4.11) *with initial condition* (4.12) *and boundary conditions* (4.13)-(4.14) *in the sense of Definition 4.3.1. Such solution is the limit as* $\varepsilon \to 0$ *of the solution* $(\rho^\varepsilon, \phi^\varepsilon)$ *to* (4.16a)-(4.16b)*.*

Proof. To recover the notion of entropy solutions, we consider again the regularised equation

$$\rho_t = (\rho f^2(\rho)\phi_x)_x + \varepsilon\rho_{xx}. \tag{4.39}$$

We multiply this equation by $\eta'(\rho - k)\psi$ (with η' defined in (4.28)) and integrate over

$\Omega_T = [-1,1] \times [0,T]$

$$\iint\limits_{\Omega_T} \eta'(\rho-k)\rho_t\psi \; dxdt = \iint\limits_{\Omega_T} \eta'(\rho-k)(g(\rho)\phi_x)_x\psi \; dxdt + \varepsilon \iint\limits_{\Omega_T} \eta'(\rho-k)\rho_{xx}\psi \; dxdt.$$

Adding

$$0 = \iint\limits_{\Omega_T} \eta'(\rho-k)g(k)\phi_x\psi_x \; dxdt - \iint\limits_{\Omega_T} \eta'(\rho-k)g(k)\phi_x\psi_x \; dxdt$$

and integrating by parts leads to

$$\begin{aligned}
&\iint\limits_{\Omega_T} \eta'(\rho-k)\rho_t\psi \; dxdt = -\iint\limits_{\Omega_T} \eta'(\rho-k)[g(\rho)-g(k)]\psi_x\phi_x \; dxdt \\
&+ \iint\limits_{\Omega_T} \eta'(\rho-k)g(k)\phi_{xx}\psi \; dxdt - \iint\limits_{\Omega_T} \eta''(\rho-k)[g(\rho)-g(k)]\phi_x\rho_x\psi \; dxdt \\
&- \int_0^T \eta'(k)(g(0)-g(k))\phi_x\psi|_{x=\pm 1}dt - \varepsilon \iint\limits_{\Omega_T} \eta''(\rho-k)\rho_x^2\psi \; dxdt \\
&-\varepsilon \iint\limits_{\Omega_T} \eta'(\rho-k)\rho_x\psi_x \; dxdt + \int_0^T \varepsilon\eta'(\rho-k)\rho_x\psi|_{x=\pm 1}dt \\
\leq &- \iint\limits_{\Omega_T} \eta'(\rho-k)[g(\rho)-g(k)]\psi_x\phi_x \; dxdt \\
&+ \iint\limits_{\Omega_T} \eta'(\rho-k)g(k)\psi\phi_{xx} \; dxdt - \eta'(k)\int_0^T [g(0)-g(k)]\phi_x\psi|_{x=\pm 1} \; dt \\
&-\varepsilon \iint\limits_{\Omega_T} \eta(\rho-k)\rho_x\psi_x \; dxdt - \eta'(k)\int_0^T \varepsilon\rho_x\psi|_{x=\pm 1} \; dt \\
&- \iint\limits_{\Omega_T} \eta''(\rho-k)[g(\rho)-g(k)]\phi_x\rho_x\psi \; dxdt
\end{aligned}$$

Next we integrate the first term by parts and multiply it by -1. Then taking the limit as $\gamma \to 0$ is justified by the dominated convergence theorem and the boundedness of ϕ_x and ψ, cf. Remark 4.3.6. The last term on the right hand side vanishes in the limit (due

to the continuity of g) and we obtain

$$\begin{aligned}
&\iint_{\Omega_T} |\rho - k|\psi_t \, dxdt + \int_{-1}^{1} \rho_I(x)\psi(x,0) \, dx \\
&\quad \geq \iint_{\Omega_T} \operatorname{sgn}(\rho - k)[g(\rho) - g(k)]\psi_x\phi_x \, dxdt \\
&\quad - \iint_{\Omega_T} \operatorname{sgn}(\rho - k)g(k)\psi\phi_{xx} \, dxdt + \operatorname{sgn}(k) \int_0^T [g(0) - g(k)]\phi_x\psi|_{x=\pm 1} \, dt \\
&\quad + \varepsilon \iint_{\Omega_T} |\rho - k|\rho_x\psi_x \, dxdt + \operatorname{sgn}(k) \int_0^T \varepsilon\rho_x\psi|_{x=\pm 1} \, dt.
\end{aligned} \tag{4.40}$$

Next we consider the limit $\varepsilon \to 0$. Using Lemma 4.3.5, the fourth term on the right hand side can be estimated by

$$\left| \varepsilon \iint_{\Omega_T} |\rho - k|\rho_x\psi_x \, dxdt \right| \leq \varepsilon C \|\psi_x(t)\|_{L^\infty(\Omega)}, \tag{4.41}$$

and thus tends to zero. To compute the limit for the last term, i.e.

$$\lim_{\varepsilon \to 0} \varepsilon \int_0^T \rho_x\psi|_{x=\pm 1} \, dt,$$

we introduce (following [17]), for some $\kappa > 0$ the function $\xi_\kappa \in C^2([-1,1])$ with the following properties

$$\begin{cases} \xi_\kappa(x) = 1 & \text{on } x = \pm 1, \\ \xi_\kappa(x) = 0 & \text{on } \{x \in [-1,1] \,;\, \operatorname{dist}(x, \partial[-1,1]) \geq \kappa\}, \\ 0 \leq \xi_\kappa(x) \leq 1 & \text{on } (-1,1). \end{cases} \tag{4.42}$$

Furthermore, defining $\mathcal{M}([-1,1])$ as the space of Radon measures on $[-1,1]$, we choose ξ_κ such that

$$\partial_x \xi_\kappa \to \mu|_{\{-1,1\}} \in \mathcal{M}([-1,1]) \text{ as } \kappa \to 0,$$

defined as

$$\mu = \delta_{x=1} - \delta_{x=-1}.$$

Now we obtain

$$\varepsilon \iint\limits_{\Omega_T} \rho_{xx}\psi\xi_\kappa \; dxdt = -\varepsilon \iint\limits_{\Omega_T} \rho_x(\psi\xi_\kappa)_x \; dxdt + \varepsilon \int_0^T \rho_x\psi|_{x=\pm 1} \; dt.$$

The second term in this equation

$$-\varepsilon \iint\limits_{\Omega_T} \rho_x(\psi\xi_\kappa)_x \; dxdt = -\varepsilon \iint\limits_{\Omega_T} \rho_x(\psi_x\xi_\kappa + \phi(\xi_\kappa)_x) \; dxdt$$

vanishes in the limit $\epsilon \to 0$ due to the L^∞ bounds on ψ, ψ_x, ξ_κ, $(\xi_\kappa)_x$ (given for $\kappa > 0$ since $\xi_\kappa \in C^2([-1,1])$) and the L^1-boundedness of ρ_x. Using (4.39) we therefore obtain

$$\begin{aligned}\lim_{\varepsilon\to 0}\left(\varepsilon \int_0^T \rho_x\psi|_{x=\pm 1} \; dt\right) = &- \iint\limits_{\Omega_T} \left(\rho\psi_t - g(\rho)\phi_x\psi_x\right)\xi_\kappa \; dxdt + \int_\Omega \rho\psi\xi_k \; dx\Big|_{t=0} \\ &+ \iint\limits_{\Omega_T} g(\rho)\phi_x\psi(\xi_\kappa)_x \; dxdt - \int_0^T g(0)\phi_x\psi|_{x=\pm 1} \; dt.\end{aligned}$$

Finally letting $\kappa \to 0$, the first term on the right hand side tends to zero while the second tends to an evaluation on the boundary. Due to the continuity of ρ and ψ the boundary term resulting from the integration by parts in time vanishes as the support of ξ_κ converges to a set of Lebesgue measure zero (i.e. $\{-1,1\}$). Thus we have

$$\lim_{\varepsilon\to 0} \varepsilon \int_0^T \rho_x\psi|_{x=\pm 1} \; dt = \int_0^T (g(\operatorname{Tr}\rho) - g(0))\phi_x(s,t)\psi|_{x=\pm 1} \; dt.$$

Combining this result with (4.40) we finally obtain the entropy formulation as in Definition 4.3.1 and this completes the proof. □

Next we prove that the boundary condition (4.13) can be recovered by the definition of entropy solution.

Lemma 4.3.11. *Let ρ be an entropy solution given by Definition 4.3.1. Then, the following inequality holds for all $k \in [0, \operatorname{Tr}\rho]$*

$$g(\operatorname{Tr}\rho) \geq g(k) \quad \text{at } x = \pm 1. \tag{4.43}$$

Proof. In (4.15), we choose the special test function $\psi = \nu(t)\omega_\kappa$ with $\nu \in \mathcal{C}^2(]0,T[)$ positive and $\omega_\kappa \in C^2([-1,1])$ with the following properties:

$$\begin{cases} \omega_\kappa(x) = 1 & \text{on } x = -1, \\ \omega_\kappa(x) = 0 & \text{on } \{x \in [-1,1]\,;\, |x+1| \geq \kappa\}, \\ 0 \leq \omega_\kappa(x) \leq 1 & \text{on } (-1,1). \end{cases} \tag{4.44}$$

Similarly as before for ξ_κ, we choose ω_κ such that

$$\partial_x \omega_\kappa \to -\delta_{x=-1} \text{ as } \kappa \to 0,$$

where $\delta_{x=-1}$ denotes the Dirac delta measure centered at -1. Then, in the limit $\kappa \to 0$ (4.15) converges to

$$\int_0^T \operatorname{sgn}(\operatorname{Tr}\rho - k)[g(\operatorname{Tr}\rho) - g(k)]\phi_x|_{x=-1}\nu(t)\,dt$$
$$+ \operatorname{sgn}(k)\int_0^T [g(\operatorname{Tr}\rho) - g(k)]\phi_x|_{x=-1}\nu(t)\,dt \geq 0,$$

for all $k \in \mathbb{R}$. Thus, almost everywhere in $\{-1\} \times (0,T)$ we have

$$(\operatorname{sgn}(\operatorname{Tr}\rho - k) + \operatorname{sgn}(k))[g(\operatorname{Tr}\rho) - g(k)]\phi_x \geq 0.$$

To conclude the proof we note that ϕ_x is always (i.e. independently of the given ρ) non-negative at $x = -1$. This is a consequence of the fact that $\phi = 0$ at $x = \pm 1$ (boundary conditions) and positive on the whole domain, due to a trivial minimum principle for the equation (4.16b). Employing Hopf's Lemma we therefore conclude strict positivity of ϕ_x at $x = -1$. In a similar way, one can construct a function ω_k concentrating on $x = 1$ with a derivative converging to a Dirac delta at $x = 1$. The same inequality is obtained since the change of sign in the derivative of concentrator ω_k is balanced by the change of sign in ϕ_x (non-increasing at $x = 1$). To conclude, we note that $(\operatorname{sgn}(\operatorname{Tr}\rho - k) + \operatorname{sgn}(k)) = 0$ for all $k \notin [0, \operatorname{Tr}\rho]$ (as $\operatorname{Tr}\rho \geq 0$) and equal to 2 otherwise. □

4.3.4 Uniqueness

Next we shall prove that the entropy solution in the sense of Definition 4.3.1 is unique.

Theorem 4.3.12 (Uniqueness of entropy solutions)**.** *There exists at most one entropy solution* (ρ, ϕ) *to the system* (4.11) *with initial condition* (4.12) *and boundary conditions* (4.13)-(4.14) *in the sense of Definition 4.3.1.*

The above stated result is a consequence of the following stability theorem, which follows the same technique developed in [56]. Here the authors use the variables doubling technique originally introduced in [62]. A similar strategy was also used e.g. [9, 10].

We state the following useful result:

Lemma 4.3.13. *([56]) Consider a function $z = z(x)$ belonging to $L^\infty(\mathbb{R}^d) \cap BV(\mathbb{R}^d)$ and let h be Lipschitz on the interval $I_z := [-\|z\|_{L^\infty}, \|z\|_{L^\infty}]$. Then $h(z)$ belongs to $L^\infty(\mathbb{R}^d) \cap BV(\mathbb{R}^d)$ and*

$$\left|\frac{\partial}{\partial x_j} h(z)\right| \leq \|h\|_{Lip(I_z)} \left|\frac{\partial}{\partial x_j} z\right|$$

in the sense of measures for $j = 1, \ldots, d$.

Uniqueness can be deduced from the following theorem:

Theorem 4.3.14. *Let (ρ, ϕ), $(\bar{\rho}, \bar{\phi})$ be the two entropy solutions to system (4.11) according to Definition 4.3.1 with initial data ρ_I, $\bar{\rho}_I \in L^\infty([-1,1]) \cap BV([-1,1])$ respectively. Then for almost all $t \in (0,T)$,*

$$\begin{aligned}\|\rho(t) - \bar{\rho}(t)\|_{L^1(\Omega)} \leq \|\rho_I - \bar{\rho}_I\|_{L^1(\Omega)} &+ t\|g\|_{L^\infty(\Omega)} \|\phi_{xx}(t) - \bar{\phi}_{xx}(t)\|_{L^\infty((0,T);L^1(\Omega))} \\ &+ t\|g\|_{Lip(\Omega)} \|\rho_x(t)\|_{L^1(\Omega)} \|\phi_x(t) - \bar{\phi}_x(t)\|_{L^\infty((0,T);L^\infty(\Omega))}\end{aligned}$$

holds.

Combining this result with (4.35) and (4.36) from Lemma 4.3.9 we obtain

$$\|\rho(t) - \bar{\rho}(t)\|_{L^1(\Omega)} \leq \|\rho_I - \bar{\rho}_I\|_{L^1(\Omega)} + tC\|\rho(t) - \bar{\rho}(t)\|_{L^1(\Omega)}, \tag{4.45}$$

for some positive constant C. Choosing t small enough this inequality contradicts the existence of two different solutions ρ and $\bar{\rho}$ having the same initial datum and thus implies uniqueness. It remains to prove Theorem 4.3.14.

Proof. We first note that in this proof there will sometimes, after integration by parts, be terms which insolve derivatives of the sgn. To be precise, the sgn needs to be approximated in these situations, as in the proof of Lemma 4.3.5. However, to increase the readability of this proof, we will omit this detail here. Consider a non-negative, compactly supported, Lipschitz continuous function $\psi(x,t,\bar{x},\bar{t})$, defined on $[-1,1] \times [0,T[\times [-1,1] \times [0,T[$. Furthermore, let ψ be zero on $\{-1,1\} \times [0,T)$. Next, we take two admissible solutions $\rho(x,t)$, $\bar{\rho}(\bar{x},\bar{t})$ and write (4.15) as

$$\begin{aligned}&\iint\limits_{\Omega_T} |\rho - \bar{\rho}|\psi_t \, dxdt - \iint\limits_{\Omega_T} \operatorname{sgn}(\rho - \bar{\rho})[g(\rho) - g(\bar{\rho})]\psi_x \phi_x(x,t) \, dxdt \; + \\ &\iint\limits_{\Omega_T} \operatorname{sgn}(\rho - \bar{\rho}) g(\bar{\rho}) \psi \phi_{xx}(x,t) dxdt - \operatorname{sgn}(\bar{\rho}) \int_0^T [g(\operatorname{Tr}\rho) - g(\bar{\rho})]\phi_x(x,t)\psi \mid_{x=\pm 1} dt \geq 0.\end{aligned}$$

and

$$\iint\limits_{\Omega_T} |\bar{\rho}-\rho|\psi_{\bar{t}}\, d\bar{x}d\bar{t} - \iint\limits_{\Omega_T} \operatorname{sgn}(\bar{\rho}-\rho)[g(\bar{\rho})-g(\rho)]\psi_{\bar{x}}\bar{\phi}_{\bar{x}}(\bar{x},\bar{t})\, d\bar{x}d\bar{t} \;+$$

$$\iint\limits_{\Omega_T} \operatorname{sgn}(\bar{\rho}-\rho)g(\rho)\psi\bar{\phi}_{\bar{x}\bar{x}}(\bar{x},\bar{t})\, d\bar{x}d\bar{t} - \operatorname{sgn}(\rho)\int_0^T [g(\operatorname{Tr}\bar{\rho})-g(\rho)]\bar{\phi}_{\bar{x}}(\bar{x},\bar{t})\psi\,|_{\bar{x}=\pm 1}\, d\bar{t} \geq 0.$$

Integrating both the above inequalities over $\Omega_T := \Omega \times [0,T[$, the first with respect to $\bar{x}$, $\bar{t}$ and the second with respect to x, t and adding the resulting equations leads to

$$\begin{aligned}
&\iiiint\limits_{\Omega_T\times\Omega_T} |\rho-\bar{\rho}|(\psi_t+\psi_{\bar{t}})\, dzd\bar{z}\\
&-\iiiint\limits_{\Omega_T\times\Omega_T} \underbrace{\left[\operatorname{sgn}(\rho-\bar{\rho})\left(g(\rho)\phi_x(x,t)-g(\bar{\rho})\bar{\phi}_x(\bar{x},\bar{t})\right)(\psi_x+\psi_{\bar{x}})\right]}_{:=I_1} dzd\bar{z}\\
&-\iiiint\limits_{\Omega_T\times\Omega_T} \underbrace{\left[\operatorname{sgn}(\rho-\bar{\rho})\left(g(\bar{\rho})\psi_x\left(\bar{\phi}_{\bar{x}}(\bar{x},\bar{t})-\phi_x(x,t)\right)+g(\rho)\psi_{\bar{x}}\left(\bar{\phi}_{\bar{x}}(\bar{x},\bar{t})-\phi_x(x,t)\right)\right)\right]}_{:=I_{2,1}} dzd\bar{z}\\
&+\iiiint\limits_{\Omega_T\times\Omega_T} \underbrace{\left[\operatorname{sgn}(\rho-\bar{\rho})(g(\bar{\rho})\phi_{xx}(x,t)-g(\rho)\bar{\phi}_{\bar{x}\bar{x}}(\bar{x},\bar{t}))\psi\right]}_{:=I_{2,2}} dzd\bar{z}\\
&=\iiiint\limits_{\Omega_T\times\Omega_T} \left(|\rho-\bar{\rho}|(\psi_t+\psi_{\bar{t}})+I_1+I_{2,1}+I_{2,2}\right) dzd\bar{z} \geq 0.
\end{aligned}$$

Here $z=(x,t)$ and $\bar{z}=(\bar{x},\bar{t})$. We take a symmetric function $\delta \in \mathcal{C}^\infty(\mathbb{R})$ with total mass one and $\operatorname{supp}(\delta) \subset (-1,1)$. We define

$$\delta_h(\cdot) := \frac{1}{h}\delta\left(\frac{\cdot}{h}\right)$$

and choose the following test function

$$\psi = \nu\left(\frac{t+\bar{t}}{2}, \frac{x+y}{2}\right)\delta_h\left(\frac{t-\bar{t}}{2}\right)\delta_h\left(\frac{x-\bar{x}}{2}\right).$$

From this definition we conclude

$$\begin{aligned}
&\iiiint\limits_{\Omega_T\times\Omega_T} \left(|\rho-\bar{\rho}|(\psi_t+\psi_{\bar{t}})+I_1\right)\, dxdtd\bar{x}d\bar{t}\\
&=\iiiint\limits_{\Omega_T\times\Omega_T} \left(|\rho-\bar{\rho}|\nu_t+\operatorname{sgn}(\rho-\bar{\rho})\left(g(\rho)\phi_x(x,t)-g(\bar{\rho})\bar{\phi}_{\bar{x}}\right)\nu_x\right)\times\\
&\qquad\qquad \times\delta_h\left(\frac{t-\bar{t}}{2}\right)\delta_h\left(\frac{x-\bar{x}}{2}\right)\, dxdtd\bar{x}d\bar{t}.
\end{aligned}$$

We now consider the term $I_{2,1}$

$$\begin{aligned}
I_{2,1} = &- \operatorname{sgn}(\rho-\bar\rho)\left[\bar\phi_x(\bar x,\bar t)\left(g(\bar\rho)+g(\rho)\right) - \phi_x(x,t)\left(g(\bar\rho)+g(\rho)\right)\right]\frac{1}{2}\nu_x\delta_h\delta_h \\
&- \operatorname{sgn}(\rho-\bar\rho)\left[\bar\phi_x(\bar x,\bar t)\left(g(\bar\rho)-g(\rho)\right) - \phi_x(x,t)\left(g(\bar\rho)-g(\rho)\right)\right]\nu(\delta_h\delta_h)_x \\
=:& \; I_{2,1,1} + I_{2,1,2}.
\end{aligned}$$

Here, we used that by definition we have $\nu_{\bar x} = \frac{1}{2}\nu_x$ and $(\delta_h\delta_h)_{\bar x} = -(\delta_h\delta_h)_x$. Integrating by parts in $I_{2,1,2}$ leads to

$$\begin{aligned}
&-\iiiint\limits_{\Omega_T\times\Omega_T} \operatorname{sgn}(\rho-\bar\rho)\left[\bar\phi_x(\bar x,\bar t)\left(g(\bar\rho)-g(\rho)\right) - \phi_x(x,t)\left(g(\bar\rho)-g(\rho)\right)\right]\times \\
&\qquad\qquad \times \nu(\delta_h\delta_h)_x \; dxdtd\bar x d\bar t \\
&= \iiiint\limits_{\Omega_T\times\Omega_T} \operatorname{sgn}(\rho-\bar\rho)\left[\bar\phi_x(\bar x,\bar t)\left(g(\bar\rho)-g(\rho)\right) - \phi_x(x,t)\left(g(\bar\rho)-g(\rho)\right)\right]\times \\
&\qquad\qquad \times \frac{1}{2}\nu_x\delta_h\delta_h \; dxdtd\bar x d\bar t \\
&+ \iiiint\limits_{\Omega_T\times\Omega_T} \bar\phi_{\bar x}[(\operatorname{sgn}(\rho-\bar\rho)(g(\bar\rho)-g(\rho)))_x - \phi_{xx}(x,t)\operatorname{sgn}(\rho-\bar\rho)\left(g(\bar\rho)-g(\rho)\right)]\times \\
&\qquad\qquad \times \nu\delta_h\delta_h \; dxdtd\bar x d\bar t \\
&+ \iiiint\limits_{\Omega_T\times\Omega_T} -\phi_x(x,t)(\operatorname{sgn}(\rho-\bar\rho)\left(g(\bar\rho)-g(\rho)\right))_x\nu\delta_h\delta_h \; dxdtd\bar x d\bar t.
\end{aligned}$$

Noticing that

$$\begin{aligned}
&-\phi_{xx}(x,t)\operatorname{sgn}(\rho-\bar\rho)\left(g(\bar\rho)-g(\rho)\right) + I_{2,2} \\
&\qquad\qquad = -\operatorname{sgn}(\rho-\bar\rho)(\bar\phi_{\bar x\bar x}(\bar x,\bar t) - \phi_{xx}(x,t))g(\rho)\nu\delta_h\delta_h
\end{aligned}$$

and adding again $I_{2,1,1}$ we obtain

$$\begin{aligned}
&\iiiint\limits_{\Omega_T\times\Omega_T} \left(I_{2,2} + I_{2,1,2} + I_{2,1,1}\right) \; dxdtd\bar x d\bar t \\
&\qquad = \iiiint\limits_{\Omega_T\times\Omega_T} -\operatorname{sgn}(\rho-\bar\rho)(\bar\phi_{\bar x\bar x}(\bar x,\bar t) - \phi_{xx}(x,t))g(\rho)\nu\delta_h\delta_h \; dxdtd\bar x d\bar t \\
&\qquad + \iiiint\limits_{\Omega_T\times\Omega_T} (\bar\phi_{\bar x} - \phi_x)(\operatorname{sgn}(\rho-\bar\rho)(g(\bar\rho)+g(\rho)))_x\nu\delta_h\delta_h \; dxdtd\bar x d\bar t \\
&\qquad + \iiiint\limits_{\Omega_T\times\Omega_T} \underbrace{\operatorname{sgn}(\rho-\bar\rho)\left[\bar\phi_x(\bar x,\bar t)g(\rho) - \phi_x(x,t)g(\rho)\right]\nu_x\delta_h\delta_h)}_{=:J} \; dxdtd\bar x d\bar t.
\end{aligned}$$

As there are no more derivatives in the terms involving $\delta_h\delta_h$, we consider the limit $h \to 0$, remove two integrals and set $x = \bar{x}$, $t = \bar{t}$. This is a rather technical point which is explained in great detail in [61]. We choose the new test function

$$\nu(x,t) = \nu_{\kappa,\tilde{h}}(x,t) = (1 - \xi_\kappa(x))\chi_{\tilde{h}}(t),$$

with for some $0 < t_1 < t_2 < T$ fixed

$$\chi_h(t) = \int_{-\infty}^{t} (\delta_h(\tau - t_1) - \delta_h(\tau - t_2))\ d\tau,$$

and ξ_κ as defined in (4.42). We observe that all terms which are bounded in L^1 and multiplied by $(\nu_{\kappa,\tilde{h}}(x,t))_x$ converge to a boundary term in the limit $\kappa \to 0$. We thus have

$$\lim_{\substack{\tilde{h}\to 0\\ \kappa\to 0}} \iint_{\Omega_T} (I_1 + J)\ dxdt = -\int_{t_1}^{t_2}\int_{\partial\Omega} \operatorname{sgn}(\operatorname{Tr}\rho - \operatorname{Tr}\bar{\rho})\bar{\phi}_x[g(\operatorname{Tr}\rho) - g(\operatorname{Tr}\bar{\rho})]\ dsdt,$$

and therefore

$$\begin{aligned}
&- \lim_{\substack{\tilde{h}\to 0,\\ \kappa\to 0}} \iint_{\Omega_T} (|\rho - \bar{\rho}|\nu_t + I_1 + I_{2,1} + I_{2,2})\ dxdt \\
&= -\int_{-1}^{1} (|\rho - \bar{\rho}|)\ dx\Big|_{t_1}^{t_2} + \int_{t_1}^{t_2}\int_{-1}^{1} -\operatorname{sgn}(\rho - \bar{\rho})(\bar{\phi}_{xx}(x,t)) - \phi_{xx}(x,t))g(\rho)\ dxdt \\
&\quad + \int_{t_1}^{t_2}\int_{-1}^{1} (\bar{\phi}_x - \phi_x)(\operatorname{sgn}(\rho - \bar{\rho})(g(\bar{\rho}) + g(\rho)))_x\ dxdt \\
&\quad + \int_{t_1}^{t_2} \operatorname{sgn}(\operatorname{Tr}\rho - \operatorname{Tr}\bar{\rho})\bar{\phi}_x[g(\operatorname{Tr}\rho) - g(\operatorname{Tr}\bar{\rho})]|_{x=\pm 1}dt \geq 0.
\end{aligned}$$

Using Lemma 4.3.13, we have

$$|(\operatorname{sgn}(\operatorname{Tr}\rho - \operatorname{Tr}\bar{\rho})(g(\operatorname{Tr}\bar{\rho}) - g(\operatorname{Tr}\rho)))_x| \leq \|g\|_{Lip(I)}|\rho_x|. \tag{4.46}$$

Collecting all the above terms we obtain

$$\begin{aligned}
\|\rho(t) - \bar{\rho}(t)\|_{L^1(\Omega)}\Big|_{t_1}^{t_2} \leq \int_{t_1}^{t_2}\int_{\Omega} &\big[|\phi_{xx}(x,t) - \bar{\phi}_{xx}(x,t)|\|g\|_{L^\infty(\Omega)} \\
&+ \|\phi_x(t) - \bar{\phi}_x(t)\|_{L^\infty(\Omega)}\|g\|_{Lip(I)}|\rho_x|\big]\ dxdt \\
&+ \int_{t_1}^{t_2}\int_{\partial\Omega} \operatorname{sgn}(\operatorname{Tr}\rho - \operatorname{Tr}\bar{\rho})\bar{\phi}_x[g(\operatorname{Tr}\rho) - g(\operatorname{Tr}\bar{\rho})]\ dsdt.
\end{aligned} \tag{4.47}$$

Following [17], we define

$$k(x,t) = \begin{cases} \operatorname{Tr}\rho & \text{if} \quad \operatorname{Tr}\rho < \operatorname{Tr}\bar{\rho}, \\ 0 & \text{if} \quad \operatorname{Tr}\rho = \operatorname{Tr}\bar{\rho}, \\ \operatorname{Tr}\bar{\rho} & \text{if} \quad \operatorname{Tr}\rho > \operatorname{Tr}\bar{\rho}. \end{cases}$$

This allows us to write, at $x = -1$

$$\begin{aligned} \operatorname{sgn}(\operatorname{Tr}\rho - \operatorname{Tr}\bar{\rho})\bar{\phi}_x(-1,t)[g(\operatorname{Tr}\rho) - g(\operatorname{Tr}\bar{\rho})] &= \operatorname{sgn}(\operatorname{Tr}\rho - k)\bar{\phi}_x(-1,t)[g(\operatorname{Tr}\rho) - g(k)] \\ &\quad + \operatorname{sgn}(\operatorname{Tr}\bar{\rho} - k)\bar{\phi}_x(-1,t)[g(\operatorname{Tr}\bar{\rho}) - g(k)]. \end{aligned}$$

Note that $\bar{\phi}_x(-1,t) > 0$. At $x = 1$, the same holds true. Using Lemma 4.3.11 we conclude that the last term on the right hand side of (4.47) is negative and can therefore be omitted. Thus letting $t_1 \to 0$ we arrive at the desired inequality and this completes the proof. □

4.4 Numerics and Examples for the Hughes' model

In this section we discuss the behaviour of solutions for the non regularised one-dimensional problem with simple initial data. Already these examples show quite interesting features which can be reproduced by numerical simulations. The content of this section is formal as we don't provide any existence and uniqueness theory. However, the characteristic calculus provides a useful tool to understand qualitatively the behaviour of the solution in the simple examples considered and is in complete agreement with the numerical results.

4.4.1 Characteristic Calculus

We consider the non-regularised problem

$$\rho_t - (\rho f^2(\rho)\phi_x)_x = 0, \tag{4.48a}$$

$$|\phi_x| = \frac{1}{f(\rho)}. \tag{4.48b}$$

In the following, we always consider the unique viscosity solution ϕ to (4.48b). We use (in a non rigorous way) the notion of a viscosity solution to be able to interpret ϕ as a biased shortest distance to the exit. Note that thus this solution has a unique turning

point $x_0(t)$ (i.e. point, where ϕ_x changes sign) given by the implicit relation

$$\int_{-1}^{x_0(t)} \frac{1}{f(\rho)}\, dx = \int_{x_0(t)}^{1} \frac{1}{f(\rho)}\, dx.$$

Thus, (4.48a) can be written as (using that $|\phi_x| = \phi_x \operatorname{sgn} \phi_x$)

$$\rho_t - (\rho f(\rho) \operatorname{sgn} \phi_x)_x = 0. \tag{4.49}$$

The natural boundary conditions (in the spirit of [17, 32]) are given by

$$f(\operatorname{Tr} \rho) \geq f(k) \qquad \text{on } x = \pm 1, \quad \text{for all } k \in [0, \operatorname{Tr} \rho], \tag{4.50}$$

which is satisfied if and only if $\operatorname{Tr} \rho$ belongs to the interval of densities corresponding to outgoing characteristics, i.e. $\operatorname{Tr} \rho \in [0, 1/2]$. As shown in [32], the boundary condition in case of incoming characteristics is determined by solving a Riemann problem between the boundary datum (i.e. zero in this case) and the trace of the density next to the boundary.

Away from the time dependent interface $x = x_0(t)$ (where ϕ_x is discontinuous) we can give sense to characteristics. They are defined by

$$\dot{x} = -(1 - 2\rho) \operatorname{sgn}(\phi_x).$$

Note that the Rankine-Hugoniot condition for a hyperbolic conservation law with flux F, i.e. $\rho_t + F(\rho)_x = 0$ is given by

$$[[F(\rho)]] = \dot{x}_0(t)\, [[\rho]]\,. \tag{4.51}$$

Here, $[[\cdot]]$ denotes the jump at the discontinuity x_0.

Constant initial data

We would like to understand the behaviour of the solution in the very simple case of constant initial data. Here we are particularly interested in the three cases which correspond to different characteristic speeds, i.e. ρ_I less, equal or greater than $1/2$. In particular we consider the cases $\rho_I = 1/4$, $\rho_I = 1/2$ and $\rho_I = 3/4$. In the case of constant initial data, the interface is constant in time, i.e. $\dot{x}_0 = 0$ and located at $x = 0$. Thus $\operatorname{sgn} \phi_x = -\operatorname{sgn} x$ and (4.48a) can be written as

$$\rho_t + (\rho f(\rho) \operatorname{sgn} x)_x = 0. \tag{4.52}$$

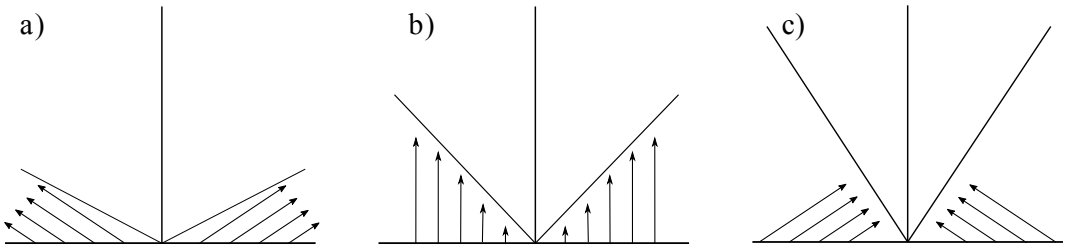

Figure 4.2: a) $\rho = 0.25$ b) $\rho = 0.5$ c) $\rho = 0.75$

The RH condition (4.51) for this flux $F(\rho) = \rho f(\rho) \operatorname{sgn} x$ reads

$$f(\rho^+) + f(\rho^-) = 0,$$

where $\rho^\pm$ denote the right and left limit of ρ at the interface $x = 0$. An immediate consequence of this is that constant functions $\rho(x,t) = c$ with $c \in (0,1)$ do not satisfy the RH condition (4.51) and are not weak solutions. If we start with a constant initial datum we expect the equation to "correct" this by forcing $\rho(0,t) = 0$ in arbitrary small time ($\rho(0,t) = 1$ would also create a solution, which however does not fulfil the entropy condition). Then two shocks originate between $\rho(0,t) = 0$ and $\rho(x,t) = c$ for $x \neq 0$, which move towards the boundary. The slope of these shocks is determined by the RH condition (4.51). In the three cases considered we obtain

$$\dot{x} = \begin{cases} \pm\frac{3}{4} & \rho_I(x) = \frac{1}{4} \\ \pm\frac{1}{2} & \rho_I(x) = \frac{1}{2} \\ \pm\frac{1}{4} & \rho_I(x) = \frac{3}{4}. \end{cases}$$

This situation, locally around $x = 0$, is sketched in Fig. 4.2. Around the center $x = 0$ where no information is transported to, we expect the solution to be either zero or a rarefaction wave. In case of a rarefaction wave we make the ansatz $\rho(x,t) = u\left(\frac{x}{t}\right)$ and deduce from (4.52) that

$$u_{\mathrm{RF}}(x,t) = \frac{x+t}{2t}.$$

This solution continuously connects the two outgoing shocks but creates the constant value $1/2$ at $x = 0$ and is thus not admissible. Therefore, the we expect formation of a vacuum in between the two shocks in all three cases. In the case $\rho = 3/4$, we encounter an additional phenomenon at the boundaries. Here the characteristics point inwards,

therefore we need to prescribe boundary conditions at $x = \pm 1$. We choose the following Dirichlet boundary conditions $\rho(\pm 1, t) = 1/2$ (maximal flux). Such condition is easily recovered by solving the Riemann problem between $\operatorname{Tr}\rho = 3/4$ and the boundary value zero (cf. [32]).

This implies that the characteristics at the boundary are vertical while characteristics of slope $1/2$ transport the value $3/4$ into the domain. Hence we obtain two wedges (one at each boundary) in which no information is transported by characteristics. If we make again the ansatz $\rho(x,t) = u\left(\frac{x+1}{t}\right)$ (shifted to the left boundary), we obtain the following rarefaction wave

$$\rho(x,t) = \frac{x+1+t}{2t},$$

which is an admissible solution. Thus we expect rarefaction waves at both boundaries. At time $t = 4/3$, these rarefaction waves will hit the shocks coming from the interface (at $x = \pm 1/3$, respectively). To calculate the new slope of the shock we use the RH condition (4.51) which results in the following ODE

$$\dot{s}(t) = -\frac{s(t)}{2t} + \frac{t-1}{2t}, \quad s\left(\frac{4}{3}\right) = -\frac{1}{3}.$$

Using standard techniques we obtain the solution

$$s(t) = -\sqrt{t}\left(\frac{1+t}{\sqrt{t}} - \sqrt{3}\right).$$

A complete picture of the case $\rho_I(x) = 3/4$ is given in Fig. 4.3. In the next section we will see that all these phenomena can be observed in numerical simulations.

Remark 4.4.1 (Boundary conditions in the regularised and non regularised case)**.** At a first glance there is a clear discrepancy between the boundary conditions in the regularised case (4.13) and the ones prescribed above for the non regularised model. In the latter case, the set of admissible boundary data is determined via the monotonicity of f at the boundary, whereas in the former case this set is determined via the function g. Hence, there is the possibility of a boundary layer in a possible limit as $\delta_1 \to 0$. However, the regularised problem has a source term $g(\rho)\phi_{xx}$, and this fact could possibly imply some compensation phenomena at the boundary which can avoid the boundary layer. This issue will be the topic of future study.

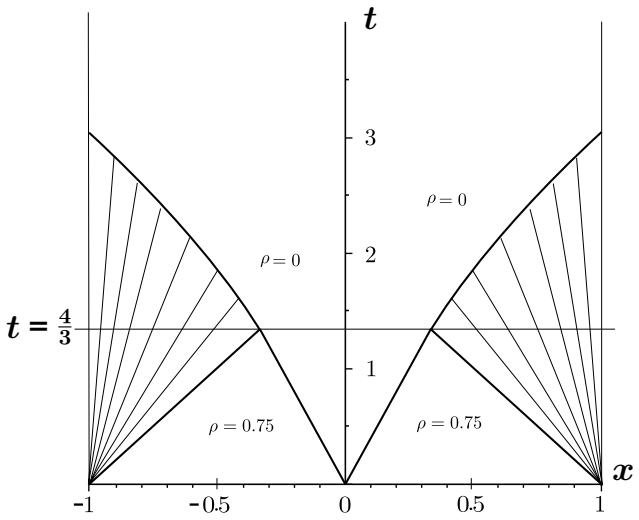

Figure 4.3: Details for the case $\rho_I(x) = 3/4$

4.4.2 Numerical simulations

Next we present numerical simulations of (4.48) relating the results to the previous discussion in Section 4.4.1. We consider the regularised system on the domain $\Omega = [-1, 1]$

$$\rho_t - \operatorname{div}(\rho f(\rho) \operatorname{sgn} \phi_x) = \varepsilon \rho_{xx} \tag{4.53a}$$

$$|\phi_x| = \frac{1}{f(\rho)} \tag{4.53b}$$

with a regularization parameter $\varepsilon \geq 0$. The system is supplemented with the initial condition $\rho(x, 0) = \rho_I(x)$ and inhomogeneous Dirichlet boundary conditions $\rho(\pm 1, t) = \rho_D$. We use these boundary conditions to be consistent with the characteristic calculus presented in Sec. 4.4.1. This allows us to compare the numerical results with these computations. We solve (4.53) in an iterative manner, i.e.

1. Given ρ solve the eikonal equation (4.53b) with fast sweeping method.

2. Solve the non-linear conservation law (4.53a) for a given ϕ using an ENO scheme or resp. a Godunov scheme.

We choose the following discretisation. The domain $\mathbb{R}$ is divided into cells $I_j = [x_{j-\frac{1}{2}}, x_{j+\frac{1}{2}}]$ with centers at points $x_j = j\Delta x$ for $j \in \mathbb{Z}$. The time domain $(0, \infty)$ is discretised in the same manner via $t^n = n\Delta t$ resulting in time strips $I^n = [t^n, t^{n+1}]$.

We used two different schemes to compare and understand the behaviour of solutions. In the first approach we use an ENO scheme with small diffusion on the whole domain $\Omega = [-1, 1]$. In the second approach we split the domain into two parts $\Omega = \Omega_1 \cup \Omega_2$ where $\Omega_1 = [0, x(t)]$ and $\Omega_2 = [x(t), 1]$, solve equation (4.53a) with a Godunov scheme (and no diffusion, i.e. $\varepsilon = 0$) on Ω_1 and Ω_2 and concatenate both solutions.

ENO scheme

J. Towers presented convergence results for an ENO scheme for conservation laws with discontinuous flux in [108]. This ansatz can be used in Step (2) to solve (4.53a) with small diffusion on the whole domain $\Omega = [-1, 1]$. Let χ_j^n denote the characteristic function on the rectangle $R_j^n = I_j \times I^n$. The finite difference scheme then generates for every mesh size Δx and Δt a piecewise constant solution ρ^Δ given by

$$\rho^\Delta(x,t) = \sum_{n\geq 0} \sum_{-\infty}^{\infty} \chi_j^n \rho_j^n.$$

The approximations ρ_j^n are generated by an explicit algorithm

$$\rho_j^{n+1} = \rho_j^n - \lambda_1(k_{j+\frac{1}{2}} h_{j+\frac{1}{2}} - k_{j-\frac{1}{2}} h_{j-\frac{1}{2}}) + \lambda_2(d_{j+\frac{1}{2}} - d_{j-\frac{1}{2}}). \tag{4.54}$$

Here $\lambda_1 = \frac{\Delta t}{\Delta x}$, $\lambda_2 = \frac{\varepsilon \Delta t}{\Delta x^2}$ and $k_{j\pm\frac{1}{2}} = \operatorname{sgn} \phi_x(x_{j\pm\frac{1}{2}})$. The diffusive flux is given by $d_{j+\frac{1}{2}}^n := \rho_{j+1}^n - \rho_j^n$, the convective one $\mathrm{h}_{\mathrm{j}+\frac{1}{2}} := h(v,u)$ is chosen such that it is consistent with the actual flux, i.e. $h(\rho,\rho) = g(\rho) = \rho f(\rho)$. To guarantee monotonicity the flux is transposed when $k_{j+\frac{1}{2}}$ changes sign, i.e.

$$\mathrm{h}_{\mathrm{j}+\frac{1}{2}} = \begin{cases} h(\rho_{j+1}, \rho_j) & \text{if } k_{j+\frac{1}{2}} \geq 0 \\ h(\rho_j, \rho_{j+1}) & \text{if } k_{j+\frac{1}{2}} < 0. \end{cases}$$

We choose the ENO flux [39] which is given by

$$h(v,u) = \frac{1}{2}\left(g(u) + g(v)\right) + \frac{1}{2}\int_u^v |g_u| du. \tag{4.55}$$

Godunov scheme The Godunov scheme is derived by using the exact solution operator for $\rho_t + (F(\rho))_x = 0$ with piecewise constant initial data. The resulting numerical flux is $h(v,u) = F(u^G(v,u))$, where $u^G(v,u)$ is the similarity solution of the resulting Riemann problem with right and left state v and u evaluated anywhere on the vertical

half-line $t > 0$ where the jump in the initial data occurs. The Godunov flux [88] is given by

$$h(v,u) = \begin{cases} \min_{[u,v]} F(w) & \text{if } u \leq v \\ \max_{[u,v]} F(w) & \text{if } u \geq v. \end{cases} \tag{4.56}$$

Constant initial data First we would like to validate the characteristic calculus presented in section 4.4.1. We choose constant initial data $\rho_I(x)$ that is smaller or larger than $1/2$. The time discretisation is set to $\Delta t = 10^{-4}$, the spatial discretisation to $\Delta x = 10^{-2}$. Here we solved the non regularised problem with $\varepsilon = 0$ using Godunovs' method. First we choose $\rho_I(x) = 1/4$, the evolution is depicted in Figure 4.4. In this case the characteristics point outward, therefore we prescribe numerical boundary conditions instead of physical ones. In our second example we set $\rho_I(x) = 3/4$. Here we observe a

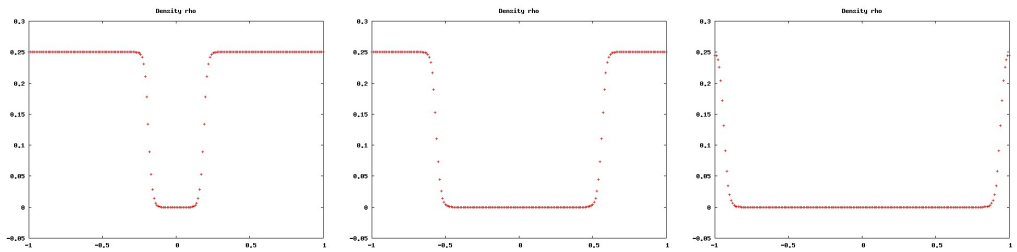

(a) $t = \frac{1}{4}$ (b) $t = \frac{3}{4}$ (c) $t = \frac{5}{4}$

Figure 4.4: Evolution of ρ with initial datum $\rho_I(x) = 0.25$

good agreement of the numerical simulation with the theoretical results, see Figure 4.5. Note that the shock hits the rarefaction waves at $t = 4/3$ and that the subsequent shock hits the boundary at $t = 3$ (as predicted by our characteristic calculus).

Other examples Finally we would like to illustrate the behavior with other examples. We choose the following initial guess

$$\rho_I(x) = \begin{cases} 0.8 & \text{if } -0.8 \leq x \leq -0.5 \\ 0.6 & \text{if } -0.3 \leq x \leq 0.3 \\ 0.9 & \text{if } \quad 0.4 \leq x \leq 0.75, \end{cases}$$

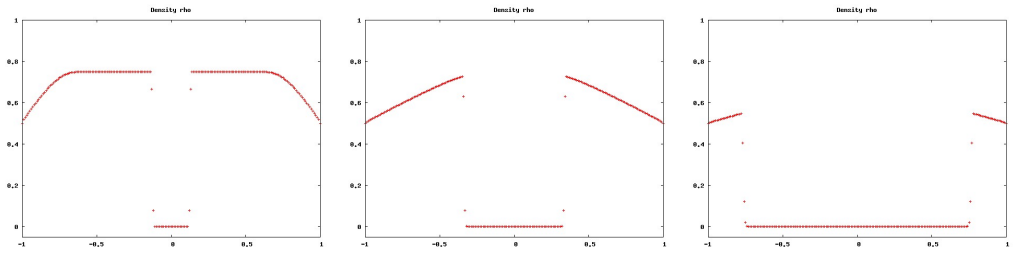

(a) $t = \frac{1}{2}$ (b) $t = \frac{4}{3}$ (c) $t = \frac{5}{2}$

Figure 4.5: Evolution of ρ with initial datum $\rho_I(x) = 0.75$ and Dirichlet boundary conditions $\rho(\pm 1) = 0.5$

representing three groups which would like to exit at $x = 1$ or $x = -1$. We set the spatial discretisation to $\Delta x = 10^{-3}$, the discretisation in time to $\Delta t = 10^{-4}$. Here we solve (4.53a) on the whole domain using an ENO flux and $\varepsilon = 10^{-4}$. The evolution of the densities is illustrated in Figure 4.6. Here the y axis corresponds to time, running from 0 (top) to 1.5 (bottom). The right group (located between $0.4 \leq x \leq 0.75$) splits at the beginning, a small part moves to the left while the rest moves towards the right exit. We observe that the part of the group which was moving to the left changes direction and moves towards the right.

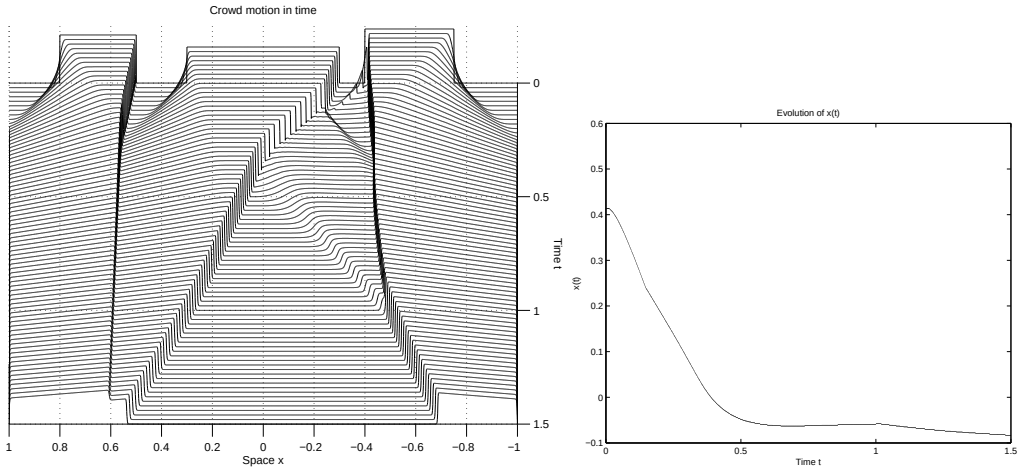

(a) $\rho(x,t)$ (b) $x(t)$

Figure 4.6: Evolution of ρ and $x(t)$

4.5 Alternative Regularization

In this section we prove that the alternative regularised problem

$$\begin{cases} \rho_t - (\rho f^2(\rho)\phi_x)_x = 0 \\ -\delta\phi_{xx} + f(\rho)^2|\phi_x|^2 = 1 \end{cases} \tag{4.57}$$

admits at least an entropy solution. The initial condition and the boundary data are posed exactly in the same way as in the previous model, therefore we shall omit them. We shall only provide a sketch of the proof. Throughout this section we will consider (4.16a), (4.16b) with homogeneous Dirichlet boundary conditions for ρ and ϕ and $\rho_I \geq 0$ as initial datum.

As we did in the previous case, we approximate the scalar conservation law by the viscous approximation

$$\rho_t - (\rho f^2(\rho)\phi_x)_x = \varepsilon\rho_{xx}.$$

In order to prove existence of smooth solutions to the approximated model, one can cut off the term $f(\rho)^2|\phi_x|^2$ in the elliptic equation and send the cut-off parameter to the limit.

In order to obtain a limit for ρ_ε as $\varepsilon \to 0$, one can try to estimate the BV norm of ρ, as done in the previous approximation. Using the same arguments as in the proof of Lemma 4.3.5 we immediately have

$$\|\rho_x\|_{L^1(\Omega)} \leq C_1 e^{C_2 t}. \tag{4.58}$$

The next step would now be to derive an estimate on ρ_t. However, this has not been possible as we were not able to control terms of the form ϕ_{xt} or ϕ_{xxt}. Indeed, the time dependence of ϕ is introduced only by ρ in the term $f(\rho)|\phi_x|^2$. However, as there are no time derivatives, it is by no means straight forward to derive bounds on time derivatives of ϕ. To still obtain existence of a weak solution, we will use the following Aubin-Lions like argument (see, e.g. [106, Chapter 3.2, Thm 2.1]), using in particular the L^1 bound on ρ_x obtained above.

We consider the three Banach spaces $W^{1,1} \subset L^2 \subset H^{-1}$ with continuous injections. Note that H^{-1} is reflexive and the injection $W^{1,1} \to L^2$ is compact. Let $T > 0$ and consider the space

$$\mathcal{Y} = \left\{ v \in L^2((0,T); W^{1,1}),\ \dot{v} = \frac{dv}{dt} \in L^2((0,T); H^{-1}) \right\}$$

which, equipped with the norm

$$\|\rho\|_{\mathcal{Y}} = \|v\|_{L^2((0,T);W^{1,1}} + \|v'\|_{L^2((0,T);H^{-1})}$$

is a Banach space which is embedded in $L^2((0,T);L^2)$. Then we want to proof the following theorem

Theorem 4.5.1. *In the above setting, the injection of $\mathcal{Y}$ into $L^2((0,T);L^2)$ is compact.*

Proof. We consider a sequence ρ_m uniformly bounded in $\mathcal{Y}$. We need to show that there exists a subsequence ρ_μ which strongly converges in $L^2((0,T);L^2(\Omega))$. First we note that $W^{1,1}$ is compactly embedded into L^2. We now define the space

$$\bar{\mathcal{Y}} = \left\{ v \in L^2((0,T);L^2),\ \dot{v} = \frac{dv}{dt} \in L^2((0,T);H^{-1}) \right\}$$

which is obviously a reflexive Banach space. As the sequence ρ_m is also bounded in this space, there exist subsequences

$$\rho_\mu \rightharpoonup \rho, \text{in } L^2((0,T);L^2(\Omega))$$
$$(\rho_\mu)_t \rightharpoonup \rho_t \text{ in } L^2((0,T);H^{-1}(\Omega)).$$

Thus what we need to show is that $v_\mu = \rho_\mu - \rho$ converges strongly in $L^2((0,T);L^2)$. Assuming for a moment that $\rho_\mu - \rho$ converges to 0 strongly in $L^2((0,T);H^{-1})$ we have, due to the classical Aubin-Lions Lemma [106, Ch.2.1, Lemma 2.1]

$$\|v_\mu\|_{L^2((0,T);L^2)} \leq \eta \|v_\mu\|_{L^2((0,T);W^{1,1})} + c_\eta \|v_\mu\|_{L^2((0,T);H^{-1})}. \tag{4.59}$$

Since our sequence is bounded in $\mathcal{Y}$ we know

$$\|v_\mu\|_{L^2((0,T);L^2)} \leq \eta c + c_\eta \|v_\mu\|_{L^2((0,T);H^{-1})} \tag{4.60}$$

and as η can be chosen arbitrary we conclude

$$\lim_{\mu\to\infty} \|v_\mu\|_{L^2((0,T);L^2)} = 0.$$

Thus we only need to prove strong convergence of v_μ in $L^2((0,T);H^{-1})$. First we observe that

$$\mathcal{Y} \subset \mathcal{C}([0,T];H^{-1})$$

with a continuous injection. From this we know that there exists a constant c such that

$$\|v_\mu(t)\|_{H^{-1}} \leq c \quad \forall\, t \in [0,1], \quad \forall\, \mu.$$

Therefore, due to Lebesgue's theorem we only need to show that for almost every t in $[0,T]$,

$$v_\mu(t) \to 0 \,\text{in}\, H^{-1} \text{ strongly, as } \mu \to \infty.$$

We prove this for $t = 0$ and we write

$$v_\mu(0) = v_\mu(t) - \int_0^t v'_\mu(\tau)\, d\tau.$$

Integrating this gives

$$v_\mu(0) = \frac{1}{s}\left(\int_0^s v_\mu(t)\, dt - \int_0^s \int_0^t v'_\mu(\tau)\, d\tau dt\right). \tag{4.61}$$

Thus

$$v_\mu(0) = a_\mu + b_\mu$$

with

$$a_\mu = \frac{1}{s}\int_0^s v_\mu(t)\, dt, \qquad b_\mu = -\frac{1}{s}\int_0^s (s-t) v'_\mu(\tau)\, d\tau dt$$

Knowing that v'_μ converges weakly in H^{-1} we conclude the boundedness of $\|v'_\mu(t)\|_{H^{-1}}$ and can thus always find a s such that

$$\|b_\mu\|_{H^{-1}} \leq \int_0^s \|v'_\mu(t)\|_{H^{-1}}\, dt \leq \frac{\varepsilon}{2}.$$

□

In view of (4.58) the only thing left to show in order to apply this theorem is $\rho_t \in L^2((0,T); H^{-1})$. Multiplying (4.16a) by ρ and integrating leads

$$\begin{aligned}\frac{d}{dt}\int \frac{\rho^2}{2}\, dx &= -\varepsilon \int |\nabla \rho|^2\, dx - \int \underbrace{\rho f^2(\rho)}_{=:F'(\rho)} \nabla\rho \cdot \nabla\phi\, dx \\ &= -\varepsilon \int |\nabla\rho|^2\, dx + \int F(\rho)\Delta\phi\, dx\end{aligned}$$

By integrating with respect to time we obtain

$$\sqrt{\varepsilon}\nabla\rho \in L^2((0,T);L^2),\ \rho \in L^\infty((0,T);L^2)$$

and thus, via the equation we obtain

$$\rho_t \in L^2((0,T);H^{-1}).$$

Thus using Theorem 4.5.1 we conclude the compactness of ρ^ε in $L^2((0,T);L^2(\Omega))$ and therefore, by compactness, the existence of a weak solution (ρ,ϕ) to (4.57).

Chapter 5

Continuous Limit of a Crowd Motion and Herding Model

5.1 Introduction

This Chapter deals with the analysis and numerical simulation of a macroscopic model for the motion of a human crowd, derived by (formally) passing to a continuous limit from a microscopic cellular automata model developed by Kirchner and Schadschneider, cf. [59]. In their approach, the crowd is considered as a group of a finite number of individuals located on a rectangular two-dimensional grid. Giving a discrete time step, the model provides for each individual in a given cell the probability to jump into a neighbouring cell. This probability is determined by several factors. First of all, individuals are not allowed to jump to an occupied cell (size exclusion, cf. [103]). Furthermore, there exist two driving forces, called "floor fields", cf. [16], respectively, a static field S and a dynamic field D on which the jump-probability depends exponentially. The static field provides the individuals with a sense of their environment, increasing towards locations they want to reach, such as doors. Being zero at the initial time, its value is increased whenever a particle leaves a cell. Thus it models the tendency of people to follow others, called herding. The term herding originates from animal herds. For human crowds it can "be broadly defined as the alignment of the thoughts or behaviours of individuals in a group (herd) through local interaction and without centralized coordination", cf. [92]. To study the herding capabilities (and limitations) of the model under consideration is one of the main goals of this paper. Interestingly, herding is not only observed

in the movement of human crowds but also in its behaviour on financial markets, cf. [8, 87, 28]. We emphasize that the dynamic field is created by a local interaction and is thus in agreement with this definition of herding.
We finally remark that this model can be seen as a (non-linear) variant of the famous Patlak-Keller-Segel model for chemotatic movement of cells (cf. [57, 52, 53]). In chemotaxis, the random movement of (biological) cells is biased by a chemical substance. This so-called chemoattractant is a chemical emitted by the cells if e.g. they found a food source and which has the function to lead other cells to this source. The dynamical behaviour of the chemoattractant is subject to degradation and diffusion. In our model, the dynamic floor field has a similar function. A striking difference however is that it does not correspond to a physical substance. Thus it may be called a "virtual chemoattractant", cf. [59]. Due to the finite size exclusion in the microscopic approach, this model features a non-linear mobility, proportional to $1-\rho$. This has also been discussed in the context of chemotaxis, cf. [89]. It prevents the model from showing a blow-up phenomena as known from the original Keller-Segel model for initial data with a mass above a certain threshold (cf. [6]). In this Chapter we will consider analytical issues such as linear stability of stationary solutions which, as we shall explain below, is closely linked to congestion. We provide extensive numerical simulations in one and two space dimensions, using specially designed experiments to analyse herding effects.
We shall also provide several results yielding improved understanding of the model by Kirchner and Schadschneider.

- A continuum limit exhibiting connections to (non-linear) chemotaxis and animal herding models (Section 2).
- A discussion of appropriate boundary conditions for modelling crowds in contained environments and a discussion of stationary states, related to the possibility of congestion.
- A discussion of numerical schemes allowing efficient simulations in set-ups with complicated geometries (Section 4).
- A discussion of particular limitations of the herding model, which occurs in a simulation with non-convex obstacles. Here the local definition of the dynamic fields yields counter-intuitive behaviour since the herding only affects local movement of the crowd but not the trend to follow those finding escape routes (Section 5).

5.2 The Microscopic Model

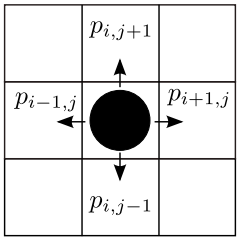

Figure 5.1: A particle on the two-dimensional cell grid

In this Section we shall give a more detailed description of the microscopic model, especially how it incorporates herding effects. As mentioned in the introduction, the model is set up on a two-dimensional rectangular grid and is discrete in time. The size of one cell is typically about $40 \times 40\,\mathrm{cm}^2$, cf. [95]. This value originates from a maximal density of 6.25 people per m^2, cf. [110]. In the following we assume a grid of size $N \times M$. An agent located in a given cell (i, j), $i = 1, \ldots, N$, $j = 1, \ldots, M$, can, at each time step, jump into one of its neighbouring cells, as depicted in Figure 5.1. Since the empirical determined average speed of a person is around $1.3\,\mathrm{m/s}$, cf. [110], a person would need about 0.3 seconds to walk through one cell. This naturally defines a time scale for the model, cf. [58]. For each cell there is a probability to jump into it and the particle chooses the cell with the highest probability. This probability is determined by three basic principles:

1. **Size exclusion**: A cell can only be occupied by one particle at each time step, i.e. its occupation number $n_{i,j}$ is either one or zero. This corresponds to the obvious assumption that there exist a maximal number of people that can occupy a certain amount of space. The model is set up such that each cell can accommodate no more than one individual.

2. **Static floor field** S: The static floor field is, as its name suggests, given and constant in time. It is used to lay down the attractiveness of certain space regions. A typical choice is the distance to an exit (given in e.g. the Euclidean or Manhattan norm) but it could also used to mark places within the domain which people want to reach, a ticket counter for example. The convention in the model is that the field increases in more attractive regions.

3. **Dynamic floor field** D: This second floor field accounts for the effect of herding. The basic idea is that, in a large crowd, people are more likely to walk into directions where they see other people moving. This is because they assume that the density in these regions is relatively low and that by moving into them they can increase their speed and reach their target earlier. Thus the dynamic field on a cell increases whenever a particle leaves it. Of course, as the distribution of particles changes, this information is only valid for a short time. This is modelled by a degradation effect. Finally, as the observations people make are not assumed to be precise, the dynamic field is also assumed to diffuse. How the field is calculated exactly in the discrete setting will be explained below.

With these ingredients at hand, the probability to jump to a cell i, j is given by

$$P_{i,j} = N_{i,j} \exp\left(k_D D_{i,j}\right) \exp\left(k_S S_{i,j}\right)(1 - n_{i,j})\xi_{i,j}.$$

The term $(1 - n_{i,j})$ accounts for the size exclusion effect rendering the probability zero if a cell is occupied. The positive constants k_D and k_S regulate the relative influence of the two floor fields. Obstacles such as walls, tables and so on are incorporated via $\xi_{i,j}$ which is zero if a cell belongs to an obstacle and one otherwise. Finally, $N_{i,j}$ is a normalisation factor given by

$$1\,/N_{i,j} = \sum_{k=i-1,i+1} \sum_{l=j-1,j+1} e^{k_D D_{k,l}} e^{k_S S_{k,l}}.$$

5.2.1 Calculation of the Dynamic Floor Field

At the beginning of a simulation, the dynamic field is zero on every cell. It is then updated in each time step t_k using the following rules

- It is increased by one whenever a particle left a cell, i.e.

$$D_{i,j}^{k+1} = \begin{cases} D_{i,j}^k + 1 & \text{if } (n_{i,j}^k - n_{i,j}^{k+1}) = 1 \\ D_{i,j}^k & \text{otherwise} \end{cases}$$

- If $D \geq 1$, it decreases by a given probability $\delta > 0$, i.e. given a random number p

$$D_{i,j}^{k+1} = \begin{cases} D_{i,j}^k - 1 & \text{if } p < \delta \\ D_{i,j}^k & \text{otherwise} \end{cases}$$

- The diffusion is implemented in the following way: Given is a fixed constant $\kappa \in \mathbb{R}_+$, in each time step, a random number p is generated. If $p < \kappa$, the D field is lowered by one and increased by one on a randomly chosen neighbouring cell.

Note that these rules imply that the value of D is always a non-negative integer.

5.2.2 Herding Effects

As mentioned in the introduction a remarkable feature of the model is to incorporate herding effects via the dynamic field. We consider the following example: a number of the people is situated in a room and want to leave it using a single door (i.e. in an evacuation). In their original paper, cf. [59], the authors simulated this situation and obtained that the evacuation time, i.e. the time until the room is empty, becomes smaller the larger the coupling parameter k_D is. The intuitive explanation is that once people found a way to the door, other people start following them. We shall however show that in more complicated geometries, the dynamic field might also yield a larger evacuation time, cf. Section 5.7.

5.3 Derivation of the Macroscopic Model

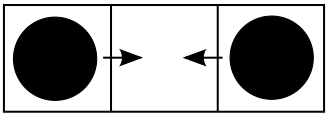

Figure 5.2: The microscopic setting in one space dimension.

In this Section we shall derive a system of partial differential equations from the discrete model, cf. [104, 103]. We perform this procedure only in one space dimension as it is analogous in higher dimensions. Thus were a dealing with row of N cells of width h as shown in Figure 5.2. We assume a scaling such that the total length of the row is one, i.e. $hN = 1$. To pass to the limit, we need to rephrase the model in the following way: First, we denote by x_i the midpoint of cell i, $i = 1, \ldots, N$. Next we introduce the following functions

$$S : [0,1] \times \mathbb{R}_+ \to \mathbb{R}_+ \quad D : [0,1] \times \mathbb{R}_+ \to \mathbb{R}_+ \quad \rho : [0,1] \times \mathbb{R}_+ \to [0,1] \tag{5.1}$$

The function S is the continuous analogue to the static floor field and assumed to be given. By $\rho(x,t)$ we denote the probability to find an particle at position x and time t. $D = D(x,t)$ is a random variable whose expected value corresponds to the value to the dynamic floor field at (x,t). The probability to jump into cell i at time $t_k = k\Delta t$, $k \in \mathbb{N} \setminus 0$ is given by

$$P(x_i) = Ne^{k_D D(x_i,t_k)} e^{k_S S(x_i)} (1 - \rho_i(x_i,t_k))\xi_i, \tag{5.2}$$

with

$$N(x_i) = \frac{1}{\sum_{k=i-1}^{i+1} e^{k_D D(x_i,t_k)} e^{k_S S(x_i)}}.$$

Remark 5.3.1 (Closure Assumption)**.** *We remark, that the above probability already contains a closure assumption. A priori, only $n_{i,j}$, i.e. the information whether cell (i,j) is occupied or not is known. However, in* (5.2) *we used the probability of the cell being occupied or not. In cases in which the macroscopic limit can be justified rigorously, this closure assumption turned out to be the right one, cf. [43], which motivates our choice.*

With this notation at hand we have the following update rule for ρ

$$\begin{aligned} \rho(x_i,t_{k+1}) = {} & P(x_i,t_k)(\rho(x_{i-1},t_k) + \rho(x_{i+1},t_k)) \\ & + \rho(x_i,t)(1 - P(x_{i-1},t_k) - P(x_{i+1},t_k)), \end{aligned} \tag{5.3}$$

i.e. the probability to find a particle at x, $t + \Delta t$ is given by the probability that a particle jumps into this cell minus the probability that a particle leaves the cell if it was already occupied and

$$D(x_i,t_{k+1}) = D(x_i,t_k) + (\Delta t)\rho(x_i,t_k)(P(x_{i-1},t_k) + P(x_{i+1},t_k)) - \delta D(x_i,t_k), \tag{5.4}$$

i.e. value of D increases, whenever a particle leaves an occupied field and decreases with rate $\delta > 0$. We first take a closer look at eq. (5.3). Taylor expansion of the right hand side leads to

$$\begin{aligned} \rho(x_i,t+\Delta t) - \rho(x_i,t) &= h^2 P(x_i,t)\frac{\partial \rho}{\partial x}(x_{i+1},t) - h^2\rho(x_i,t)\frac{\partial P}{\partial x}(x_{i+1},t) \\ &= h^2 P(x_i,t)\frac{\partial \rho_i}{\partial x}(t) - h^2\rho(x_i,t)\frac{\partial}{\partial x}\left(Ne^{k_S S}e^{k_D D}\left[(1-\rho(x_i,t))(\nabla D + \nabla S) - \frac{\partial \rho(x_i,t)}{\partial x}\right]\right) \\ &= h^2\frac{\partial}{\partial x}\left(Ne^{k_S S}e^{k_D D}\frac{\partial \rho(x_i,t)}{\partial x}\right) - h^2\frac{\partial}{\partial x}\left(Ne^{k_S S}e^{k_D D}\rho(x_i,t)(1-\rho(x_i,t))(\nabla D + \nabla S)\right). \end{aligned}$$

Dividing this expression by h^2, choosing the scaling $\Delta t = h^2$ and passing to the limit $h \to 0$ we obtain the following limiting equation

$$\partial_t \rho + \frac{1}{3}\mathrm{div}(\rho(1-\rho)(k_S \nabla S + k_D \nabla D)) = \frac{1}{3}\Delta\rho. \tag{5.5}$$

Here we made use of

$$F_i(h^2) := e^{k_D D(x_i)} e^{k_S S(x_i,t)} N_i = \frac{e^{k_D D(x_i,t)} e^{k_S S(x_i)}}{3e^{k_D D(x_i,t)} e^{k_S S(x_i)} + O(h^2)} \overset{h\to 0}{\longrightarrow} \frac{1}{3}. \tag{5.6}$$

For (5.4), we apply the same procedure yielding

$$\begin{aligned}
\frac{D(x_i, t+\Delta t) - D(x_i,t)}{\Delta t} &= \rho_i(t)(P(x_{i+1},t) + P(x_{i-1},t)) - \delta D(x_i,t_k) \\
&= \rho(x_i,t)(F_{i+1}(h^2)(1-\rho(x_{i+1},t) + F_{i-1}(h^2)(1-\rho(x_{i-1},t)) - \delta D(x_i,t_k) \\
&= \rho(x_i,t)\left(F_{i+1}(h^2)(1-\rho(x_i,t) + F_{i-1}(h^2)(1-\rho(x_i,t)\right) - \delta D(x_i,t_k) \\
&+ \rho(x_i,t)\left(h\left(F_{i+1}(h^2)\frac{\partial\rho(x_i,t)}{\partial x} - F_{i-1}(h^2)\frac{\partial\rho(x_i,t)}{\partial x}\right)\right) - \delta D(x_i,t_k) \\
&+ O(h^2)
\end{aligned}$$

In the limit $\Delta t = h^2 \to 0$, the last term on the r.h.s vanishes and we obtain

$$\partial_t D = -\delta D + \frac{2}{3}\rho(1-\rho).$$

As it is well known that the diffusion algorithm described in Subsection 5.2.1 yields, in the continuum limit a term $\kappa\Delta D$, we arrive at

$$\partial_t D = \kappa\Delta D - \delta D + \frac{2}{3}\rho(1-\rho). \tag{5.7}$$

Remark 5.3.2. *In [58, Sec. 3.5.2], an alternative definition of the dynamic field is given, namely that the value of the D in a certain cell is increased whenever the cell is occupied, i.e.*

$$D_i(t+\Delta t) = D_i(t) + (\Delta t)\rho_i(t).$$

We remark that in the continuous limit, this results in a system with a linear coupling in the D equation which reads

$$\partial_t \rho = \Delta\rho - \mathrm{div}(\rho(1-\rho)(k_D\nabla D + k_S \nabla S)), \tag{5.8}$$

$$\partial_t D = \Delta D - \delta D + \rho. \tag{5.9}$$

This system has already been analysed extensively in the context of chemotaxis, cf. [29].

5.4 Basic Properties of the Model

In this Section we shall discuss properties of the system derived above. First we note that with an appropriate scaling of t and D, we obtain an diffusion coefficient equal to one in the equation for ρ and can also remove the factor $\frac{2}{3}$ in front of the non-linear coupling in the equation for D. We arrive at

$$\rho_t = \Delta\rho - \operatorname{div}(\rho(1-\rho)(k_D\nabla D + k_S\nabla S)), \tag{5.10}$$

$$D_t = \kappa\Delta D - \delta D + \rho(1-\rho). \tag{5.11}$$

We denote by j the total flux in ρ, i.e.

$$j := \rho(1-\rho)(k_D\nabla D + k_S\nabla S) - \nabla\rho$$

5.4.1 Boundary Conditions

For the boundary conditions, we prescribe homogeneous Neumann conditions for D, i.e.

$$\nabla D \cdot n = 0 \text{ on } \partial\Omega$$

where n denotes the outward normal on $\partial\Omega$. This means that the total mass of the dynamic field only changes via its creation and degradation within the domain. To define realistic boundary boundary conditions on ρ is not as straightforward as for D. First, we divide the boundary into two parts, namely doors and walls

$$\partial\Omega := \partial\Omega_D \cup \partial\Omega_W.$$

In our approach, we assume that as soon as people reached a door, they leave the domain with a given outflow velocity v_0 of Euclidean norm 1 pointing outside. Of course, people leave the domain proportional to their density at the door and thus we have

$$j \cdot n = \rho v_0 \cdot n \text{ on } \partial\Omega_D.$$

This means in particular that the size exclusion no longer holds once people reached the door, i.e. the space behind the door is assumed to be large enough to allow everybody to exit with speed v_0. A typical choice for v_0 would be $k_S\nabla S$. On the wall segments, we prescribe no-flux boundary conditions, i.e.

$$j \cdot n = 0 \text{ on } \partial\Omega_W.$$

Note that due to the Neumann conditions on D, if $\nabla S \cdot n = 0$, this is equivalent to homogeneous Neumann conditions on ρ (assuming no vacuum and no saturation on $\partial\Omega_w$). Furthermore, we supplement the system with the initial conditions

$$\rho(t=0) = \rho_I,$$
$$D(t=0) = D_I.$$

5.4.2 Well-posedness

Under appropriate conditions on the initial datum $u_I = (\rho_I, D_I)$, existence and uniqueness of a weak solution for this system is well-known. For the sake of simplicity we will only state the result with the simplification of homogeneous Dirichlet boundary conditions. We define

$$\mathcal{V} := \left\{(u,v) \mid (u,v) \in W^{1,p}(\Omega;\mathbb{R}^2),\ 0 \le u \le 1, 0 \le v \text{ on } \bar{\Omega},\ u = v = 0 \text{ on } \partial\Omega\right\}.$$

We note that existence of a solution in $\mathcal{V}$ especially implies that the ρ is always less or equal to one. This reflects the size exclusion present in the microscopic model. Furthermore, also the non-negativity of D is preserved. We have the following theorem

Theorem 5.4.1 ([112, Thm. 2.1])**.** *Assume $p > n$, $p \ge 2$. If furthermore $(u_I, D_I) \in \mathcal{V}$ then for arbitrary $t > 0$ there exist unique global solutions (u, D) of* (5.10), (5.11) *with $(u(t), D(t)) \in \mathcal{V}$.*

We remark that for the realistic boundary conditions stated above, we expect less regularity of the solutions. In particular, the flux may become discontinuous at the edges of doors. The regularity of the flux will depend on the geometry and regularity of the boundary, cf. [77, 46].

5.4.3 Stationary Solutions

In this Section we examine the stationary system, i.e.

$$0 = \operatorname{div}(\nabla\rho_\infty - \rho_\infty(1-\rho_\infty)(k_S\nabla S + k_D\nabla D_\infty)), \tag{5.12}$$
$$0 = \kappa\Delta D_\infty - \delta D_\infty + \rho_\infty(1-\rho_\infty). \tag{5.13}$$

Here we assume no flux boundary conditions on ρ and D. For the first equation, it suffices to find ρ_∞ such that the total flux is zero, i.e.

$$0 = \rho_\infty(1-\rho_\infty)(k_S\nabla S + k_D\nabla D_\infty) + \nabla\rho_\infty.$$

Dividing by $\rho_\infty(1-\rho_\infty)$ leads to

$$0 = \frac{\nabla\rho_\infty}{\rho_\infty(1-\rho_\infty)} + (k_S\nabla S + k_D\nabla D_\infty) = \nabla\left(\log\left(\frac{\rho_\infty}{1-\rho_\infty}\right) + k_S S + k_D D_\infty\right).$$

Integrating this equation we obtain

$$\log\left(\frac{\rho_\infty}{1-\rho_\infty}\right) = k - k_S S - k_D D,$$

and thus (with $K = e^k$)

$$\rho_\infty = \frac{Ke^{-k_S S - k_D D_\infty}}{1 + Ke^{-k_S S - k_D D_\infty}}. \tag{5.14}$$

The constant K is implicitly determined by the total mass

$$M := \int_\Omega \rho \, dx. \tag{5.15}$$

To obtain the stationary solutions D_∞ to the second equation, we have to solve the following non-linear elliptic mean-field problem

$$\kappa\Delta D_\infty - \delta D_\infty = -\rho_\infty(1-\rho_\infty)$$

where the right hand side

$$-\rho_\infty(1-\rho_\infty) = -\frac{Ke^{-k_S S - k_D D_\infty}}{(1 + Ke^{-k_S S - k_D D_\infty})^2}.$$

is bounded between zero and minus one. We point out that uniqueness of a solution can be obtained by Banach's fixed point theorem if either δ is large or k_D is small enough.

Remark 5.4.2 (Constant Stationary Solutions)**.** *We consider the special case of constant stationary solutions. We note that $\rho_\infty = const$, $D_\infty = const$ solves* (5.12)*, if $S = 0$. From* (5.15) *we find*

$$\rho_\infty = \frac{|\Omega|}{M}.$$

Assuming $\delta > 0$, equation (5.13) *reduces to the following simple algebraic expression*

$$D_\infty = \frac{1}{\delta}\rho_\infty(1-\rho_\infty).$$

Thus as long as $\delta > 0$, there always exists constant stationary solutions (ρ_∞, D_∞), uniquely determined by the total mass M.

Linear Stability

We shall now derive stability properties of the stationary solutions considered above. Constant stationary solutions correspond to situations without congestion and it is thus important to understand if they prevail under perturbation. Consider the following example: A long corridor (e.g. in an airport) with people moving only in one direction. Assume that approximately the same amount of people leave and enter the corridor. After some time, this system can assumed to be in the stationary regime. If people can move freely through the corridor, we expect a constant density depending only on the amount of people entering or leaving as well as their preferred speed. A congestion however would be a region of higher density located somewhere in the corridor. An important question from the application point of view is under which conditions the constant state is stable under small perturbations (i.e. some people stopping for a short time creating a small region of slightly increased density). The linear stability analysis gives an answer to the question in terms of the value of the constant density ρ_∞ as well as the parameters k_D, κ and δ. For simplicity, we set $S = 0$ in the following and examine the perturbation of the constant equilibria ($(u, v) \in \mathcal{V}$)

$$\tilde{\rho} = \rho_\infty + \epsilon u, \quad \tilde{D} = D_\infty + \epsilon v, \tag{5.16}$$

where we assume homogeneous Dirichlet boundary conditions for u and v. Using this ansatz in (5.10), (5.11), we arrive at

$$\begin{aligned}
\epsilon\partial_t u &= \Delta(\rho_\infty + \epsilon u) + \operatorname{div}((\rho_\infty + \epsilon u)(1 - (\rho_\infty + \epsilon u))k_D\nabla(D_\infty + \epsilon v)) \\
&= \Delta(\rho_\infty + \epsilon u) + \operatorname{div}((\rho_\infty(1 - \rho_\infty) - 2\epsilon u\rho_\infty + \epsilon u)(k_D\nabla D_\infty + \epsilon k_D\nabla v)) \\
&= \underbrace{\operatorname{div}(\nabla\rho_\infty + (\rho_\infty(1 - \rho_\infty)\nabla D_\infty))}_{=0} + \epsilon\Delta u + \epsilon\operatorname{div}(\rho_\infty(1 - \rho_\infty)k_D\nabla v) \\
&\quad + \underbrace{\epsilon\operatorname{div}(u(1 - 2\rho_\infty)\nabla D_\infty)}_{=0} + \mathcal{O}(\epsilon^2)
\end{aligned}$$

and

$$\epsilon\partial_t v = \underbrace{\kappa\Delta D_\infty - \delta D_\infty + \rho_\infty(1 - \rho_\infty)}_{=0} + \epsilon\kappa\Delta v - \epsilon\delta v - \epsilon u(1 - 2\rho_\infty) + \mathcal{O}(\epsilon^2).$$

Dividing by ϵ and letting $\epsilon \to 0$ we obtain the following linearisation

$$\partial_t u = \Delta u + \operatorname{div}(\rho_\infty(1 - \rho_\infty)k_D\nabla v), \tag{5.17}$$

$$\partial_t v = \kappa\Delta v - \delta v + u(1 - 2\rho_\infty). \tag{5.18}$$

We first analyse this system in one space dimension using the Fourier series method:

$$\partial_t u = u_{xx} + k_D \rho_\infty (1 - \rho_\infty) v_{xx},$$
$$\partial_t v = \kappa v_{xx} - \delta v_{xx} + u(1 - 2\rho_\infty).$$

The ansatz

$$u = \sum_{n \in \mathbb{Z}} c_n(t) e^{inx}, \quad v = \sum_{n \in \mathbb{Z}} d_n(t) e^{inx}$$

leads to (for all $n \in \mathbb{Z}$)

$$\begin{pmatrix} c_n' \\ d_n' \end{pmatrix} = \begin{pmatrix} -n^2 & -k_D k_1 n^2 \\ k_2 & -\kappa n^2 - \delta \end{pmatrix} \begin{pmatrix} c_n \\ d_n \end{pmatrix} =: M \begin{pmatrix} c_n \\ d_n \end{pmatrix}$$

with

$$k_1 := \rho_\infty(1 - \rho_\infty), \; k_2 := (1 - 2\rho_\infty).$$

The corresponding eigenvalues of this 2×2 ODE system are

$$\lambda_{1,2} = -\frac{1}{2}\delta - \frac{1}{2}n^2(\kappa + 1) \pm \frac{1}{2}\sqrt{n^4(1 - k^2) + 2n^2\delta(\kappa - 1) + \delta^2 + 4k_D k_1 k_2 n^2}.$$

Consider the larger one only, then the condition for λ_2 to be negative is

$$k_D k_1 k_2 - \delta \leq \kappa n^2 \tag{5.19}$$

Due to the homogeneous Dirichlet boundary conditions for the perturbations, the lowest order mode is zero. Thus, due to (5.21), the effect of the instability is largest in the first mode yielding the condition

$$k_D k_1 k_2 - \delta \leq \kappa. \tag{5.20}$$

We summarize these results in the following

Proposition 5.4.3 (Linear stability)**.** *Let (ρ_∞, D_∞) be a constant solution to system* (5.12)-(5.13)*. If the condition*

$$k_D k_1 k_2 - \delta \leq \kappa, \tag{5.21}$$

is fulfilled, this solution is linearly stable with respect to small perturbations.

We point out that, at least for simple geometries of Ω, this procedure also works in two space dimension. For example for the case of a quadratical domain Ω, the Fourier series is given by

$$u = \sum_{n,m\in\mathbb{Z}} c_{n,m}(t)e^{inx}e^{imy}, \quad v = \sum_{n,m\in\mathbb{Z}} d_{n,m}(t)e^{inx}e^{imy}.$$

Instead of (5.19) we obtain

$$k_D k_1 k_2 - \delta \leq \kappa(n^2 + m^2).$$

In Section 5.6.1, we shall present numerical simulations confirming this result in both one and two space dimensions.

Plateau Solutions

In the case of a constant stationary state being linearly unstable it is natural to look for other stationary solutions or at least meta-stable ones in the dynamics. As explained above these solutions are of special interest as from the modelling point of view they correspond to congestion effects. A congestion should be related to a plateau of higher density. In this Section, we shall show that non constant meta-stable solutions indeed have the form of plateaus, i.e. being asymptotically piecewise constant. In particular a large coupling constant k_D and a small diffusion coefficient κ are promising parameters to vary, as suggested by the linear stability condition. Rescaling the coupling coefficient to 1 would correspond to a small diffusion coefficient in the equation for ρ. For small diffusion coefficients meta-stable plateau solutions have indeed already been observed:

- In the Keller-Segel model with volume filling, which corresponds to our model with $\rho(1-\rho)$ replaced by ρ, i.e.

  $$\partial_t D = \kappa\Delta D - \delta D + \rho.$$

  This equation corresponds to an attractive force, the bacteria want to concentrate on or near their food source yielding the positive coupling term. Meta-stable plateau solutions are obtained for small diffusion coefficients in the equation for ρ (cf. [31, 10]).

- In the Poisson-Nernst-Planck equations with size exclusion, corresponding to

  $$\partial_t D = \kappa\Delta D - \rho.$$

Here, the repulsive Coulomb force between equally charged ions accounts for the negative coupling term $-\rho$. Stationary solutions are obtained in the presence of additional external potentials for small diffusion coefficients in the Poisson equation (the equation for D, cf. [13]). This is corresponding to the well-studied limit of small Debye length in the semiconductor drift-diffusion equations (cf. [78]).

We are facing a mixed situation compared to the two types of models above, which are either based on attractive of repulsive interactions. Even though the coupling term $\rho(1-\rho)$ itself is always positive, in our case interactions are attractive for small densities, but repulsive for large densities. We illustrate this using a simplified version of the model. Consider the quasi-stationary case with zero diffusion in D, i.e.

$$D = \frac{1}{\delta}\rho(1-\rho),$$

which, inserted in (5.10), yields the forward-backward diffusion equation

$$\rho_t = \operatorname{div}\left(1 - \frac{k_D}{\delta}\rho(1-\rho)(1-2\rho)\nabla\rho\right). \tag{5.22}$$

Note that the equation is always forward parabolic for $\rho \geq \frac{1}{2}$ and around $\rho = 0$, however for $\gamma := \frac{k_D}{\delta}$ large there exist intermediate densities such that the diffusion coefficient becomes negative, yielding backward diffusion which corresponds to an attractive force. We will thus investigate asymptotics of plateau-like stationary solutions for small parameter $\epsilon = \frac{\sqrt{\kappa}}{\delta}$ in the stationary system

$$\begin{aligned} \operatorname{div}(\nabla\rho_\infty - \gamma\rho_\infty(1-\rho_\infty)\nabla D_\infty) &= 0 \\ -\epsilon^2\Delta D_\infty + D_\infty &= \rho_\infty(1-\rho_\infty). \end{aligned} \tag{5.23}$$

or

$$\rho_\infty = \frac{e^{\gamma D_\infty}}{c_K + e^{\gamma D_\infty}}. \tag{5.24}$$

with $c_K = 1/K$. In order to gain understanding of the asymptotics it is convenient to assume c_K is given (we then obtain solutions for different masses by varying c_K), which we shall do in the following. Setting directly $\epsilon = 0$ we obtain $D_\infty = \rho_\infty(1-\rho_\infty)$ and thus the fixed-point equation

$$\rho_\infty = \frac{e^{\gamma\rho_\infty(1-\rho_\infty)}}{c_K + e^{\gamma\rho_\infty(1-\rho_\infty)}} = F(\rho_\infty). \tag{5.25}$$

This equation has at least one fixed point since $0 < \frac{1}{c_K+1} = F(0) = F(1) < 1$. For many values of c_K and γ, it has a unique fixed point, thus we only expect the regular asymptotics of constant stationary solutions. The situation is more interesting if there are multiple fixed points, namely two stable (i.e. $F' < 0$) and one unstable (i.e. $F' > 0$) one. Using a piecewise constant approximation of the numerically obtained solution shown in Figure 5.7 yields approximately $c_K = 91$. Choosing $\gamma = 20$, we indeed obtain three fixed points, see Figure 5.3. Denoting by a and b the two stable fixed ones, we expect plateau-like solutions of the form

$$\bar{\rho}_\infty = \begin{cases} a & \text{in } \bar{\Omega}, \\ b & \text{else} \end{cases} \quad \text{and} \quad \bar{D}_\infty = \bar{\rho}_\infty(1 - \bar{\rho}_\infty)$$

which indeed appear in numerical simulations as we shall see below. To obtain an

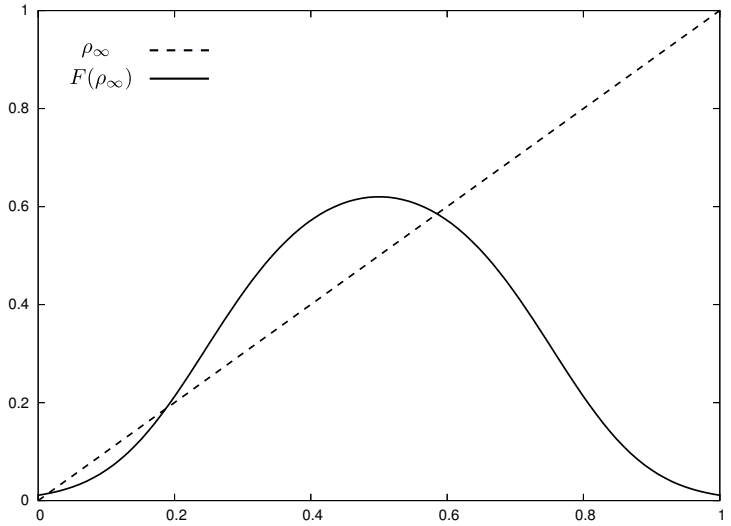

Figure 5.3: Solutions to $F(\rho_\infty) = \rho_\infty$ for $c_K = 91$ and $\gamma = 20$

(formal) analytical confirmation that solutions of this form exist, we now eliminate ρ_∞ via (5.24) and work with the resulting equation for D

$$-\epsilon^2 \delta D_\infty + D_\infty = \frac{c_K e^{\gamma D_\infty}}{(c_K + e^{\gamma D_\infty}))^2}. \tag{5.26}$$

We define $\Gamma := \partial\bar{\Omega} \setminus \partial\Omega$ and denote by d the signed distance to $\Gamma(t)$, where we choose d to be negative outside and positive inside the plateau. In order to resolve the local change in normal direction we define a local variable $z := \frac{d(x)}{\epsilon}$ and expand the solutions

in the form

$$\rho_\infty = \sum_{j=0}^{\infty} f_j\,(x,z)\,\epsilon^j$$
$$D_\infty = \sum_{j=0}^{\infty} g_j\,(x,z)\,\epsilon^j.$$

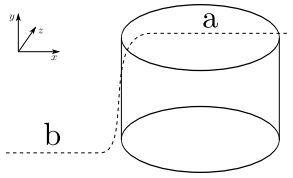

Figure 5.4: New coordinates close to plateau solutions

The leading order equation in the interfacial layer is given by

$$-\partial_{zz} g_0 + g_0 = \frac{c_K e^{\gamma g_0}}{(c + e^{\gamma g_0})^2} \tag{5.27}$$

supplemented with the conditions

$$g_0 \to a(1-a) \text{ for } z \to \infty$$
$$g_0 \to b(1-b) \text{ for } z \to -\infty.$$

This equation determines the exact form of the transition between the boundary values on the plateaus.

The next order is given by

$$-\partial_{zz} g_1 - \partial_z g_0 \Delta d - 2\nabla_x \partial_z g_0 \cdot \nabla d = F'(g_0) g_1 \tag{5.28}$$

with homogeneous boundary values. In one spatial dimension (due to the absence of curvature effects, $\Delta d = 0$) we have

$$-\partial_{zz} g_1 = F'(g_0) g_1,$$

which has a trivial solution $g_1 = 0$.

In higher spatial dimension the mean curvature (equal to Δd) in the first-order determines the shape of the interface. In order to extract the appropriate equation, we use the non-trivial solution $\psi_1(z)$ of the homogeneous problem

$$-\psi_1'' = \lambda F'(g_0)\psi_1,$$

where $0 < \lambda < 1$ is the smallest eigenvalue of the operator. Multiplying the first-order equation by ψ and integrating with respect to z we obtain

$$A(x)\Delta d + 2\nabla_x A(x) \cdot \nabla d = B(x), \tag{5.29}$$

with the coefficients

$$A(x) = \int \psi_1(z)\partial_z g_0(z)\ dz, \quad B(x) = (\lambda - 1) \int \psi_1(z)F'(g_0)g_1\ dz.$$

The simplest solution we expect to be radially symmetric. Thus we chose an ansatz which only depends on z and not explicitly on x and therefore

$$\Delta d = \text{const.} \tag{5.30}$$

This means in 2 spatial dimensions there indeed exist solutions such that the interface is a circle or a part of a circle if cut by $\partial\Omega$. As we shall see below such solutions appear in numerical simulations.

5.5 Numerical Simulations

In this Section we shall discuss numerical methods used for computational experiments. All numerical simulations are carried out on a domain of size one, i.e. $\Omega = [0, 1]$ in one and $\Omega = [0, 1] \times [0, 1]$ in two space dimensions. Note that we will not give any details on the calculation of the static field S. In the original definition of the model, attractive regions such as doors or escape routes can be modelled as regions where the value of S is large compared to other parts of the domain, cf. [58]. In the cases we are concerned with here we only consider the case where S is given by a constant minus the distance to the door, i.e.

$$S(x) = S_{max} - \text{dist}(x, \text{“door”}).$$

The constant S_{max} is typically defined as the maximum distance to the door. This ensures that S assumes is maximum value at and decreases with increasing distance from the door. As the geometry in our examples is very simple, the distance to the door can be obtained by basic geometric considerations. However, for more complex geometries, it might be necessary to use an Euclidean shortest path algorithm such as Dijkstra's algorithm, cf. [30]. Finally we remark that to visualise the results of the two dimensional finite element simulations, we used the freely available tool Visit (cf. [2]).

5.5.1 Simulations in one space dimension

In one space dimension, we use a simple semi-implicit finite difference scheme to solve a linearised version of system (5.10), (5.11), namely

$$\begin{aligned}\rho_t &= \rho_{xx} - (\rho(1-\tilde{\rho})(k_D\tilde{D}_x + k_S S_x))_x,\\ D_t &= \kappa D_{xx} - \delta D + \rho(1-\tilde{\rho}),\end{aligned}$$

with $x \in \Omega_1 := [0,1]$ and supplemented with an initial datum ρ_0. As we are interested in the linear stability properties we prescribe homogenious Neumann boundary conditions for both ρ and D, i.e. we assume a domain with no doors. We divide the domain into N equidistant intervals of length Δh and denote by

$$\rho_i(t) := \rho(i\Delta x, t),\ D_i(t) := D(i\Delta x, t),$$

and so on, the values of the solution at each grid point at time t. We also discretise time in portions of size Δt and write $t_k := k\Delta t$. Then our semi-implicit scheme reads

$$\begin{aligned}\frac{\rho_i(t_k) - \rho_i(t_{k-1})}{\Delta t} &= \frac{\rho_{i+1}(t_n) - 2\rho_i(t_n) + \rho_{i-1}(t_n)}{(\Delta x)^2}\\ &\quad - \partial_x^i\left((\rho_i(t_k)(1-\rho_i(t_{k-1}))(k_D\partial_x^i D(t_{k-1}) + k_S\partial_x^i S)\right),\end{aligned}$$

and

$$\frac{D_i(t_k) - D_i(t_{k-1})}{\Delta t} = \kappa\frac{D_{i+1}(t_n) - 2D_i(t_n) + D_{i-1}(t_n)}{(\Delta x)^2} - \delta D_i(t_k) + \rho_i(t_k)(1-\rho_i(t_{k-1})),$$

where ∂_x^i denotes the discrete first derivative at the ith grid point obtained by a central difference quotient, i.e.

$$\partial_x^i D(t_k) = \frac{D_{i+1}(t_k) - D_{i-1}(t_k)}{2\Delta x}.$$

To implement the scheme, we used matrix and vector classes from the NgSolve package, cf. [98] and use the sparse direct solver Pardiso, cf. [96, 97].

5.5.2 Simulations in two space dimensions

In two space dimensions, we use a hybrid discontinuous Galerkin method as described in [36]. This method has initially been developed for equations of the form

$$\rho_t = \operatorname{div}(\nabla\rho + \rho v),$$

with some given velocity vector field v. The method already includes upwind stabilisation for the convection turn and we shall apply it to the linearised system

$$\begin{aligned}\rho_t &= \operatorname{div}(\nabla\rho - \rho(1-\tilde{\rho})(k_D\nabla\tilde{D} + k_S\nabla S)),\\ D_t &= \kappa\Delta D - \delta D + \rho(1-\tilde{\rho}).\end{aligned}$$

Here, $\tilde{\rho}$ and $\tilde{D}$ are assumed to be given functions. In our implementation, at time t_n we take $\tilde{\rho} = \rho(t_{n-1})$ and $\tilde{D} = D(t_{n-1})$. Then, we solve the complete linearised system to obtain $\rho(t_{n+1})$ and $D(t_{n+1})$ and repeat this procedure until we reach $t = t_{\text{final}}$.

Remark 5.5.1. *To guarantee the continuity of the normal component of the numerical flux*

$$j := \rho(1-\tilde{\rho})(k_D\nabla\tilde{D} + k_S\nabla S)$$

over interior element edges we project j onto the space $H^1(\Omega)$ in every time step. This is necessary to strictly enforce the mass conserving property of the scheme. A similar strategy and more details can be found in [5].

5.5.3 Monte-Carlo Simulation

In order to check the consistency between our PDE and the original model, we implemented a Monte Carlo scheme following the steps described in Section 5.2, cf. [59]. We used a Mersenne twister, cf. [80] to create the pseudo random numbers needed. The main issue here is to deal with so-called "conflicts", i.e. the case when two particles want to jump into the same cell. In our implementation, we followed the strategy described in [58]. The basic idea is the following: A new parameter $\lambda \in [0,1]$ in introduced. If two or more particles want to jump to the same cell, this new parameter determines their behaviour: With probability λ, none of the particles jumps and the cell remains empty. With probability $(1-\lambda)$, one particle is chosen randomly and jumps into the target cell. One step in the simulation thus consists of:

- Create a random number for each occupied cell
- For each empty cell, find all neighbouring particles that want to jump into this cell
- Resolve the conflicts using the procedure described above
- Update the dynamic floor field

5.6 Examples

5.6.1 Linear Stability

In this Section we will use the numerical schemes described above to verify the impact of our linear stability analysis in one and two space dimensions. In the one dimensional case, we choose the constant stationary states $\rho_\infty = 0.25$ and $D_\infty = 0.75$. We chose the mesh size $h = 5e-4$ and time steps $\Delta t = 0.1$. Furthermore, we choose the parameter $\epsilon = 1$, $\kappa = 0.001$ and $\delta = 0.25$. From the linear stability analysis (5.21), we expect the system to become unstable for $k_D \geq 2.66$. To verify this behaviour numerically, we add at time $t = 0.5$, the perturbation $u = 0.01\sin(\pi x)$ to ρ and D. The results in Fig. 5.5 illustrate the numerical behaviour for different k_D. (Note that for $k_D = 3$, the instability develops very slowly and thus can hardly be seen in the plotted figure). The results confirm our analytical calculations, cf. (5.19). Furthermore, we can see that the form of the new non-constant equilibria and the speed at which they are approached depend heavily on the value of k_D.
We experience the same behaviour in the two dimensional case. Here, the perturbation is $u_{2D} = 0.01\sin(\pi x)\sin(\pi y)$. In Fig. 5.6, we only show the case $k_D = 3$ as an example. Videos for both the one- and two-dimensional case are available at [1].

5.6.2 Plateau Solutions

Neglecting the time derivative in (5.11), choosing $\kappa = 10^{-4}$ we are in the situation of Section 5.4.3. Starting with a constant initial guess $\rho = 0.25$, $D = 0.75$, both perturbed by $0.01\sin(\pi x)\sin(\pi y)$, we can numerically confirm the emergence of plateau solutions as described in Section 5.4.3 in one as well as in two space dimensions, cf. Fig 5.7, 5.8.

5.7 Limitations of the Model: Non-convex Obstacles

In this Subsection, we present the results of a numerical test designed to examine the herding behaviour of our model. The basic set-up is shown in Fig. 5.9(a): A group of people is located behind an obstacle that prevents them from seeing the exit of the room (i.e. $S = 0$ behind the obstacle, cf. 5.9(b). However, due to the diffusion in the model, after a certain time some people will move around the obstacle and reach a position from which is it possible to see the door ($S \neq 0$). Naively, one would expect that other people

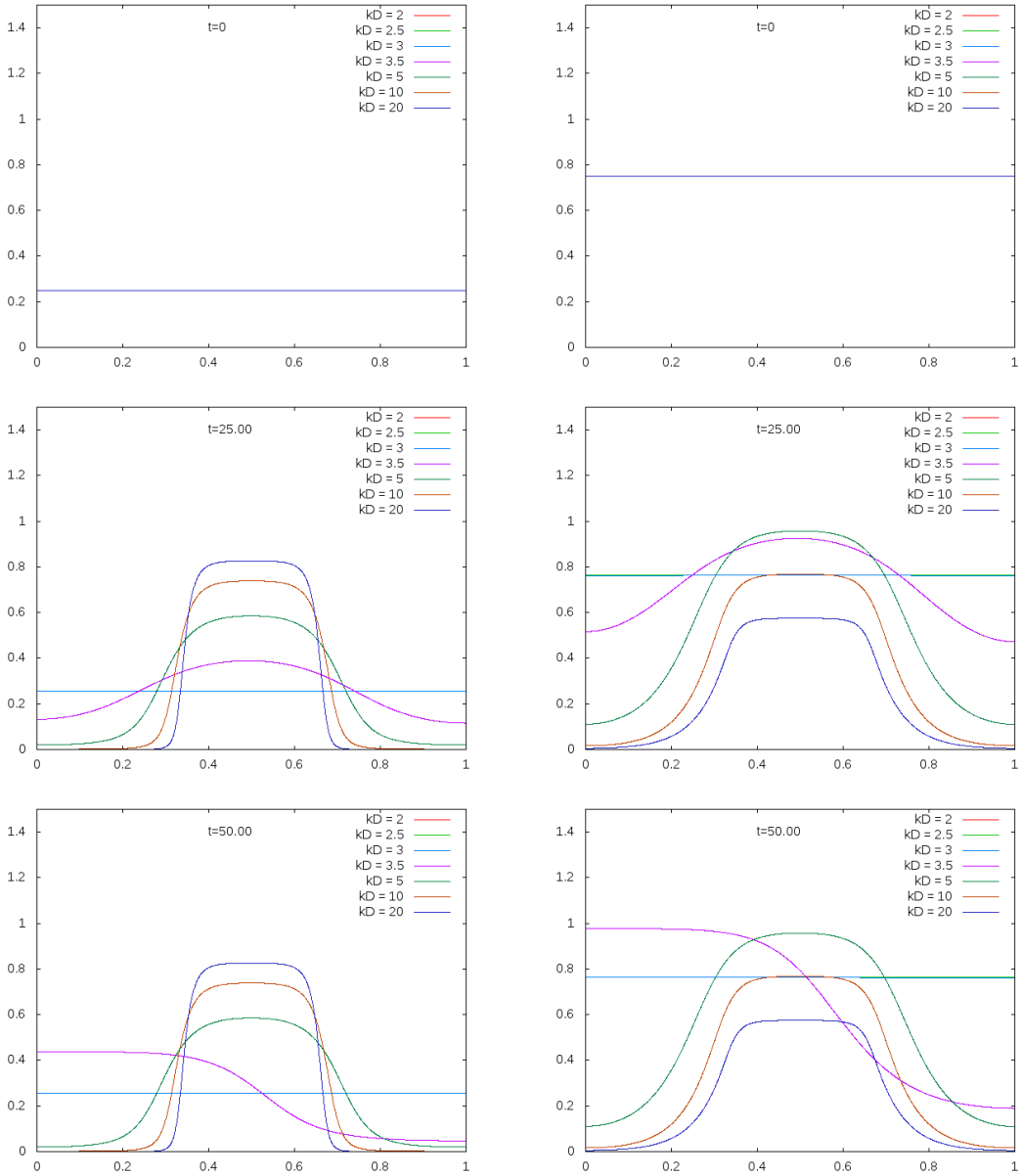

Figure 5.5: Linear stability in 1 D: ρ (left column) and D (right column) at time $t = 0$, $t = 25$ and $t = 50$

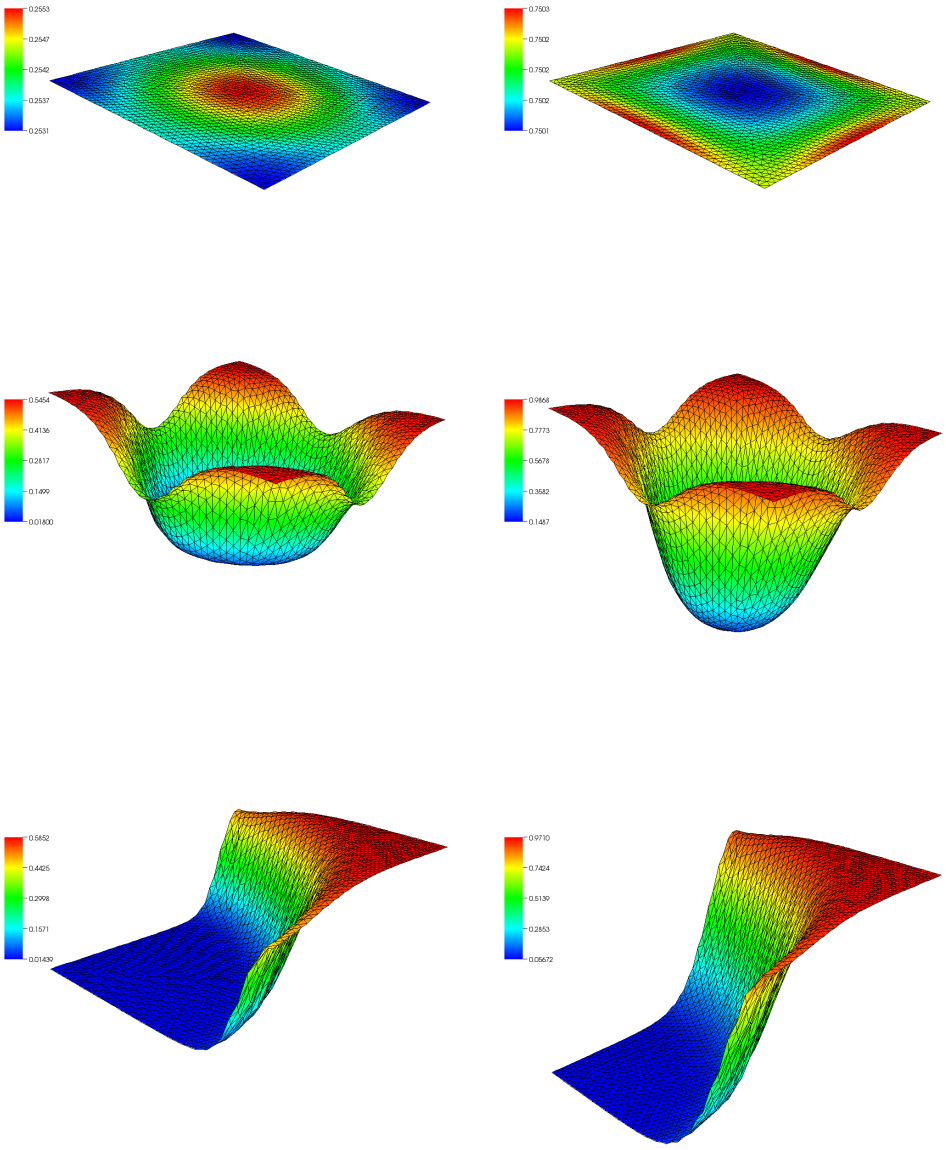

Figure 5.6: Linear stability in 2 D: ρ (left column) and D (right column) at time $t = 0$, $t = 60$ and $t = 300$. The computational domain is the two-dimensional unit square.

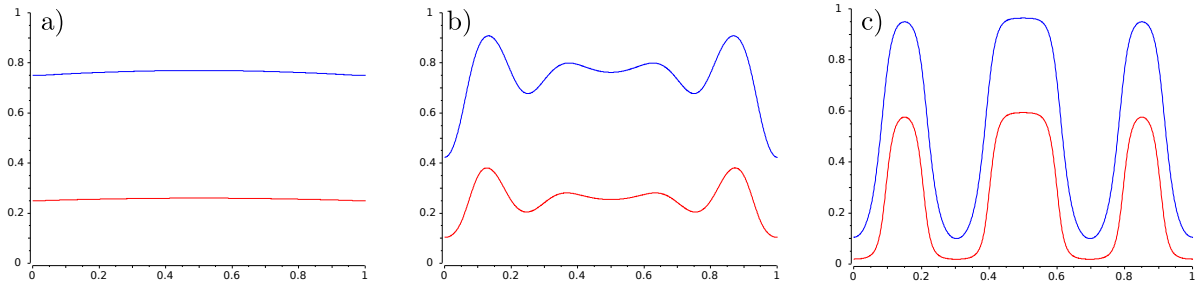

Figure 5.7: Plateau solutions (ρ: red, D: blue) in 1 D at a) $t = 0$, b) $t = 0.025$ and c) $t = 0.6$

will follow these people and therefore be able find their way to the exit faster and that this effect increases with the value of k_D. To verify this, we did simulations with several values of k_D (namely 0, 1, 3 and 5) and compared the loss of mass versus time, cf. Fig. 5.10. However, the results shown confirm this expectation neither in the discrete nor in the continuous case. In fact, people behind the obstacle moving around due to diffusion are creating a large D-field within the obstacle. The stronger the coupling, the more people are held back within the obstacle.

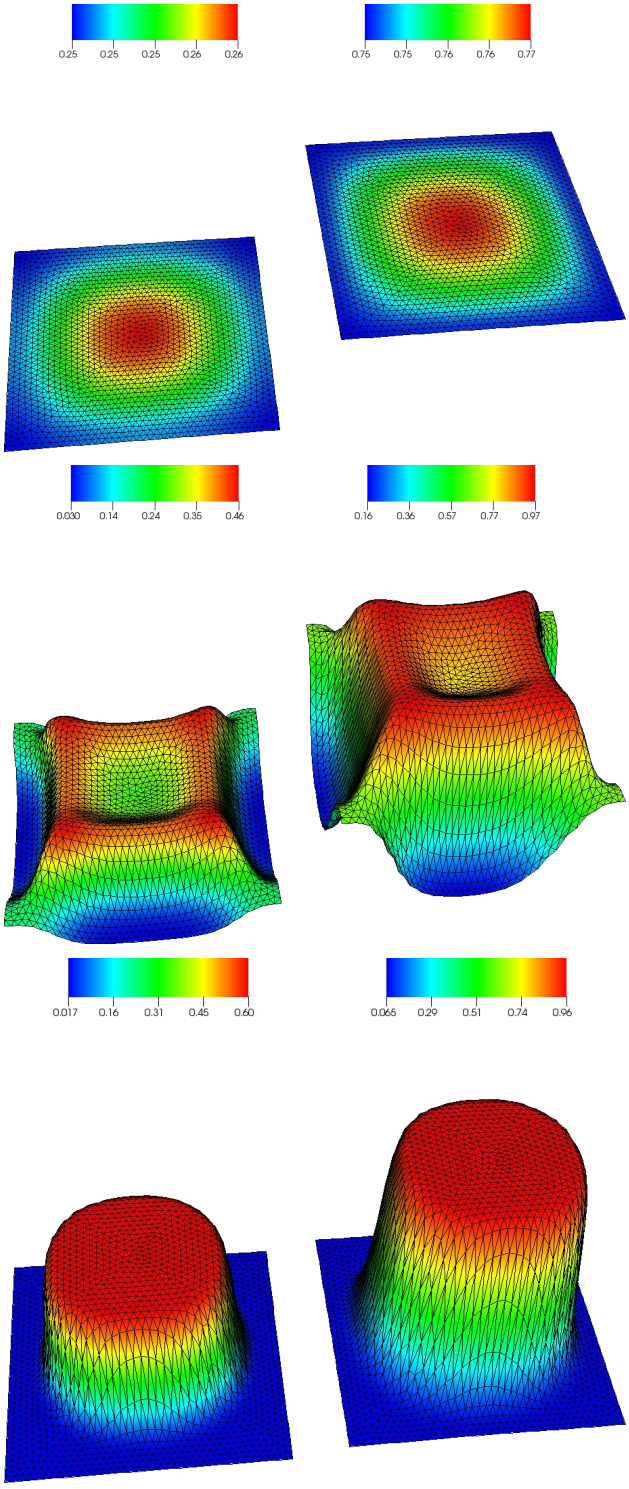

Figure 5.8: Plateau solutions in 2 D: ρ (left column) and D (right column) at time $t = 0$, $t = 7$ and $t = 70$. The computational domain is the two-dimensional unit square.

a)

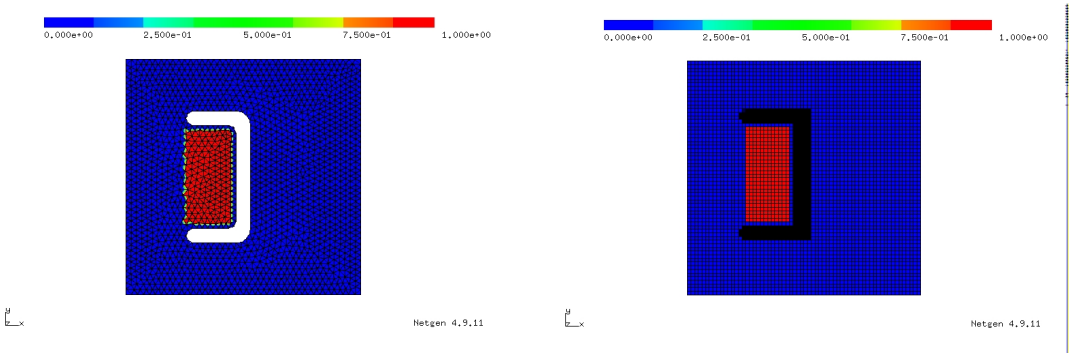

b)

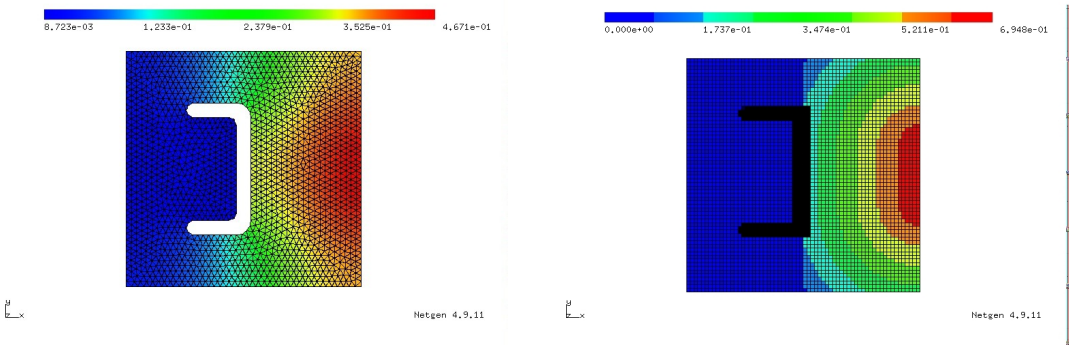

Figure 5.9: The initial conditions in the PDE (a, left) and Monte Carlo (a, right) setting and the static field S in the PDE (b, left) and Monte Carlo (b, right) setting

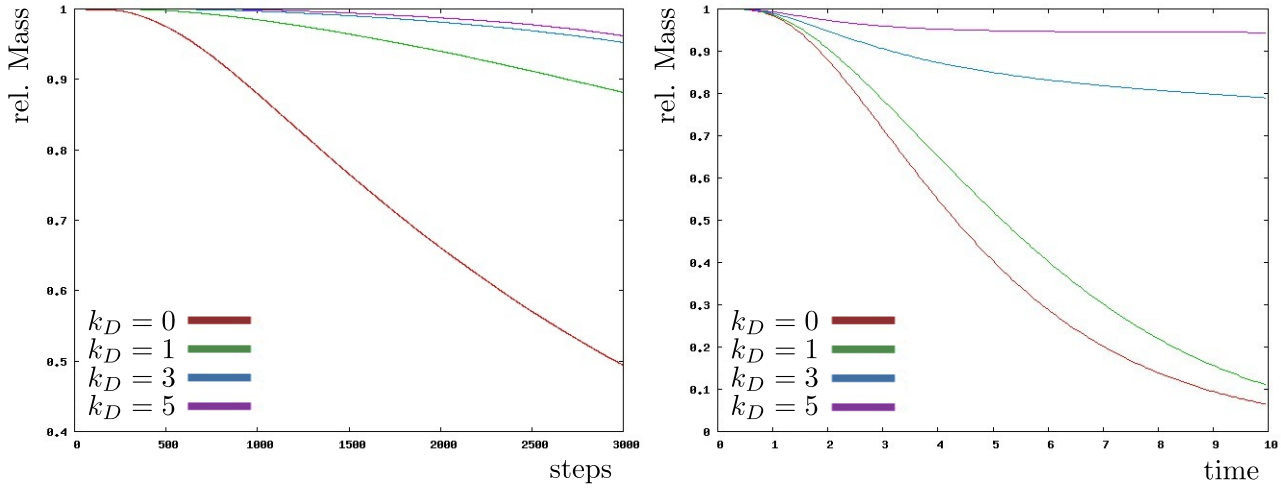

Figure 5.10: The loss of mass vs. time for several values of k_D for the PDE case (left) and the Monte Carlo simulation (right)

Chapter 6

Conclusions and Future Work

The first part of this thesis dealt with a mean-field price formation model. We were able to show local existence, but the problem of global existence of a smooth solution on the whole real line is still open. In [71], a sketch of such a proof is given, however it seems difficult to make it rigorous. The main obstructions are the regularity and boundedness of the free boundary (i.e the price).
For the data assimilation problem we were able to provide analytical and numerical results for a known price $p(t)$ in the assimilation interval. We provided numerical experiments showing the influence of inverse crime, noise and imperfect measurements. Interesting open problems are:

- If not only the price, but the price and the transaction rate are known, will this improve the results?
- Improve the performance of the numerical algorithm, e.g. by including a backtracking line search, cf. [27], to determine the damping parameter. Furthermore, the update step could be performed in a higher norm such as H^1, i.e.

  $$\langle f_I^{k+1}, v\rangle = \langle f_I^k, v\rangle - \tau J'(f_I^k)v, \quad v \in H^1(\Omega).$$

  This would correspond to an additional regularisation term.
- Application to real data. This will help in particular to get a feeling about the modelling error.

Concerning the crowd motion models considered in the second part of this thesis, the following points are worthwhile to address:

- For Hughes's model, it would be interesting to consider the two dimensional situation. While the model is given for any space dimension, it is not completely clear whether the definition of the potential makes sense in a domain including obstacles. Thus a numerical scheme which would be able to handle the 2d case including obstacles would be useful to consider more realistic geometries. Due to the hyperbolic structure of the model, specialised numerical algorithms, such as (weighted) essentially non-oscillatory, cf. [47, 101, 102] and [24, Chapter 4], or hybrid discontinuous Galerkin schemes, cf. [23, 36], are necessary. Some work in this direction has been done, cf. [76], but the obstacles have not been considered.

- For the continuous model considered in Chapter 5, possible future work would be to apply the numerical algorithm implemented to more realistic set-ups (e.g. stadiums, metro stations, etc.) and compare the results with other existing models.

- In some situations, it might also be desirable to consider a coupling of the discrete (Monte Carlo) and the continuous finite element scheme. For example, for very large buildings, a particle simulation near crucial points such as exits coupled with the finite element method in regions which are not critical would lead to a significant reduction of simulation time.

- In [11], the author in collaboration M. Burger, C. Di Francesco and B. Schlake studied a continuum model for diffusion of multiple species incorporating size exclusion effects. It can be deduced from a microscopic hopping model in the same manner as the Schadschneider & Kirchner model in Chapter 5. In the aforementioned work, only the case of a given, time independent potential has been considered. Well-posedness of strong solutions close to equilibrium as well as global existence of weak solutions is proven. Thus a natural extension would be to couple this model with the mean-field equation (5.11) (or, more precisely, two or more mean field equations - one for each species) and employ it for the simulation of human crowds. Most likely, at least the well-posedness proof can be adapted. Furthermore, already the model without mean field equations is able to produce lane formation (as instability of certain stationary states). This is quite remarkable for a continuum limit and it is worthwhile to explore whether this property persists or how it changes in the presence of the dynamic field. Finally, the results could again be compared with discrete (Monte Carlo) simulations.

- Finally, as explained in the introduction, a very important question in the modelling of human crowds is how to obtain realistic models. The same holds true for other situations involving high densities (i.e. the classical mean field hypothesis is not fulfilled), such as ion channels. One possible way to deal with this issue is to start from a generic, non-linear drift diffusion model and try to obtain the structure of the non-linearities from measured data. This is an (inverse) parameter identification problem. The advantage of this approach is obvious: the model is already generated from measured data and thus reflects the "real" behaviour. However, due its non-linear and inverse structure, the problem is not easy to treat. The development of a theoretical framework and numerical algorithms is ongoing work in collaboration with M. Burger and M.-T. Wolfram, cf. [12].

Bibliography

[1] Videos for linear stability. http://www.jfpietschmann.eu/crowdmotion. 112

[2] Visit visualization environment. Available at http://www.llnl.gov/visit/home.html. 109

[3] S. Al Gadhi and H. Mahmassani. Simulation of crowd behaviour and movement: fundamental relations and application. *Transp. Res. Rec.*, 1991. 8

[4] A. Aw and M. Rascle. Resurrection of "second order" models of traffic flow. *SIAM J. Appl. Math.*, 60(3):916–938 (electronic), 2000. 9

[5] P. Bastian and B. Rivière. Superconvergence and H(div)-projection for discontinuous Galerkin methods. *Int. J. Numer. Meth. Fluids.*, 42(10):1043–1057, 2003. 111

[6] A. Blanchet, J. Dolbeault, and B. Perthame. Two-dimensional Keller-Segel model: optimal critical mass and qualitative properties of the solutions. *Electron. J. Differential Equations*, pages No. 44, 32 pp. (electronic), 2006. 94

[7] F. Brezzi and P. A. Markowich. A convection-diffusion problem with small diffusion coefficient arising in semiconductor physics. *Boll. Un. Mat. Ital. B (7)*, 2(4):903–930, 1988. 62

[8] M. Brunnermeier. *Asset Pricing under Asymmetric Information: Bubbles, Crashes, Technical Analysis and Herding.* Oxford University Press: Oxford, 2001. 94

[9] M. Burger, M. Di Francesco, and Y. Dolak-Struss. The Keller-Segel model for chemotaxis: linear vs. nonlinear diffusion. *SIAM J. Math. Anal.*, 38:1288–1315., 2006. 76

[10] M. Burger, Y. Dolak-Struss, and C. Schmeiser. Asymptotic analysis of an advection-dominated chemotaxis model in multiple spatial dimensions. *Commun. Math. Sci.*, 6:1–28, 2008. 76, 105

[11] M. Burger, M. D. Francesco, J.-F. Pietschmann, and B. Schlake. Nonlinear cross-diffusion with size exclusion. *SIAM Journal on Mathematical Analysis*, 42(6):2842–2871, 2010. 120

[12] M. Burger, J.-F. Pietschmann, and M.-T. Wolfram. Identification of nonlinearities in transport-diffusion models for size exclusion. submitted, 2011. 9, 121

[13] M. Burger, B. Schlake, and W. M.-T. Nonlinear poisson-nernst planck equations for ion flux through confined geometries. *preprint*, 2010. 106

[14] R. Bürger, , K. Karlsen, and J. Towers. A conservation law with discontinuous flux modelling traffic flow with abruptly changing road surface conditions. In *Hyperbolic Problems: Theory, Numerics and Applications*, volume 67 of *Proceedings of Symposia in Applied Mathematics*, pages 455–464, 2009. 58

[15] R. Bürger, G. A., K. Karlsen, and J. Towers. Difference schemes, entropy solutions and speedup impulse for an inhomogeneous kinetamtic traffic flow model. *Networks and heterogeneous media*, 3(2):1–41, 2008. 58

[16] C. Burstedde, K. Klauck, A. Schadschneider, and J. Zittartz. Simulation of pedestrian dynamics using a two-dimensional cellular automaton. *Physica A: Statistical Mechanics and its Applications*, 295(3-4):507–525, 2001. 93

[17] J. C. N. C. Bardos, A. Y. Leroux. First order quasilinear equations with boundary conditions. *Comm. Partial Differential Equations*, 4:1017–1034, 1979. 62, 63, 67, 74, 81, 82

[18] L. A. Caffarelli, P. A. Markowich, and J.-F. Pietschmann. On a price formation free boundary model by lasry & lions. *C. R. Acad. Sci. Paris, Ser. I*, 349:621–624, 2011. 6

[19] L. A. Caffarelli, P. A. Markowich, and M.-T. Wolfram. On a price formation free boundary value model by lasry & lions: The neumann problem. *C. R. Acad. Sci. Paris, Ser. I*, 349:841–844, 2011. 6

[20] B. K. Chakrabarti, A. Chakraborti, and A. Chatterjee, editors. *Econophysics and Sociophysics: Trends and Perspectives*. Wiley-VCH Verlag GmbH & Co. KGaA, 2006. 5

[21] U. Chattaraj, A. Seyfried, and P. Chakroborty. Comparison of Pedestrian Fundamental Diagram Across Cultures. *Advances in Complex Systems*, 12(03):393–405, 2009. 8

[22] L. Chayes, M. d. M. González, M. P. Gualdani, and I. Kim. Global existence and uniqueness of solutions to a model of price formation. *SIAM J. Math. Anal.*, 41(5):2107–2135, 2009. 6

[23] B. Cockburn, J. Gopalakrishnan, and R. Lazarov. Unified hybridization of discontinuous galerkin, mixed, and continuous galerkin methods for second order elliptic problems. *SIAM Journal on Numerical Analysis*, 47(2):1319–1365, 2009. 120

[24] B. Cockburn, C.-W. Shu, C. Johnson, E. Tadmor, and C.-W. Shu. Essentially non-oscillatory and weighted essentially non-oscillatory schemes for hyperbolic conservation laws. In *Advanced Numerical Approximation of Nonlinear Hyperbolic Equations*, volume 1697 of *Lecture Notes in Mathematics*, pages 325–432. Springer Berlin / Heidelberg, 1998. 10.1007/BFb0096355. 120

[25] R. M. Colombo and M. D. Rosini. Pedestrian flows and non-classical shocks. *Math. Methods Appl. Sci.*, 28(13):1553–1567, 2005. 9

[26] M. G. Crandall and T. M. Liggett. Generation of semi-groups of nonlinear transformations on general banach spaces. *American Journal of Mathematics*, 93(2):265–298, 1971. 15

[27] J. E. Dennis, Jr. and R. B. Schnabel. *Numerical methods for unconstrained optimization and nonlinear equations*, volume 16 of *Classics in Applied Mathematics*. Society for Industrial and Applied Mathematics (SIAM), Philadelphia, PA, 1996. Corrected reprint of the 1983 original. 119

[28] A. Devenow and I. Welch. Rational herding in financial economics. *European Economic Review*, 40(3-5):603 – 615, 1996. Papers and Proceedings of the Tenth Annual Congress of the European Economic Association. 94

[29] M. Di Francesco and J. Rosado. Fully parabolic Keller-Segel model for chemotaxis with prevention of overcrowding. *Nonlinearity*, 21(11):2715–2730, 2008. 99

[30] E. W. Dijkstra. A note on two problems in connexion with graphs. *Numer. Math.*, 1, 1959. 109

[31] Y. Dolak and S. C. The keller-segel model with logistic sensitivity function and small diffusivity. *SIAM J. Appl. Math.*, 66:286–308, 2005. 105

[32] F. Dubois and P. LeFloch. Boundary conditions for nonlinear hyperbolic systems of conservation laws. *J. Differential Equations*, 71(1):93–122, 1988. 62, 63, 82, 84

[33] B. Düring, P. Markowich, J.-F. Pietschmann, and M.-T. Wolfram. Boltzmann and Fokker-Planck equations modelling opinion formation in the presence of strong leaders. *Proc. R. Soc. Lond. Ser. A Math. Phys. Eng. Sci.*, 465(2112):3687–3708, 2009. 5

[34] B. Düring, D. Matthes, and G. Toscani. Kinetic equations modelling wealth redistribution: a comparison of approaches. *Phys. Rev. E (3)*, 78(5):056103, 12, 2008. 5

[35] B. Düring, D. Matthes, and G. Toscani. A Boltzmann-type approach to the formation of wealth distribution curves. *Riv. Mat. Univ. Parma (8)*, 1, 2009. 5

[36] H. Egger. A class of hybrid mortar finite element methods for interface problems with non-matching meshes. *Technical Report AICES-2009-2*, submitted. 110, 120

[37] H. W. Engl. *Integralgleichungen*. Springer Lehrbuch Mathematik. [Springer Mathematics Textbook]. Springer-Verlag, Vienna, 1997. 20

[38] H. W. Engl, M. Hanke, and A. Neubauer. *Regularization of inverse problems*, volume 375 of *Mathematics and its Applications*. Kluwer Academic Publishers Group, Dordrecht, 1996. 45

[39] B. Engquist and S. Osher. One-sided difference schemes and transonic flow. *Proc. Nat. Acad. Sci. U.S.A.*, 77(6):3071–3074, 1980. 86

[40] L. C. Evans. *Partial differential equations*, volume 19 of *Graduate Studies in Mathematics*. American Mathematical Society, Providence, RI, 1998. 24, 25, 34

[41] L. C. Evans and R. F. Gariepy. *Measure Theory and Fine Properties of Functions.* Crc Pr Inc, 1991. 72

[42] M. Fukui and Y. Ishibashi. Self-organized phase transitions in CA-models for pedestrians. *J. Phys. Soc. Japan*, 8:2861–2863, 1999. 9

[43] G. Giacomin and J. L. Lebowitz. Phase segregation dynamics in particle systems with long range interactions. I. Macroscopic limits. *J. Statist. Phys.*, 87(1-2):37–61, 1997. 98

[44] M. d. M. González and M. P. Gualdani. Asymptotics for a symmetric equation in price formation. *Appl. Math. Optim.*, 59(2):233–246, 2009. 6, 15, 43

[45] M. d. M. González and M. P. Gualdani. Asymptotics for a free-boundary problem in price formation. *Nonlinear Analysis: Theory, Methods & Applications*, 74(10):3269–3294, 2011. 6, 15, 16

[46] P. Grisvard. *Elliptic problems in nonsmooth domains*, volume 24 of *Monographs and Studies in Mathematics.* Pitman (Advanced Publishing Program), Boston, MA, 1985. 101

[47] A. Harten, B. Engquist, S. Osher, and S. R. Chakravarthy. Uniformly high-order accurate essentially nonoscillatory schemes. III. *J. Comput. Phys.*, 71(2):231–303, 1987. 120

[48] D. Helbing. Traffic and related self-driven many-particle systems. *Rev. Mod. Phys.*, 73(4):1067–1141, Dec 2001. 9

[49] D. Helbing, I. J. Farkas, P. Molnar, and T. Vicsek. Simulation of pedestrian crowds in normal and evacuation situations. *in: M. Schreckenberg and S. D. Sharma (eds.)* Pedestrian and Evacuation Dynamics *(Springer, Berlin).*, pages 21–58, 2002. 9

[50] D. Helbing, A. Johansson, and H. Z. Al-Abideen. The dynamics of crowd disasters: An empirical study. *Physical Review E (Statistical, Nonlinear, and Soft Matter Physics)*, 75(4), 2007. 8

[51] L. F. Henderson. The statistics of crowd fluids. *Nature*, 229:381–383, 1971. 9

[52] D. Horstmann. From 1970 until present: the Keller-Segel model in chemotaxis and its consequences. I. *Jahresber. Deutsch. Math.-Verein.*, 105(3):103–165, 2003. 94

[53] D. Horstmann. From 1970 until present: the Keller-Segel model in chemotaxis and its consequences. II. *Jahresber. Deutsch. Math.-Verein.*, 106(2):51–69, 2004. 94

[54] R. L. Hughes. A continuum theory for the flow of pedestrians. *Transportation Research Part B: Methodological*, 36(6):507 – 535, 2002. 10, 57, 58

[55] R. L. Hughes. The flow of human crowds. *Annual Review of Fluid Mechanics*, 35:169–182, 2003. 57

[56] K. H. Karlsen and N. H. Risebro. On the uniqueness and stability of entropy solutions of nonlinear degenerate parabolic equations with rough coefficients. *Discrete Contin. Dyn. Syst.*, 9(5):1081–1104, 2003. 58, 76, 77

[57] E. Keller and L. Segel. Initiation of slide mold aggregation viewed as an instability. *J. Theor. Biol.*, 26:399–415, 1970. 94

[58] A. Kirchner. Modellierung und statistische physik biologischer und sozialer systeme. PhD Thesis, 2002. 95, 99, 109, 111

[59] A. Kirchner and A. Schadschneider. Simulation of evacuation processes using a bionics-inspired cellular automaton model for pedestrian dynamics. *Physica A: Statistical Mechanics and its Applications*, 312(1-2):260 – 276, 2002. 10, 93, 94, 97, 111

[60] R. A. Klausen and N. H. Risebro. Stability of conservation laws with discontinuous coefficients. *J. Differential Equations*, 157(1):41–60, 1999. 58

[61] C. Klingenberg and N. H. Risebro. Convex conservation laws with discontinuous coefficients. Existence, uniqueness and asymptotic behavior. *Comm. Partial Differential Equations*, 20(11-12):1959–1990, 1995. 80

[62] S. N. Kružkov. First order quasilinear equations in serveral independent variables. *Math. USSR Sb*, 10:217–243, 1970. 61, 63, 76

[63] A. Lachapelle and M.-T. Wolfram. On a mean field game approach modeling congestion and aversion in pedestrian crowds. *Transportation Research Part B: Methodologica*, 2011. to appear. 9

[64] O. A. Ladyzhenskaia and N. N. Uraltseva. *Linear and quasilinear elliptic equations [by] Olga A. Ladyzhenskaya and Nina N. Uraltseva. Translated by Scripta Technica. Translation editor: Leon Ehrenpreis.* Academic Press, New York,, 1968. 64

[65] J.-M. Lasry and P.-L. Lions. Jeux à champ moyen. I. Le cas stationnaire. *C. R. Math. Acad. Sci. Paris*, 343(9):619–625, 2006. 6

[66] J.-M. Lasry and P.-L. Lions. Jeux à champ moyen. II. Horizon fini et contrôle optimal. *C. R. Math. Acad. Sci. Paris*, 343(10):679–684, 2006. 6, 15

[67] J.-M. Lasry and P.-L. Lions. Towards a self-consistent theory of volatility. *J. Math. Pures Appl. (9)*, 86(6):541–551, 2006. 6

[68] J.-M. Lasry and P.-L. Lions. Instantaneous self-fulfilling of long-term prophecies on the probabilistic distribution of financial asset values. *Ann. Inst. H. Poincaré Anal. Non Linéaire*, 24(3):361–368, 2007. 6

[69] J.-M. Lasry and P.-L. Lions. Large investor trading impacts on volatility. In *Paris-Princeton Lectures on Mathematical Finance 2004*, volume 1919 of *Lecture Notes in Math.*, pages 173–190. Springer, Berlin, 2007. 6

[70] J.-M. Lasry and P.-L. Lions. Large investor trading impacts on volatility. *Ann. Inst. H. Poincaré Anal. Non Linéaire*, 24(2):311–323, 2007. 6

[71] J.-M. Lasry and P.-L. Lions. Mean field games. *Jpn. J. Math.*, 2(1):229–260, 2007. 6, 9, 15, 36, 39, 119

[72] R. J. LeVeque. *Numerical methods for conservation laws.* Lectures in Mathematics ETH Zürich. Birkhäuser Verlag, Basel, second edition, 1992. 58

[73] J. Lewis, S. Lakshmivarahan, and S. Dhall. *Dynamic Data Assimilation: A Least Squares Approach*, volume 104 of *Encyclopedia of Mathematics and its Applications.* Cambridge University Press, 2006. 46

[74] A. Liddle, J. andSeyfried, W. Klingsch, T. Rupprecht, A. Schadschneider, and A. Winkens. An experimental study of pedestrian congestions: Influence of bottleneck width and length, 2009. 8

[75] M. J. Lighthill and G. B. Whitham. On kinematic waves. ii. a theory of traffic flow on long crowded roads. *Royal Society of London Proceedings Series A*, 229:317–345, May 1955. 58

[76] H. Ling, S. C. Wong, M. Zhang, C.-H. Shu, and W. H. K. Lam. Revisiting hughes' dynamic continuum model for pedestrian flow and the development of an efficient solution algorithm. *Transportation Research Part B: Methodological*, 43(1):127–141, 2009. 58, 120

[77] P. A. Markowich. *The stationary semiconductor device equations*. Computational Microelectronics. Springer-Verlag, Vienna, 1986. 101

[78] P. A. Markowich, C. A. Ringhofer, and C. Schmeiser. *Semiconductor equations*. Springer-Verlag New York, Inc., New York, NY, USA, 1990. 106

[79] P. A. Markowich and P. Szmolyan. A system of convection-diffusion equations with small diffusion coefficient arising in semiconductor physics. *J. Differential Equations*, 81(2):234–254, 1989. 62

[80] M. Matsumoto and T. Nishimura. Mersenne twister: a 623-dimensionally equidistributed uniform pseudo-random number generator. *ACM Trans. Model. Comput. Simul.*, 8(1):3–30, 1998. 111

[81] D. Matthes and G. Toscani. On steady distributions of kinetic models of conservative economies. *J. Stat. Phys.*, 130(6):1087–1117, 2008. 5

[82] B. Maury, A. Roudneff-Chupin, and F. Santambrogio. A macroscopic crowd motion model of the gradient-flow type. *M3AS*, 20(10):1787–1821, 2010. 9

[83] M. Muramatsu and T. Nagatani. Jamming transition in two-dimensional pedestrian traffic. *Physica A*, 275:281 – 291, 2000. 9

[84] U. Nations. Population division: World urbanization prospects, the 2009 revision. online, 2010. 9

[85] N. Nichols. Mathematical concepts of data assimilation. In W. L. et al., editor, *Data Assimilation*. Springer Berlin, 2010. 46

[86] J. Nocedal and S. J. Wright. *Numerical optimization*. Springer Series in Operations Research and Financial Engineering. Springer, New York, second edition, 2006. 49

[87] J. R. Nofsinger and R. W. Sias. Herding and feedback trading by institutional and individual investors. *The Journal of Finance*, 54(6):2263–2295, 1999. 94

[88] S. Osher. Riemann solvers, the entropy condition, and difference approximations. *SIAM J. Numer. Anal.*, 21(2):217–235, 1984. 87

[89] K. J. Painter and T. Hillen. Volume-filling and quorum-sensing in models for chemosensitive movement. *Can. Appl. Math. Q.*, 10(4):501–543, 2002. 94

[90] B. Piccoli and A. Tosin. Pedestrian flows in bounded domains with obstacles. *Contin. Mech. Thermodyn.*, 21(2):85–107, 2009. 9

[91] A. Portz and A. Seyfried. Analyzing stop-and-go waves by experiment and modeling, 2010. 8

[92] R. M. Raafat, N. Chater, and C. Frith. Herding in humans. *Trends in Cognitive Sciences*, 13(10):420–428, 2009. 93

[93] P. I. Richards. Shock waves on the highway. *Operations Research*, 4(1):42–51, 1956. 58

[94] N. Rodriguez and A. Bertozzi. Local existence and uniqueness of solutions to a pde model for criminal behavior. *Mathematical Models and Methods in Applied Sciences (M3AS)*, 20:1425–1457, 2010. 5

[95] A. Schadschneider, W. Klingsch, H. Kluepfel, T. Kretz, C. Rogsch, and A. Seyfried. *Encyclopedia of Complexity and System Science, R. A. Meyers, (ed.)*, volume 3, chapter Evacuation Dynamics: Empirical Results, Modeling and Applications, page pp. 3142. Springer, 2009. 95

[96] O. Schenk and K. Gärtner. Solving unsymmetric sparse systems of linear equations with pardiso. *Journal of Future Generation Computer Systems*, 20:475–487, 2004. 110

[97] O. Schenk and K. Gärtner. On fast factorization pivoting methods for symmetric indefinite systems. *Elec. Trans. Numer. Anal*, 23:158–179, 2006. 110

[98] J. Schöberl. Netgen an advancing front 2d/3d-mesh generator based on abstract rules. *Computing and Visualization in Science*, 1:41–52, 1997. 110

[99] A. Seyfried, 2001. taken from Video recordings available at http://www2.fz-juelich.de/jsc/appliedmath/ped. 8

[100] M. B. Short, P. J. Brantingham, A. L. Bertozzi, and G. E. Tita. Dissipation and displacement of hotspots in reaction-diffusion models of crime. *Proceedings of the National Academy of Sciences*, 107(9):3961–3965, 2010. 5

[101] C.-W. Shu and S. Osher. Efficient implementation of essentially nonoscillatory shock-capturing schemes. *J. Comput. Phys.*, 77(2):439–471, 1988. 120

[102] C.-W. Shu and S. Osher. Efficient implementation of essentially nonoscillatory shock-capturing schemes. II. *J. Comput. Phys.*, 83(1):32–78, 1989. 120

[103] M. Simpson, K. Landman, and B. Hughes. Diffusing populations: ghosts or folks? *Australasian Journal of Engineering Education*, 15:59–67, 2009. 93, 97

[104] A. Sopasakis and M. A. Katsoulakis. Stochastic modeling and simulation of traffic flow: Asymmetric single exclusion process with arrhenius look-ahead dynamics. *SIAM Journal on Applied Mathematics*, 66(3):921–944, 2006. 97

[105] H. Tanabe. *Equations of evolution*, volume 6. Pitman (Advanced Publishing Program), 1979. 64

[106] R. Temam. *Navier-Stokes equations. Theory and numerical analysis.* North-Holland Publishing Co., Amsterdam, 1977. Studies in Mathematics and its Applications, Vol. 2. 89, 90

[107] J. W. Thomas. *Numerical partial differential equations*, volume 33 of *Texts in Applied Mathematics*. Springer-Verlag, New York, 1999. Conservation laws and elliptic equations. 58

[108] J. D. Towers. Convergence of a difference scheme for conservation laws with a discontinuous flux. *SIAM J. Numer. Anal.*, 38(2):681–698 (electronic), 2000. 58, 86

[109] A. Treuille, S. Cooper, and Z. Popovic. Continuum crowds. In *ACM Transaction on Graphics*, volume 25, pages 1160–1168, 2006. Proceedings of SCM SIGGRAPH 2006. 9

[110] U. Weidmann. Transporttechnik der fussgänger - transporttechnische eigenschaften des fussgngerverkehrs (literaturstudie). Literature Research 90, Institut füer Verkehrsplanung, Transporttechnik, Strassen- und Eisenbahnbau IVT an der ETH Zürich, ETH-Hönggerberg, CH-8093 Zürich, March 1993. in German. 95

[111] A. Wirgin. The inverse crime. arXiv:math-ph/0401050v1, 2004. 50

[112] D. Wrzosek. Global attractor for a chemotaxis model with prevention of overcrowding. *Nonlinear Analysis*, 59(8):1293 – 1310, 2004. 101

[113] A. Yagi. Abstract quasilinear evolution equations of parabolic type in Banach spaces. *Boll. Un. Mat. Ital. B (7)*, 5(2):341–368, 1991. 64

[114] S. J. Yuhaski, Jr. and J. M. Smith. Modeling circulation systems in buildings using state dependent queueing models. *Queueing Systems Theory Appl.*, 4(4):319–338, 1989. 9

[115] M. Zhang, C.-W. Shu, G. C. K. Wong, and S. C. Wong. A weighted essentially non-oscillatory numerical scheme for a multi-class lighthill-whitham-richards traffic flow model. *Journal of Computational Physics*, 191(2):639 – 659, 2003. 58

[116] P. Zhang, S. Wong, and C.-W. Shu. A weighted essentially non-oscillatory numerical scheme for a multi-class traffic flow model on an inhomogeneous highway. *Journal of Computational Physics*, 212(2):739 – 756, 2006. 58